Structural and Dynamic Aspects of Trophic Cord Microtubules in *Rhodnius prolixus*.

Rene E. Harrison

A Thesis
Submitted to the Faculty of Graduate Studies
In Partial Fulfillment of the Requirements
for the Degree of

MASTER OF SCIENCE

Department of Zoology
Winnipeg, Manitoba

ISBN 0-612-13174-2

Canada

Name ____

Dissertation Abstracts International is arranged by broad, general subject categories. Please select the one subject which most nearly describes the content of your dissertation. Enter the corresponding four-digit code in the spaces provided.

Cell Biology
SUBJECT TERM

0379
SUBJECT CODE

U·M·I

Subject Categories

THE HUMANITIES AND SOCIAL SCIENCES

COMMUNICATIONS AND THE ARTS
Architecture 0729
Art History 0377
Cinema 0900
Dance 0378
Fine Arts 0357
Information Science 0723
Journalism 0391
Library Science 0399
Mass Communications 0708
Music 0413
Speech Communication 0459
Theater 0465

EDUCATION
General 0515
Administration 0514
Adult and Continuing 0516
Agricultural 0517
Art 0273
Bilingual and Multicultural 0282
Business 0688
Community College 0275
Curriculum and Instruction 0727
Early Childhood 0518
Elementary 0524
Finance 0277
Guidance and Counseling 0519
Health 0680
Higher 0745
History of 0520
Home Economics 0278
Industrial 0521
Language and Literature 0279
Mathematics 0280
Music 0522
Philosophy of 0998
Physical 0523
Psychology 0525
Reading 0535
Religious 0527
Sciences 0714
Secondary 0533
Social Sciences 0534
Sociology of 0340
Special 0529
Teacher Training 0530
Technology 0710
Tests and Measurements 0288
Vocational 0747

LANGUAGE, LITERATURE AND LINGUISTICS
Language
- General 0679
- Ancient 0289
- Linguistics 0290
- Modern 0291

Literature
- General 0401
- Classical 0294
- Comparative 0295
- Medieval 0297
- Modern 0298
- African 0316
- American 0591
- Asian 0305
- Canadian (English) 0352
- Canadian (French) 0355
- English 0593
- Germanic 0311
- Latin American 0312
- Middle Eastern 0315
- Romance 0313
- Slavic and East European 0314

PHILOSOPHY, RELIGION AND THEOLOGY
Philosophy 0422
Religion
- General 0318
- Biblical Studies 0321
- Clergy 0319
- History of 0320
- Philosophy of 0322

Theology 0469

SOCIAL SCIENCES
American Studies 0323
Anthropology
- Archaeology 0324
- Cultural 0326
- Physical 0327

Business Administration
- General 0310
- Accounting 0272
- Banking 0770
- Management 0454
- Marketing 0338

Canadian Studies 0385
Economics
- General 0501
- Agricultural 0503
- Commerce-Business 0505
- Finance 0508
- History 0509
- Labor 0510
- Theory 0511

Folklore 0358
Geography 0366
Gerontology 0351
History
- General 0578
- Ancient 0579
- Medieval 0581
- Modern 0582
- Black 0328
- African 0331
- Asia, Australia and Oceania 0332
- Canadian 0334
- European 0335
- Latin American 0336
- Middle Eastern 0333
- United States 0337

History of Science 0585
Law 0398
Political Science
- General 0615
- International Law and Relations 0616
- Public Administration 0617

Recreation 0814
Social Work 0452
Sociology
- General 0626
- Criminology and Penology ... 0627
- Demography 0938
- Ethnic and Racial Studies 0631
- Individual and Family Studies 0628
- Industrial and Labor Relations 0629
- Public and Social Welfare 0630
- Social Structure and Development 0700
- Theory and Methods 0344

Transportation 0709
Urban and Regional Planning 0999
Women's Studies 0453

THE SCIENCES AND ENGINEERING

BIOLOGICAL SCIENCES
Agriculture
- General 0473
- Agronomy 0285
- Animal Culture and Nutrition 0475
- Animal Pathology 0476
- Food Science and Technology 0359
- Forestry and Wildlife 0478
- Plant Culture 0479
- Plant Pathology 0480
- Plant Physiology 0817
- Range Management 0777
- Wood Technology 0746

Biology
- General 0306
- Anatomy 0287
- Biostatistics 0308
- Botany 0309
- Cell 0379
- Ecology 0329
- Entomology 0353
- Genetics 0369
- Limnology 0793
- Microbiology 0410
- Molecular 0307
- Neuroscience 0317
- Oceanography 0416
- Physiology 0433
- Radiation 0821
- Veterinary Science 0778
- Zoology 0472

Biophysics
- General 0786
- Medical 0760

EARTH SCIENCES
Biogeochemistry 0425
Geochemistry 0996
Geodesy 0370
Geology 0372
Geophysics 0373
Hydrology 0388
Mineralogy 0411
Paleobotany 0345
Paleoecology 0426
Paleontology 0418
Paleozoology 0985
Palynology 0427
Physical Geography 0368
Physical Oceanography 0415

HEALTH AND ENVIRONMENTAL SCIENCES
Environmental Sciences 0768
Health Sciences
- General 0566
- Audiology 0300
- Chemotherapy 0992
- Dentistry 0567
- Education 0350
- Hospital Management 0769
- Human Development 0758
- Immunology 0982
- Medicine and Surgery 0564
- Mental Health 0347
- Nursing 0569
- Nutrition 0570
- Obstetrics and Gynecology .. 0380
- Occupational Health and Therapy 0354
- Ophthalmology 0381
- Pathology 0571
- Pharmacology 0419
- Pharmacy 0572
- Physical Therapy 0382
- Public Health 0573
- Radiology 0574
- Recreation 0575
- Speech Pathology 0460
- Toxicology 0383

Home Economics 0386

PHYSICAL SCIENCES
Pure Sciences
Chemistry
- General 0485
- Agricultural 0749
- Analytical 0486
- Biochemistry 0487
- Inorganic 0488
- Nuclear 0738
- Organic 0490
- Pharmaceutical 0491
- Physical 0494
- Polymer 0495
- Radiation 0754

Mathematics 0405
Physics
- General 0605
- Acoustics 0986
- Astronomy and Astrophysics 0606
- Atmospheric Science 0608
- Atomic 0748
- Electronics and Electricity 0607
- Elementary Particles and High Energy 0798
- Fluid and Plasma 0759
- Molecular 0609
- Nuclear 0610
- Optics 0752
- Radiation 0756
- Solid State 0611

Statistics 0463

Applied Sciences
Applied Mechanics 0346
Computer Science 0984
Engineering
- General 0537
- Aerospace 0538
- Agricultural 0539
- Automotive 0540
- Biomedical 0541
- Chemical 0542
- Civil 0543
- Electronics and Electrical 0544
- Heat and Thermodynamics ... 0348
- Hydraulic 0545
- Industrial 0546
- Marine 0547
- Materials Science 0794
- Mechanical 0548
- Metallurgy 0743
- Mining 0551
- Nuclear 0552
- Packaging 0549
- Petroleum 0765
- Sanitary and Municipal 0554
- System Science 0790

Geotechnology 0428
Operations Research 0796
Plastics Technology 0795
Textile Technology 0994

PSYCHOLOGY
General 0621
Behavioral 0384
Clinical 0622
Developmental 0620
Experimental 0623
Industrial 0624
Personality 0625
Physiological 0989
Psychobiology 0349
Psychometrics 0632
Social 0451

STRUCTURAL AND DYNAMIC ASPECTS OF TROPHIC CORD MICROTUBULES IN RHODNIUS PROLIXUS

BY

RENE E. HARRISON

A Thesis submitted to the Faculty of Graduate Studies of the University of Manitoba in partial fulfillment of the requirements of the degree of

MASTER OF SCIENCE

I hereby declare that I am the sole author of this thesis.

I authorize the University of Manitoba to lend this thesis to other institutions or individuals for the purpose of scholarly research.

Rene Harrison

I further authorize the University of Manitoba to reproduce this thesis by photocopying or other means, in total or in part, at the request of other institutions or individuals for the purpose of scholarly research.

Rene Harrison

Abstract

The telotrophic ovariole of *Rhodnius prolixus* has one of the richest endowments of microtubules (MTs) yet described. An extensive array of MTs present in the trophic core and trophic cords links the nurse cell compartments to the growing oocytes. This system provides excellent material to study MT-based transport as the MTs are believed to play a role in transport of nurse cell-produced mitochondria, ribosomes and mRNAs to the oocytes. I investigated in this unidirectional transport system MT stability, polarity and molecular MT motors. Trophic cord MTs are stable, being highly resistant to depolymerisation by cold, colchicine and nocodozole. It is generally believed that MT stability is linked to posttranslational modifications of tubulin subunits and the presence of microtubule-associated proteins (MAPs). Using indirect immunocytochemistry and Western blotting, *Rhodnius* ovarioles were screened with antibodies against different tubulin isotypes and MAPs. The trophic cord MTs are rich in acetylated and tyrosinated α-tubulin but not detyrosinated α-tubulin. This is unique compared to other telotrophic ovarioles. Since, in *Rhodnius* only a few oocytes develop at any point in time (with earlier stages inhibited), MT stability may be especially important structurally and functionally in this highly regulated system.

The hook decoration procedure revealed that the MTs of the trophic core and

cords have their plus (+) ends in the tropharium and minus (-) ends in the oocytes. As this is similar to the single previous report of polarity in the insect *Notenecta glauca* (Stebbings and Hunt, 1983), a common polarity may exist in all telotrophic ovarioles. Presumably, the site of MT nucleation is in the oocytes and the growing or (+) ends extend towards the tropharium. The polarity suggests that a retrograde motor would be involved in MT-based transport to the oocytes. AVEC-DIC video microscopy showed that vesicle transport was saltatory, ATP-dependent, and had an average rate of 0.77 μm/sec. Movement was only towards the oocyte. Movement was inhibited by 2mM NEM (N-ethylmaleimide) and 50 μM vanadate ($NaVO_4$) but unaffected by 1 mM AMP-PNP (5'adenylylimidodiphosphate) and 5 μM vanadate. These results indicate that MTs are directly involved in nurse cell-oocyte transport involving a cytoplasmic dynein-like retrograde motor.

ACKNOWLEDGEMENTS

My Master's years has been a long and very rewarding journey and there are many people I would like to thank for both intellectual and emotional assistance. First I would like to acknowledge my parents, Eric and Jessie Harrison and my brothers Tobin and Derek for their lifetime support and encouragement which has continuously fueled me to be the best that I can be. I would also like to acknowledge a few of the many people who have touched my life during this period. These include: James Nickarz; (Constable) Leanne Zrum who kept me into trouble; Inendo Choudhury my late-night, always-dedicated colleague; Chris Waterhouse; my great "bud" Heather Simpson; my colleagues and "Bug Friends" Karen Yeow, Chris Bjornnson and Patrick Nelson; and all of the Zoology graduate students who made my time in the department a very entertaining one. Most importantly, I would like to thank my best friend Katrin ("Kat") Stedronsky who got me through all of my little "crises" smiling, and who made these last years some of the best in my life. I would like to thank my extremely helpful committee Dr. Ed Byard and Dr. Jeff Eales for all of their assistance and suggestions on my thesis. I would like like to acknowledge financial assistance from the following sources: NSERC research grant to E. Huebner; teaching assistantships and lecturer positions from the Department of Zoology and University of Manitoba Fellowship from Graduate Studies. And last, but far from least, I would like to thank Dr. Erwin Huebner for his incredible support in all aspects. Thank you Doc for being their when I needed you for my research and otherwise, and tolerating and occasionally enjoying my idiosyncrasies. You are a great inspiration as a teacher and a scientist and a friend.

Table of Contents

GENERAL INTRODUCTION: The Telotrophic Ovariole

The meroistic ovary of the hemipteran insect, *Rhodnius prolixus* serves as an ideal system for the study of microtubule (MT) structure and function. Each ovary contains seven telotrophic ovarioles that consist of an anterior trophic region of syncytial polyploid nurse cells attached around a central common trophic core via intracellular bridges. The trophic core extends posteriorly by cytoplasmic channels to a series of developing oocytes, with the most developed vitellogenic oocytes furthest away from the tropharium (for review see Huebner, 1984). The attenuated "nutritive" or "trophic" cords that extend to each oocyte up to mid-vitellogenic stage are filled with thirty to fifty thousand parallel and extremely stable MTs (Macgregor and Stebbings, 1970; Hyams and Stebbings, 1977; Huebner, 1981; Stebbings and van Bueren, 1981). This is believed to be one of the most extensive microtubular arrays in the animal kingdom (Brunt, 1970; Huebner and Anderson, 1970; MacGregor and Stebbings, 1970). These MTs are believed to participate in the movement of mitochondria and ribosomal and messenger RNA produced in the syncytium of nurse cells to each developing oocyte. Autoradiographic studies done on another hemipteran insect showed that most RNA synthesis occurred in the nurse cells, which was then seen to move to each developing oocyte (MacGregor and Stebbings, 1970). In the telotrophic ovarioles of *Dysdercus*

fasciatus, Dittmann and colleagues (1987) observed movement of mitochondria into the oocytes using AVEC-DIC (Allen video-enhanced contrast DIC) microscopy. Once mature midvitellogenic oocytes receive sufficient materials for future development, the cords are suddenly cut off and become redundant (Bennett and Stebbings, 1979; Hyams and Stebbings, 1979).

Originally it was proposed that these trophic cord MTs functioned only as a sieve, preventing the slippage of the larger nurse cell components into the trophic core and cords which could potentially block and stop any cytoplasmic flow into the oocytes (MacGregor and Stebbings, 1970). This belief arose from the fact that a popular and well understood function of MTs at the time was merely to provide a "skeletal" kind of support in cells. Trophic cord MTs would then indirectly form channels in the cell that directed and/or maintained cytoplasmic flow (Porter, 1966). However, recent evidence suggests MTs play a more active role in transport, and there are likely MT "motors" involved in this translocation system. A dynein-like motor was found in ovarioles of *Oncopeltus fasciatus* (Anastasi et al., 1990) and a motor likely exists and is responsible for trophic cord MT transport in *Rhodnius* ovarioles.

In one species examined, the trophic cord MTs were oriented with their "minus" or slow-growing ends extending in and dispersing throughout each oocyte, and their "plus" ends filling the trophic core (Stebbings and Hunt, 1983). Posttranslational modifications of tubulin, associated with stable subsets of MTs have also been examined in two hemipteran insects (Harrison et al., 1991).

My research aims to characterize the properties of the MTs of the trophic cords in *Rhodnius prolixus* ovarioles. Specifically the research focuses on: (1) determining the tubulin isotypes present in the cords and their functional implications; (2) determining the MT polarity; and, (3) determining if there is evidence for MT-based transport by an appropriate MT motor. To gain insight into the research problems, a variety of immunological, biochemical, microscopical and *in vitro* motility techniques were necessary. I utilized indirect immunocytochemisty and Western blotting to study tubulin isotypes, hook decoration procedures to establish MT polarity and AVEC-DIC video microscopy coupled with inhibitor studies to examine MT-based transport and motor involvement.

CHAPTER 1: Tubulin Posttranslational Modifications and MT Stability

INTRODUCTION

The discovery of the ubiquitous cytoskeletal component known as microtubules (Slautterback, 1963; Porter, 1966), and extensive research since has lead to a new understanding of cellular organization, compartmentalization and function. Besides acting as a structural component of cells, it is now known that MTs have significant and diverse functional roles in the cell: promoting chromosome movements during mitosis and meiosis (Inoué and Sato, 1967), the beating of cilia and flagella (Satir, 1968; Summers and Gibbons, 1971) and intracellular transport of membranous vesicles (Allen et al., 1985; Brady et al., 1985, Gilbert et al., 1985; Schnapp et al., 1985; Vale et al., 1985a,b). The cytoplasm of most eukaryotic cells is dynamic due to assembly and disassembly of MT arrays. MTs provide structural support to cells, most likely due to the limited bending of the MT fibre itself or to secondary interactions of the MT with other cytoskeletal elements (Dustin, 1984).

Microtubules are hollow circular arrays of usually 13 protofilaments arranged in a parallel fashion. Protofilaments are long polar structures (0.1-100 μm) resulting from the polymerization of inherently asymmetric tubulin heterodimers consisting of an α- and a β-tubulin subunit (Amos et al., 1976). Consequently

the two ends of the MT are structurally distinct and are called the "plus" or fast-growing end, and the "minus" or slow-growing end, reflecting their kinetic tendencies to add or lose tubulin subunits, respectively (Allen and Borisy, 1974). This "dynamic instability" of MTs may play a key role in cell shape and movement as they are seen to cause rapid formation and shrinkage of long filipodial extensions in *Reticulomyxa* and *Actinospherium* (Nauss, 1949; Tilney and Porter, 1967). It has also been proposed that the rapid assembly and disassembly of spindle MTs results in chromosomal migrations during mitosis (Cartier, 1988). On the other hand, ciliary and flagellar movement, and "saltatory" organelle transport often involves relatively stable microtubular arrays (Greer and Rosenbaum, 1989).

Within the cell, MT organization and function are controlled at a number of levels including the control of MT nucleation, MT dynamics and stability and the association between MTs and various accessory proteins (Olmsted, 1986). Because MTs play roles in many cellular activities, specific mechanisms have been proposed for regulating and controlling these functions. The diversity of MTs both structurally and functionally may be due to heterogenous α- and β-tubulin polypeptide composition and/or the binding of different MAPs (Cleveland and Sullivan, 1985). Tubulin belongs to a multigene family and most MTs are formed from a mixture of these tubulins (Sullivan, 1988). In higher vertebrates, sequencing of tubulin genes has shown the presence of about 6 α- and 6 β-tubulin isotypes (Sullivan, 1988). For instance, neurite extension in embryonic

rats correlates with high expression levels of a new α-tubulin mRNA whose protein may differ enough to allow for MT modifications (Miller et al., 1987). Posttranslational modifications of tubulin subunits may also modulate MT function *in vivo*. Although most isotypes of tubulin appear to be randomly dispersed in MTs, one finds MTs with different characteristics in the cell.

Two subpopulations of MTs often exist within the same cell based on differences in stability. These are classified as dynamic or stable depending on the rate that tubulin dimers are added or subtracted (Schulze and Kirschner, 1987). Dynamic MTs are usually disassembled by several MT-disrupting agents including cold, calcium or drugs such as colchicine, while a small fraction of drug-insensitive and cold-stable MTs are occasionally observed (Bulinski and Gundersen, 1991). Stable MTs are necessary in highly polarized structures such as axons, which can extend great distances from the cell body and contain MTs which persist for months (Sahenk and Brady, 1987). These stable MTs are involved in maintaining the elongated morphology and in axonal transport (Brady et al., 1984) and may also act as nucleating sites when MT assembly occurs within the axon (Sahenk and Brady, 1987).

The basis for MT stability is not fully understood but these subpopulations of MTs have been identified as containing predominantly specific posttranslational modifications of tubulin. Tubulin can be cyclically detyrosinated (Hallak et al., 1977; Gundersen et al., 1984; Gundersen and Bulinski, 1986; Wehland and Weber, 1987) and tyrosinated (Barra et al., 1973) as well as acetylated

(Piperno et al., 1987; Sasse et al., 1987; Diggins and Dove, 1987) and deacetylated (L'Hernault and Rosenbaum, 1983; 1985). It is believed that these modifications are related to the assembly-disassembly of these MTs (Greer and Rosenbaum, 1989; Bulinski and Gundersen, 1991). The study of the various tubulin isoforms has been greatly enhanced by the development of monospecific antibodies against tyrosinated, detyrosinated and acetylated α-tubulin and allowed examination of stable MT involvement in cell differentiation and specialization.

Acetylation of tubulin has been shown to occur preferentially on preformed MTs, rather than on free tubulin dimers (Maruta et al., 1986). Acetylation/deacetylation occurs at the ε(epsilon)-lysine 40 amino group of α-tubulin (Piperno et al., 1987). Consequently lysine residues of α-tubulin are acetylated after MT assembly and deacetylated after MT disassembly (Maruta et al., 1986). The site of acetylation then must be accessible on the surface of MTs. Since there is a preference of the tubulin acetyltransferase (acetylase) for polymerized over soluble α-tubulin as a substrate it is often correlated with stable MTs (Schulze et al., 1987). Therefore, where the enzyme is present, stabilized MTs such as those found in mitotic midbodies, ciliary axonemes or neuronal processes can be expected to contain significant amounts of acetylated α-tubulin (Acet-tubulin) (Thompson et al., 1984; Piperno et al., 1987). Work by Wolf and co-workers (1988) on *Drosophila* and Chu and Klymkowsky (1989) on *Xenopus* show that the extent and pattern of acetylated MTs change

during early development. Acetylation of MTs occurs during development of mouse oocytes and embryos (Schatten et al., 1988; Houliston and Maro, 1989) and has also been observed in *Physarum* (Sasse et al., 1987). Other MT subsets are particularly enriched in this modified tubulin include the subpellicular MT array of *Trypanosoma* (Schneider et al., 1987) and the basal bodies of *Chlamydomonas* (LeDizet and Piperno, 1986). In all organisms studied, the primary cilia and centrioles almost invariably were enriched with acetylated α-tubulin (Thompson et al., 1984; Piperno et al., 1987).

In a similar fashion, a tubulin-specific carboxypeptidase removes the C (carboxy)-terminal tyrosine after MT assembly exposing a glutamic acid at the C-terminus of α-tubulin, while tubulin tyrosine ligase rapidly adds back tyrosine to the same end after MT disassembly (Arce et al., 1978). Tyrosinated α-tubulin (Tyr-tubulin) is enriched within newly assembled and dynamic MTs (Gundersen et al., 1989). Since detyrosinated α-tubulin (Glu-tubulin) is found only in intact MTs this suggests that older, more stable MTs will more likely become substrates for the carboxypeptidase than those which are newer or more dynamic. Detyrosination is also believed to be involved in the long term stabilization of differentiated MTs as the proportion of Glu-tubulin often increases during differentiation (Gundersen et al., 1989). In fibroblasts and epithelial cells, most Glu MTs appear after 20 minutes of polymerization and persist for at least one hour, sometimes longer (Webster et al., 1987) as opposed to the majority of cellular MTs (Tyr MTs) whose half-life is 5-10

minutes (Schulze and Kirschner, 1986).

A variety of mammalian cells and other vertebrates are rich in Glu-tubulin and posttranslational loss and addition of the carboxy-terminal tyrosine seems to be a widespread feature of tubulin metabolism. Existence of both Tyr and Glu MTs has been observed in *Trypanosoma* (Sherwin et al., 1987), *Caenorhabditis* (Gabeus et al., 1983) and *Xenopus* (Preston et al., 1981). Like acetylation, detyrosination of MTs is also usually localized in stable, highly organized MT arrays such as the centrioles, basal bodies, the neuronal MT network of vertebrates and the cilia and flagella of motile cells (LeDizet and Piperno, 1986; Schulze et al., 1987; Webster et al., 1987; Piperno et al., 1987). These MT subsets are most often colchicine-resistant, show a longer half-life and are more resistant to cold-induced depolymerization than the majority of cytoplasmic MTs (Bre et al., 1987; Piperno et al., 1987; Schulze et al., 1987).

Other modifications include phosphorylation of both α- and β-tubulin polypeptides at various sites (Serrano et al., 1987) and the glutamylation of α-tubulin, which involves the addition of glutamyl units to a carboxy-terminal glutamic acid residue of α-tubulin (Eddé et al., 1990).

Although the exact functions of tubulin posttranslational modifications have not been conclusively determined, it has been proposed that the modifications directly affect the assembly properties of the MTs affecting the stability directly or modulating the binding of MAPs (Greer and Rosenbaum, 1989). On the other hand, they may indirectly play a role in differentiating the MTs for specific

functions following polymerization and stabilization via MAPs (Schulze et al., 1987). Consequently the accumulation of tubulin modifications within MT subsets may be a useful marker for MT age (Greer and Rosenbaum, 1989).

MAPs usually comprise approximately 20% of isolated MT proteins. There are several MT-associated proteins which co-purify with brain tubulin during repetitive cycles of temperature-dependent assembly and disassembly. High molecular weight (HMW) proteins (MAP1A, MAP1B and MAP2) and *tau* are the major species in neuronal tissue (Olmsted, 1986). The HMW MAPs are flexible, rod-like structures about 100-200 nm long and are components of crossbridges associated with MTs *in vivo* (Hirokawa et al., 1985). *Tau*, however is a rod-like molecule about 50 nm long, and forms short crossbridges, less than 20 nm long, between MTs *in vitro* (Hirokawa et al., 1988). It is not known whether only one, or several MAPs are involved in increasing stability to anti-MT agents and cold depolymerization.

A successful approach to understanding the role of tubulin isotypes is to study them in developmentally important systems such as the telotrophic ovariole. Within the adult ovariole, early trophic cord MTs can be compared to more mature or redundant cord MTs. Trophic cords supply oocytes at various stages of development so MT modification, cytoplasmic movement and oocyte differentiation are ongoing and highly regulated. The trophic cord MTs of *Rhodnius prolixus* ovarioles are very stable as they are highly resistant to depolymerisation by colchicine, nocodazole and cold treatments (Huebner,

unpublished results) but form MT crystals in the presence of vinblastine sulphate (Huebner and Anderson, 1970).

In two other species with telotrophic ovaries, the presence and distribution of posttranslational modifications of tubulin were examined by Harrison and colleagues (1991). They found that *Notonecta glauca* cord MTs stained strongly and uniformly for detyrosinated and acetylated MTs while tyrosinated tubulin was localized in the periphery of the trophic cords. Another species, *Oncopeltus fasciatus*, had cords which stained intensely throughout for tyrosinated tubulin but only very weakly for acetylated and detyrosinated-tubulin (Harrison et al., 1991). Because *Rhodnius* ovarioles exhibit unique feedback and regulation of oocyte growth in telotrophic ovarioles studied, it provides a good system to examine the relationship of oogenesis dynamics and MT posttranslational modifications and stability. I examined the presence and distribution of these isotypes in *Rhodnius* ovarioles. This was done by screening sections and permeabilized whole ovarioles with antibodies to tyrosinated, detyrosinated and acetylated α-tubulin using indirect immunocytochemistry as well as immunoblotting of SDS gels of whole ovariole homogenates. I also screened ovariole sections immunocytochemically for MAP 1, MAP 2 and *tau.* I found that all cords stained intensely and uniformly with tyrosinated and acetylated α-tubulin specific antibodies both with indirect immunocytochemistry and with Western blotting. Detyrosinated α-tubulin staining was absent or very weak in some cords and not observed at all by

Western blotting. MAP 1 and 2 were not seen in the cords. However it appeared that *tau* was prominent in a redundant cord. The presence and distribution of tubulin isotypes has many interesting correlations between the known stability of the MTs contained within the cords and the role of posttranslational modifications in this system.

MATERIALS AND METHODS

Animal Rearing Techniques

A colony of *Rhodnius prolixus* was maintained at high humidity and 27°C in a controlled environment chamber (Huebner and Anderson, 1972). The colony was fed using both artificial feeding (Huebner et al., 1995) and on female New Zealand white rabbits. Ovaries were dissected from mated adult females three to four days post-feed and placed in O'Donnell's *Rhodnius* Ringers solution (129 mM NaCl, 8.6 mM KCl, 2 mM $CaCl_2 \cdot 2H_2O$, 8.5 mM $MgCl_2 \cdot 6H_2O$, 34 mM dextrose and 15 mM Bis-Tris (pH 6.9)). Ovarioles containing trophic cords connected to oocytes spanning a range of developmental stages were examined.

Indirect Immunofluorescence (DGD sections)

The method used for DGD (diethylene glycol disterate)-ovariole section immunostaining followed protocols of Valdimarsson and Huebner (1989). The ovarioles were desheathed in calcium-free *Rhodnius* Ringers and fixed for 30 minutes in 3% paraformaldehyde and 0.5% gluteraldehyde in PHEM buffer (60 mM PIPES, 25 mM HEPES, 10 mM EGTA and 2 mM $MgCl_2$ (pH 6.9)) with 1 mM GTP added. The tissue was then washed in PHEM and dehydrated

through an ascending series of ethanol. DGD embedding followed procedures of Capco et al. (1984) and Capco and McGaughey (1986). Following two changes of absolute ethanol the tissue was taken through an ascending series of 1-butanol followed by an ascending series of molten DGD (diethylene glycol distearate) to which 0.5% DMSO was added. Following an overnight infiltration the samples were embedded in DGD with 0.5% DMSO in Micromolds™ and allowed to solidify at room temperature.

Semi-thin sections (2 µm) were cut with glass knives (4° angle) on a Sorval Porter Blum MT2-B Ultramicrotome and floated onto Poly-L-lysine coated coverslips (MW 70,000-150,000, Sigma Chem. Co.). The sections were then dried and adhered to the coverslips at 55°C and covered with pure glycerol until immunostaining.

DGD was removed from the sections using 3 changes of 1-butanol (1 hour each) and taken through an ascending series of ethanol to remove the butanol. The sections were then rehydrated in 3-minute changes of 95%, 70% (plus 1 mg/ml $NaBH_4$ for 10 minutes to reduce background fluorescence), 70% and 50% ethanol followed by 3 minutes in phosphate buffered saline (PBS) (8g NaCl, 0.2 g KCl, 0.2 g KH_2PO_4, 1.15g Na_2HPO_4 per litre, pH 7.3). The sections were then blocked with PBS plus 1% BSA (bovine serum albumin, type V, Sigma Chem. Co.) at 37°C for 1 hour in a humid, light-tight chamber. The blocking agent was drained off and the primary antibodies, at appropriate dilution in PBS-BSA buffer, were added and sections incubated at 37°C for 1 to

2 hours.

Primary antibodies included the monoclonals TAT-1 which recognized α-tubulin and C3B9 which recognized the acetylated α-tubulin isoform (both supplied by Dr. Keith Gull) diluted 1:5. All antibodies were diluted in PBS-BSA solutions. Dr. Wehland provided the monoclonal ID5 antibody which recognized the detyrosinated α-tubulin isoform. This was diluted 1:10. A polyclonal anti-detyrosinated antibody, obtained from Dr. T. MacCrae (anti-E) was also screened and was diluted 1:500. A monoclonal anti-tyrosinated α-tubulin antibody (Sigma, clone TUB-1A2) was diluted 1:800. The following monoclonal antibodies to MAPs were also screened: anti-MAP 1 (Sigma, clone HM-1, diluted 1:500), anti-MAP 2 (Sigma, clone HM-2, diluted 1:500) and anti-*tau* (Sigma, clone tau 2, diluted 1:1000). Following incubation, the sections were washed three times for 5-minute intervals in PBS-BSA at room temperature prior to exposure to the appropriate 2° antibody for 1 hour at 37°C. For the monoclonal antibodies a fluorescein-labelled goat anti-mouse 2° antibody (Sigma F0257) was used and diluted 1:64 in PBS-BSA buffer. For the polyclonal primary antibody a fluorescein-labelled goat anti-rabbit 2° antibody was used (Sigma F9887) and was diluted 1:64. Control slides were treated identically with the exception that they were not exposed to a 1° antibody.

Coverslips were then washed thoroughly with PBS and mounted on glass slides using PVA mounting media (20 g PVA (type II, Sigma Chem Co.) in 5 ml 1M Tris-Cl (pH 9.0), 75 ml ddH2O and 10 ml glycerol) plus 1-2 g/L

paraphenylenediamine to reduce photobleaching. The sections were examined using a Zeiss Photomicroscope II equipped for epifluorescence.

Whole Ovariole Immunostaining

Ovarioles were desheathed in Ringers and treated with 0.15% Elastase Type IV (Sigma) in Ringers for 5 minutes to remove basement membranes. Ovarioles were microdissected using tungsten wire needles to remove follicle cells and isolate trophic cords. Membranes were briefly exposed to 0.2% Triton X-100 in Ringers for 5 minutes. The tissue was then fixed in 3.7% paraformaldehyde in PHEM buffer at 4°C for 1 hour. The ovarioles were washed three times in PBS and blocked with PBS plus 0.5% BSA and 0.2% Triton X-100 for 1 hour at 37°C. The ovarioles were exposed to the above primary antibodies (C3B9 and TAT-1) at the same dilutions in the same buffer as DGD-sections at 37°C overnight. The ovarioles were washed for 3 hours before exposure to the appropriate 2° antibody at the same temperature. The ovarioles were then washed for 2 hours to remove any unbound label before examination using epifluorescence.

Electrophoretic Transfer Methods

SDS-PAGE was performed on twice-cycled porcine tubulin (see purification in Chapter 2) and whole ovariole homogenates by the method of Laemmli (1970). Ovariole homogenates were prepared by homogenizing ovarioles from

approximately 50 adult female insects in 100 mM PIPES (pH 6.9) containing 1 mM $MgSO_4$, 0.5 mM $CaCl_2$ and protease inhibitors (2 mM phenylmethyl-sulfonyl fluoride (PMSF), 1 mM dithiothrietol (DTT), 1000 µg/ml soybean trypsin inhibitor, 1 µg/ml leupeptin, 1 µg/ml pepstatin and 10 µg/ml aprotinin). The protein concentration was determined using a Bradford assay (Biorad). Between 5 and 20 µg total protein was used for each loading. MW markers were also run to determine size of the proteins (Sigma P1677, MW 30-120 kDa). Samples were mixed with equal volumes of 2x Laemmli buffer (125 mM Tris-Cl (pH 6.8, 4% w/v SDS, 20% v/v glycerol, 10% v/v 2-mercaptoethanol and 0.002% w/v bromophenol blue) which was boiled for 2 minutes prior to loading.

SDS-PAGE was performed according to the method of Laemmli (1970) with a Protean II Cell (Biorad) and LKB Bromma 2197 power supply. The separating gel contained 10% w/v acrylamide and 2.7% w/w N,N'-methylene-bis-acrylamide (10%T, 2.7%C), 375 mM Tris-Cl (pH 8.8) and 0.1% SDS. The gel was degassed, and prior to pouring 0.005% w/v ammonium persulfate and 0.03% v/v N,N,N',N' tetramethylthylenediamine (TEMED) was added for polymerization. The stacking gel was prepared identically using 5% acrylamide (5%T, 2.7%C), 0.05% w/v ammonium persulfate and 0.05% v/v TEMED. The upper and lower tank buffers contained 25 mM Tris-Cl (pH 8.3), 192 mM glycine and 0.1% w/v SDS. Gels were run at 10°C at 20 mAmperes for approximately 3 hours until the tracking dye reached approximately 1 cm from the bottom of the gel.

Western Blotting

Following electrophoresis the gel was removed and rinsed in transfer buffer (25 mM Tris (pH 8.3), 192 mM glycine, 20 % v/v methanol). A vertical slice was removed and stained with 0.1% Coomassie blue in destain solution (50% methanol and 10% acetic acid) for 4 hours then destained for 1 hour to analyze electrophoretic performance. The nitrocellulose (NC) paper and filter papers were wet by capillary action with transfer buffer and overlayed on the gel. The gel was placed in a gel holder which was inserted into a Bio-Rad Trans-blot cell containing transfer buffer and 0.1% w/v SDS maintained at 4°C. The transfer was carried out at 70V for 2 hours using a Bio-Rad Model 250/2.5 power supply. Following transfer, the gel was stained with Coomassie blue and a vertical strip of NC was stained with 0.1% Amido black in 25% propanol, 10% acetic acid to determine the efficiency of the transfer.

Immunodetection was performed on NC strips in heat-sealed baggies on an orbit shaker platform. NC blots were quenched in 1% BSA/TBST solution (50 mM Tris-Cl (pH 7.4), 150 mM NaCl and 0.05% v/v polyoxyethelene-sorbitan monolaurate (Tween-20)) for 1 hour at 40°C to block non-specific binding sites. The rest of the procedure was performed at room temperature. The strips were washed twice with TBST then incubated for 2 hours in the appropriate 1° antibody in BSA-TBST solution The NC blots were screened with same monoclonal antibodies used in indirect immunocytochemisty at the same dilutions (TAT-1 (anti-α-tubulin), C3B9 (anti-ACET-tubulin), ID5 (anti-GLU-

tubulin) and clone TUB-1A2 (anti-TYR-tub). The NC strips were washed four times (20 minutes each) in BSA-TBST and then incubated for 2 hours in alkaline-phosphatase-conjugated 2° antibody (Promega), diluted 1:7500 in BSA-TBST. The strips were then washed 2 times in TBS to remove any residual Tween-20.

The substrate reaction was carried out in 33 mg/ml nitro blue tetrazolium (NBT) and 0.165 mg/ml of 5-bromo-4-chloro-3-indolyl phosphate (BCIP) in alkaline phosphatase buffer (AP) (100 mM Tris-cl (pH 9.3), 100 mM NaCl, 0.5 mM $MgCl_2$) for 30 minutes. The reaction was stopped by dipping the NC strips in dd$H_2$0.

Photography

Immunofluorescent images were photographed using Kodak T-max 400 and developed using Kodak T-max Developer (Kodak, Inc.) according to manufacturer's instructions. Digitized images stored using Image 1 (Universal Imaging, Inc.) were recorded on Kodak Tmax 100 film using a Polaroid freeze frame. NC sheets were photographed using Kodak T-max 100 and developed as above. Negatives were printed on Ilford Polycontrast rapid paper.

RESULTS

Immunocytochemistry and Western Blotting

Indirect immunocytochemistry on DGD sections of fixed tissue and fixed whole ovarioles proved to be a useful tool for determining the presence and distribution of tubulin isotypes and MAPs in the trophic cords of *Rhodnius.* Controls were run in which the primary antibody was omitted (Fig. 2) to measure background fluorescence and verify the reliability of the technique. As well, a general antibody to α-tubulin was used as a control to assess overall MT distribution within the ovariole to compare with distributions observed for more specific antibodies (Figs. 3-5). Western blotting was utilized to confirm the specificity of the tubulin antibodies and for high sensitivity screening of whole ovariole homogenates for these tubulin isotypes.

Tyrosinated α-tubulin

Microtubules in the ovariole stained uniformly and intensely for tyrosinated tubulin using the monoclonal anti-tyrosinated α-tubulin antibody (TUB-1A2) (Figs. 6-11). The staining distribution within the entire ovariole including follicle cells, nurse cells and oocytes was very similar to that seen using the general α-tubulin antibody, TAT-1 (Figs. 3-5). The MTs within the trophic core (Fig. 6) and trophic cords (Figs. 7-11) stained quite strongly for this antibody confirming the presence of this unmodified tubulin within this MT array. The cords were not

always as distinct due to the general staining of the MTs within the surrounding tissue (Figs. 10 and 11). The specificity of the antibody to tubulin was confirmed on the Western blots as label was detected at a band which co-migrated with a labelled porcine brain tubulin band at a MW of approximately 50 kilodaltons (kD) (Fig. 35; lane 2 and 3). Porcine brain tubulin is of approximately this size and is known to contain small amounts of acetylated tubulin and a greater amount of tyrosinated and detyrosinated α-tubulin in similar amounts (Cambray-Deakin and Burgoyne, 1987). A similar sized band was found when the ovariole homogenate was screened for the general α-tubulin antibody (Fig. 35; lane 1).

Detyrosinated α-tubulin

Detyrosinated α-tubulin staining using the monoclonal ID5 was extremely weak and only seen in some of the larger cords (Figs. 14-16). The trophic core and most trophic cords did not show any detectable staining (Figs. 12-13). Very faint staining was seen in the oocytes (Figs. 14-16). Immunocytochemistry using the polyclonal obtained from Macrae showed no staining either in the cords or within the oocytes (Figs. 18-19). No staining was observed in ovariole homogenates using Western blotting with ID5 as compared to the band observed for porcine tubulin (Fig. 35; lane 4 and 5).

Acetylated α-tubulin

All trophic cord MTs examined stained intensely for acetylated α-tubulin using the monoclonal C3B9 antibody (Figs. 22-31). Qualitatively, the intensity of fluorescence within the cords paralleled that of total α-tubulin seen using TAT-1 monoclonal antibody also obtained from Dr. Keith Gull (Figs. 3-5). In some sections there appeared to be more intense staining towards the periphery of the cords but this was not consistent in all cords examined (Figs. 29-30).

MTs within the trophic core also stained with the anti-acetylated antibody as well as MTs extending into the apex of the oocyte (Figs. 20-21; 24-28). However, tissue elsewhere in the ovariole including follicle cells and the majority of the oocytes did not stain substantially with this antibody (Figs. 20-30). Whole ovariole immunostaining showed consistent results as intense fluorescence was restricted to the trophic core, trophic cords and the apex of the oocytes (Figs. 22 and 31).

Western blot analysis verified the specificity of this antibody as well as the presence of this tubulin isoform, as staining was observed intensely at a tubulin-sized band. The band co-migrated with the purified, twice cycled porcine tubulin (Fig. 35; lane 6 and 7).

Structural MAPs

Indirect immunocytochemical analysis of MAP presence and distribution showed no detection with anti-MAP1 and anti-MAP2 antibodies (Figs. 32-33).

The absence of staining was similar to control staining (Fig. 2) indicating a negative result. However, staining was observed using the anti-*tau* antibody in several sections through a particular cord (Fig. 34). This cord is believed to be a redundant cord.

FIGURE ABBREVIATIONS

C = Trophic Core

NC = Nurse Cells

O = Oocyte

T = Trophic Cord

TR = Tropharium

PLATE 1

Overview of MT Distribution in Adult Ovariole

and Immunofluorescent Controls

Figure 1. Summary illustration of the adult *Rhodnius* telotrophic ovariole (based on Huebner, 1984).

Figure 2. DGD immunofluorescence control. Arrows indicated trophic cord regions. Note faint autofluorescence and non-specific fluorescence when primary antibody is omitted during procedure. x200.

Figure 3-4. Immunofluorescence micrographs, longitudinal sections, with general anti-α-tubulin antibody (TAT-1) showing overall MT staining and large MT-rich trophic cords and core. x700, x150.

Figure 5. Immunofluorescent micrograph, cross-section, using TAT-1 antibody showing MT dense trophic cords at various stages. The inset shows an intensity profile of the same image. x800.

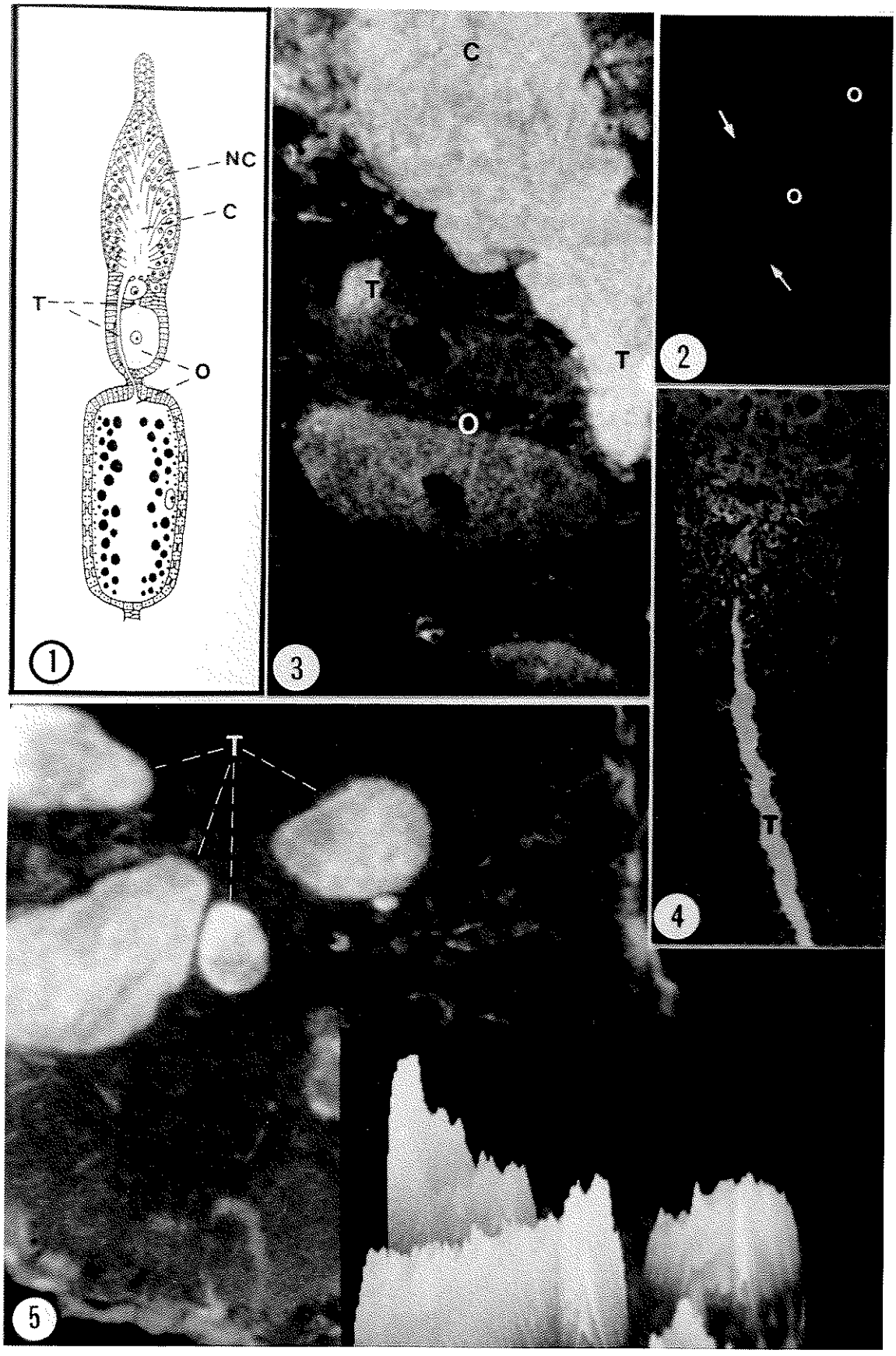
NC
C
T
O
C
T
O
T
O
T
T
1
2
3
4
5

PLATE 2

Tyrosinated α-tubulin Distribution

Figures 6-8. Immunofluorescence micrographs of longitudinal sections of DGD-embedded ovarioles illustrating the staining pattern with an anti-tyrosinated tubulin antibody (Sigma, clone TUB-1A2). Note that most tissue in the ovariole stains fluorescently with this antibody. The trophic core stains intensely as do the trophic cords. x700, x500, x550.

Figures 9-11. Immunofluorescence micrographs, cross-section with anti-Tyr antibody showing strong staining in trophic core and trophic cords (arrows) of various stages. x400, x500, x600.

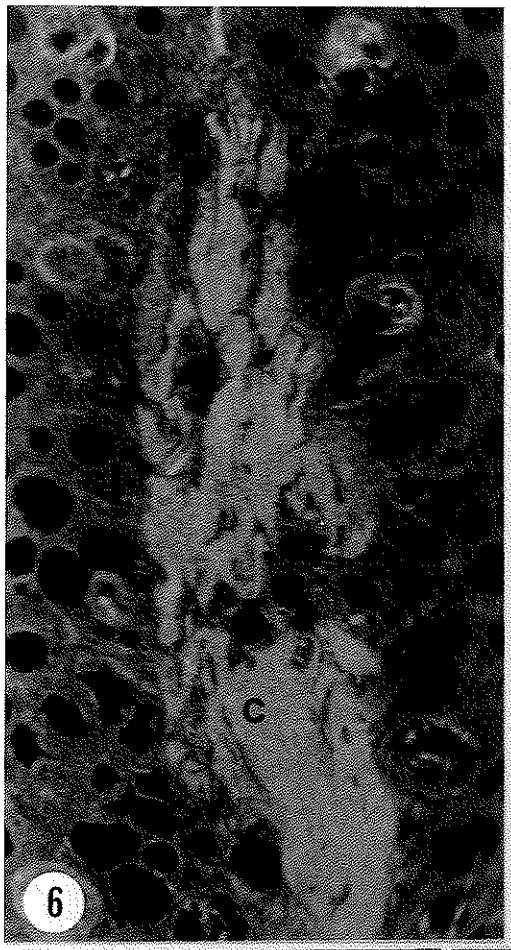
C
6

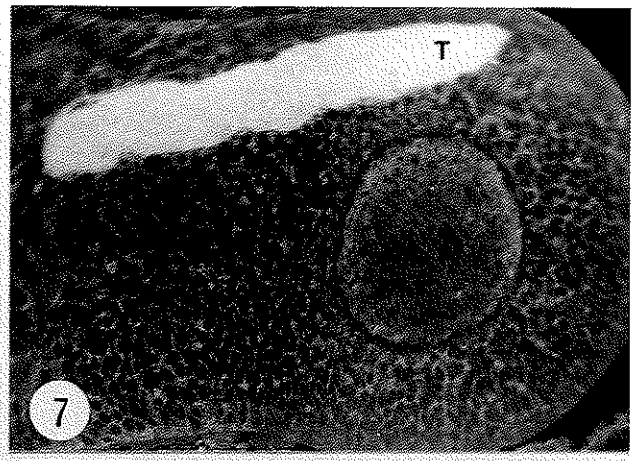
T
7

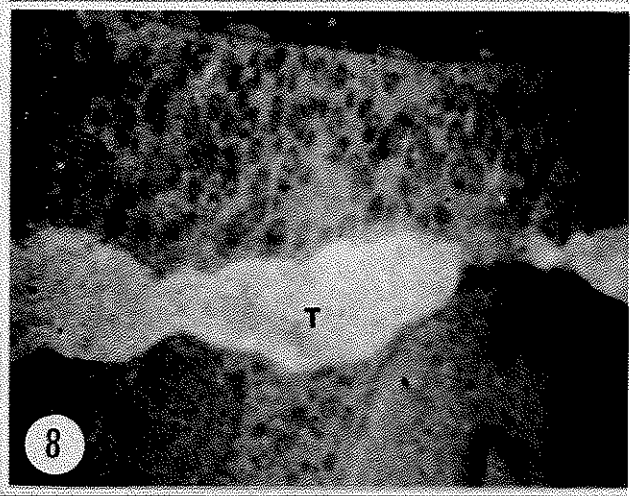
T
8

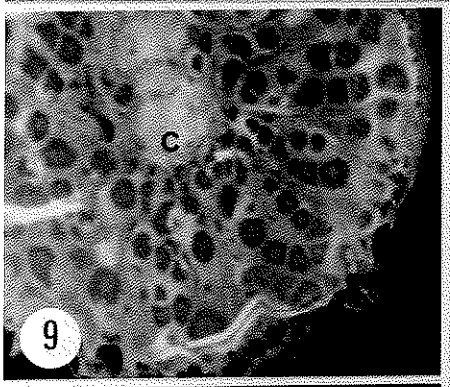
C
9

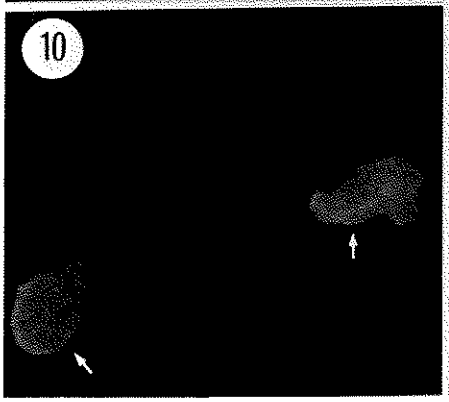
10

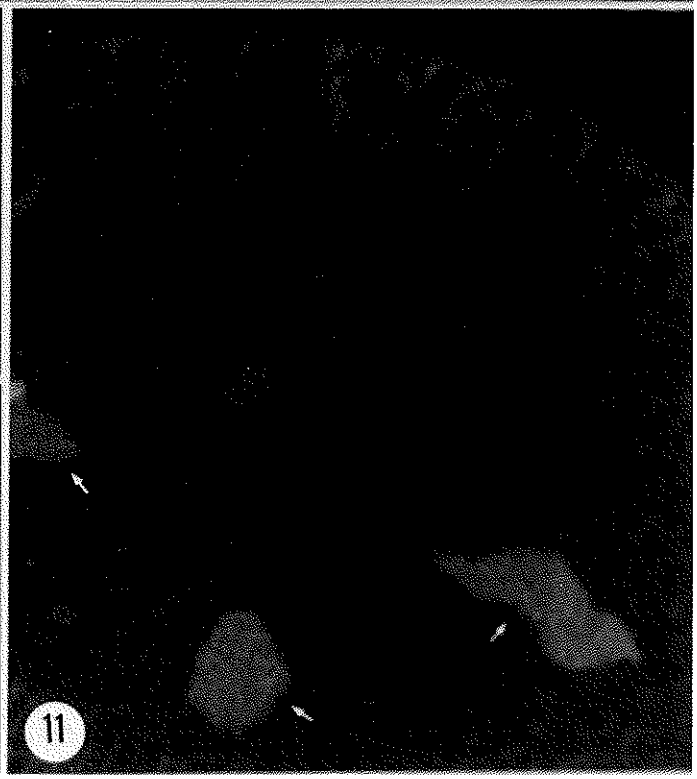
11

PLATE 3

Detyrosinated α-tubulin Distribution

Figures 12-13. Immunofluorescence micrographs, longitudinal sections, using monoclonal ID5 anti-detyrosinated tubulin antibody, showing negative results in the trophic core and trophic cord (arrow). x300, x650.

Figures 14-16. Immunofluorescence micrographs, longitudinal section, using the same anti-Glu tubulin antibody showing positive staining in the oocytes and a larger, older trophic cord (arrows). x350, x250, x150.

Figure 17. Immunofluorescence micrograph, cross-section showing no staining of ID5 antibody through a trophic cord (arrows). x650.

Figures 18-19. Immunofluorescence micrographs, longitudinal and cross-section showing negative results in the trophic cords (arrows) following staining with a polyclonal anti-Glu tubulin antibody (anti-E). x600, x500.

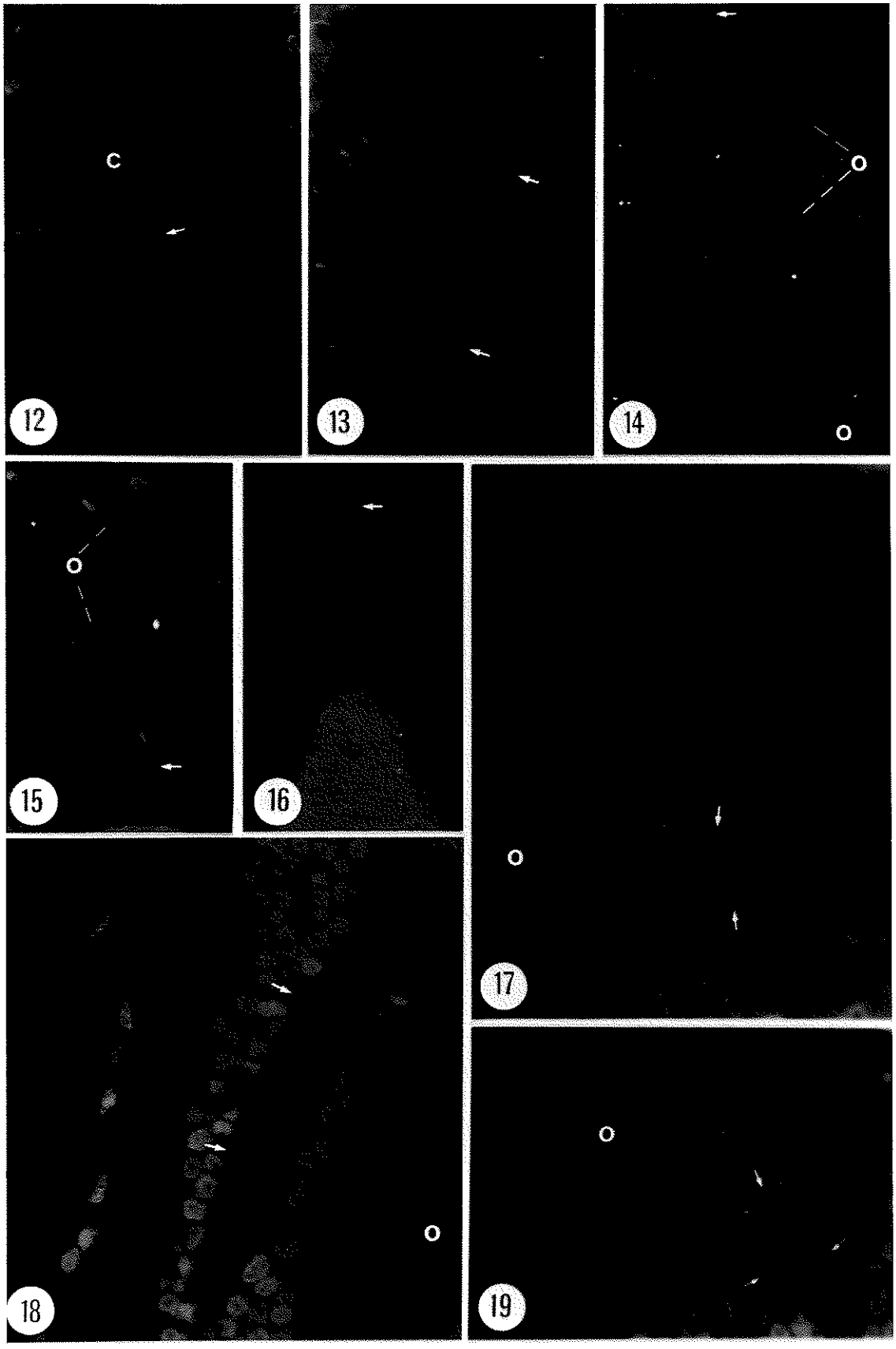
12
13
14
15
16
17
18
19

PLATE 4

Acetylated α-tubulin Distribution

Figures 20-21. Immunofluorescence micrographs through the trophic core, longitudinal and cross-section showing intense staining for the anti-acetylated tubulin antibody, C3B9. x650, x700.

Figure 22. Micrograph of whole ovariole immunostaining with C3B9 antibody showing intense staining in trophic cords from trophic core region into the apex of the oocytes. x500.

Figure 23. This immunofluorescence micrograph shows bright staining of three trophic cords in cross-section profile and the grazing view of an oocyte apex. x1000.

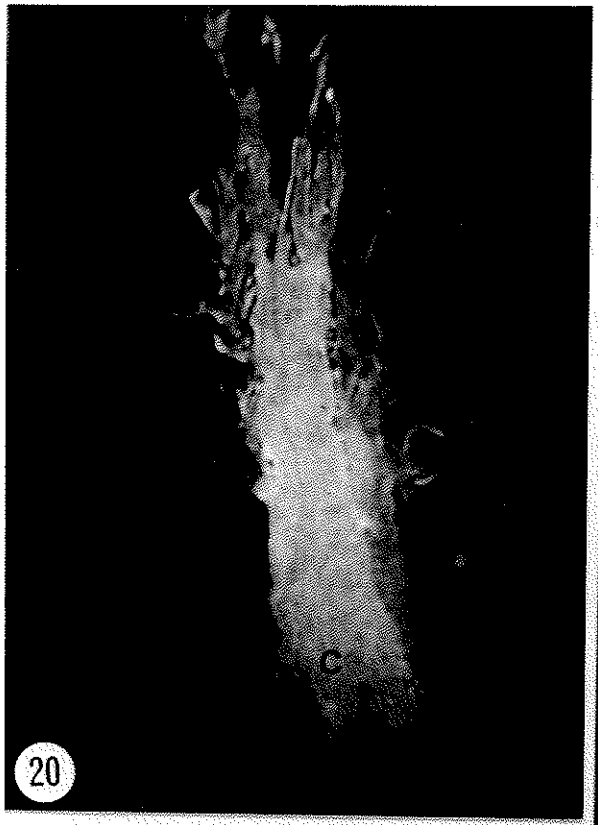
C
20

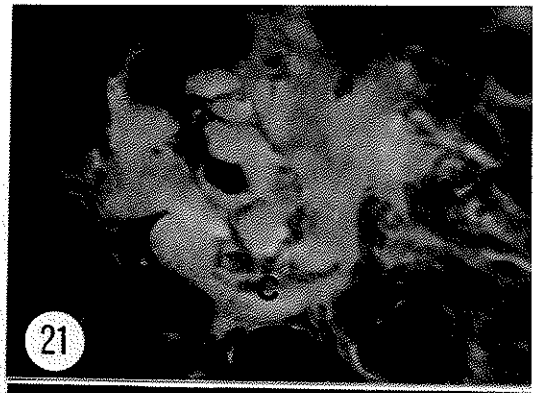
C
21

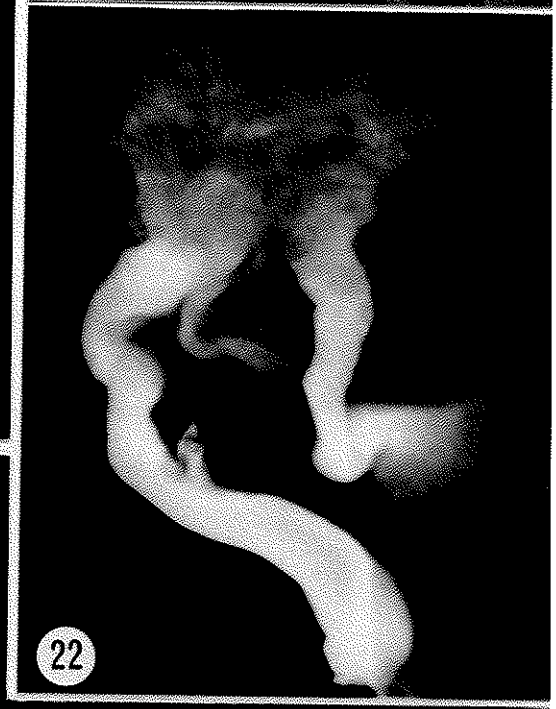
22

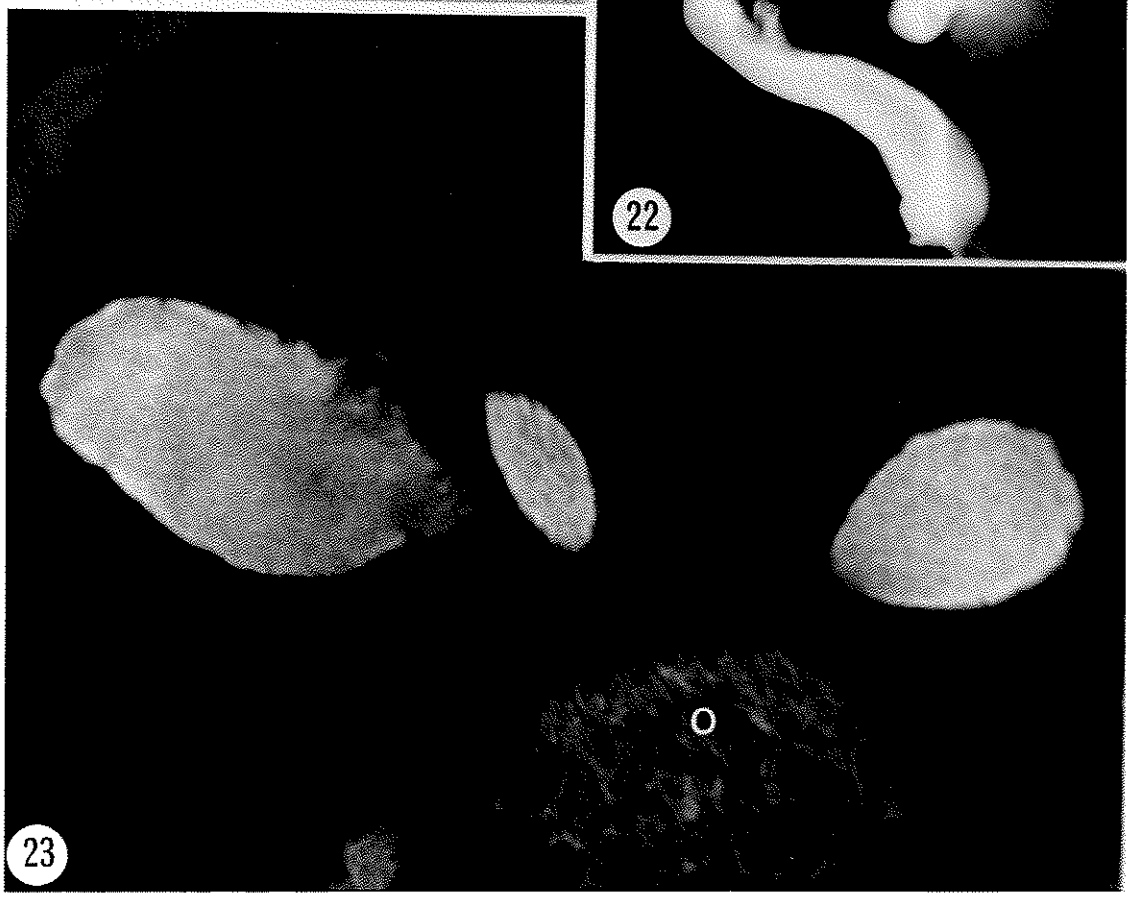
O
23

PLATE 5

Acetylated α-tubulin Distribution

Figures 24-27.These immunofluorescence micrographs show positive staining of the trophic cords at various stages in longitudinal (Figs. 24,26) and cross-section (Figs. 25,27). The apex of the oocytes also stain with the anti-acetylated α-tubulin antibody. Note the minimal staining within the centre of the oocytes. x600, x400, x300, x400.

Figure 28. The intense staining of MTs in the trophic cords and oocyte apex is seen in this micrograph and intensity profile. x450.

Figures 29-30.A fluorescently stained trophic cord with an intensity line scan shows the intense staining and its distribution across a trophic cord in cross-section. This cord is shown in an intensity profile in Figure 30. Note the stronger fluorescent signal around the periphery of the cord. x800.

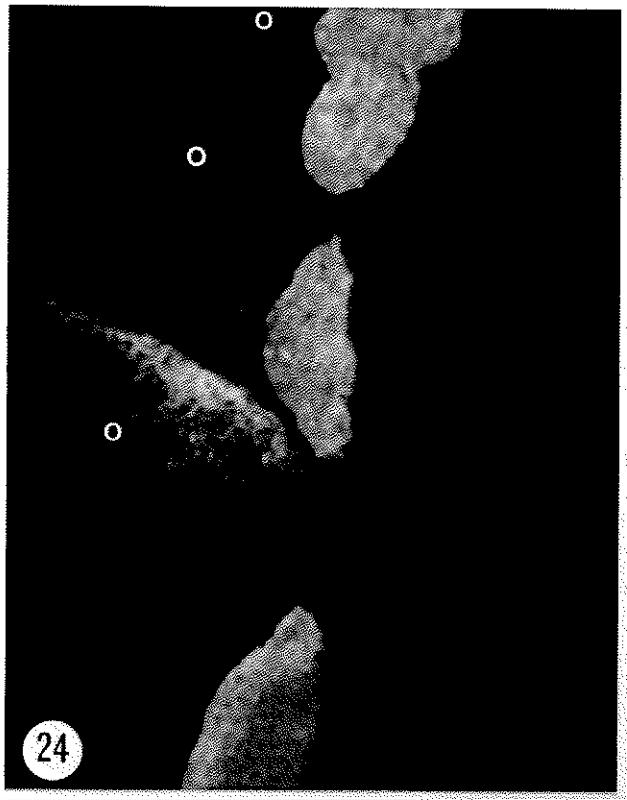

24

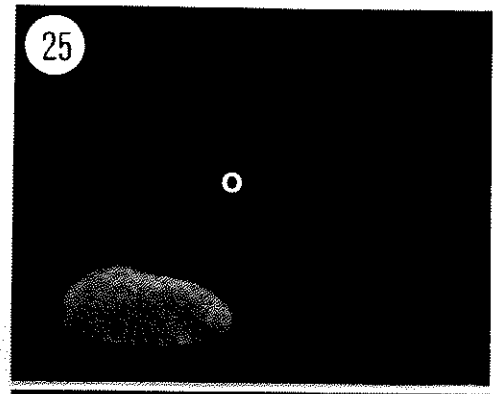

25

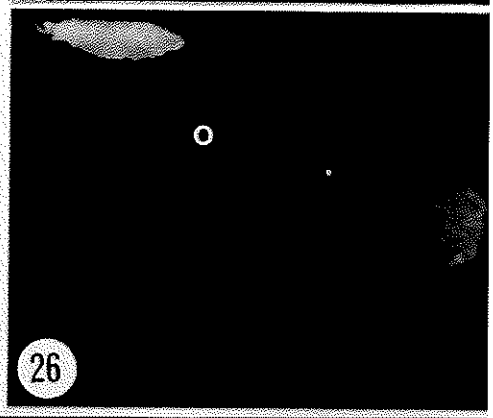

26

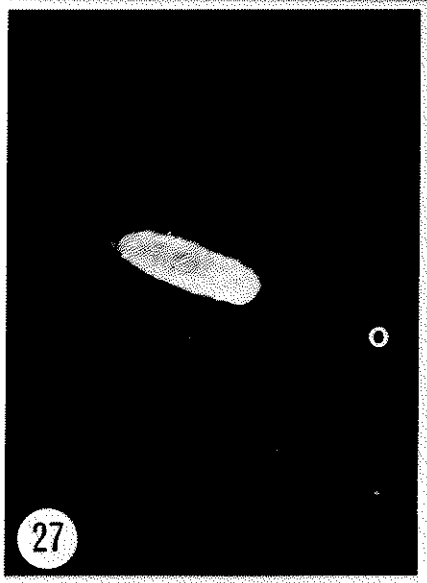

27

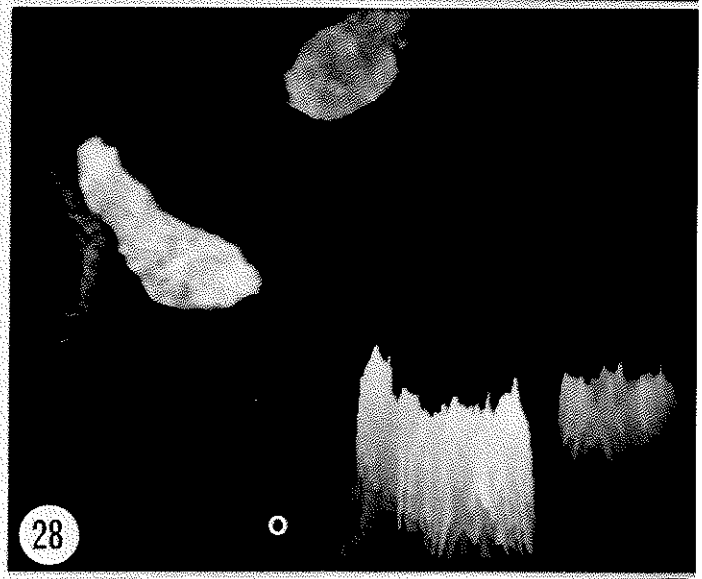

28

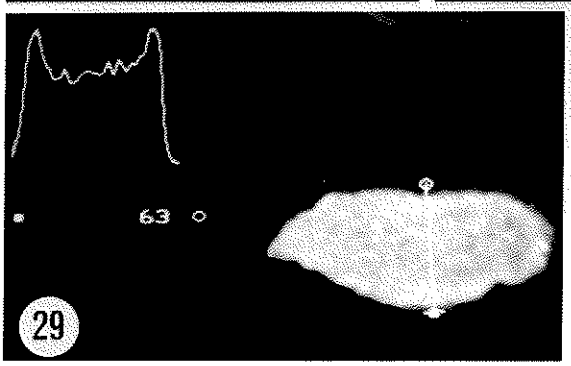

29

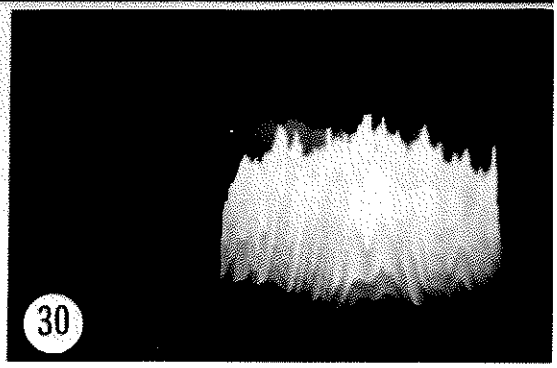

30

PLATE 6

Acetylated α-tubulin and MAP Distribution

Figure 31. Whole ovariole immunostaining using C3B9 antibody showing brilliant staining of the abundant MTs in a trophic cord leading into the apex of an oocyte. x1000.

Figure 32. Negative staining of a trophic cord (arrow) using an anti-MAP1 antibody (Sigma, clone HM-1). x250.

Figure 33. Immunofluorescent micrograph showing no fluorescent staining in a trophic cord (arrow) following screening with a anti-MAP2 antibody (Sigma, clone HM-2). x250.

Figure 34. Immunofluorescent micrograph showing staining of anti-*tau* antibody (Sigma, clone tau 2) in a presumptive redundant cord (arrow). x400.

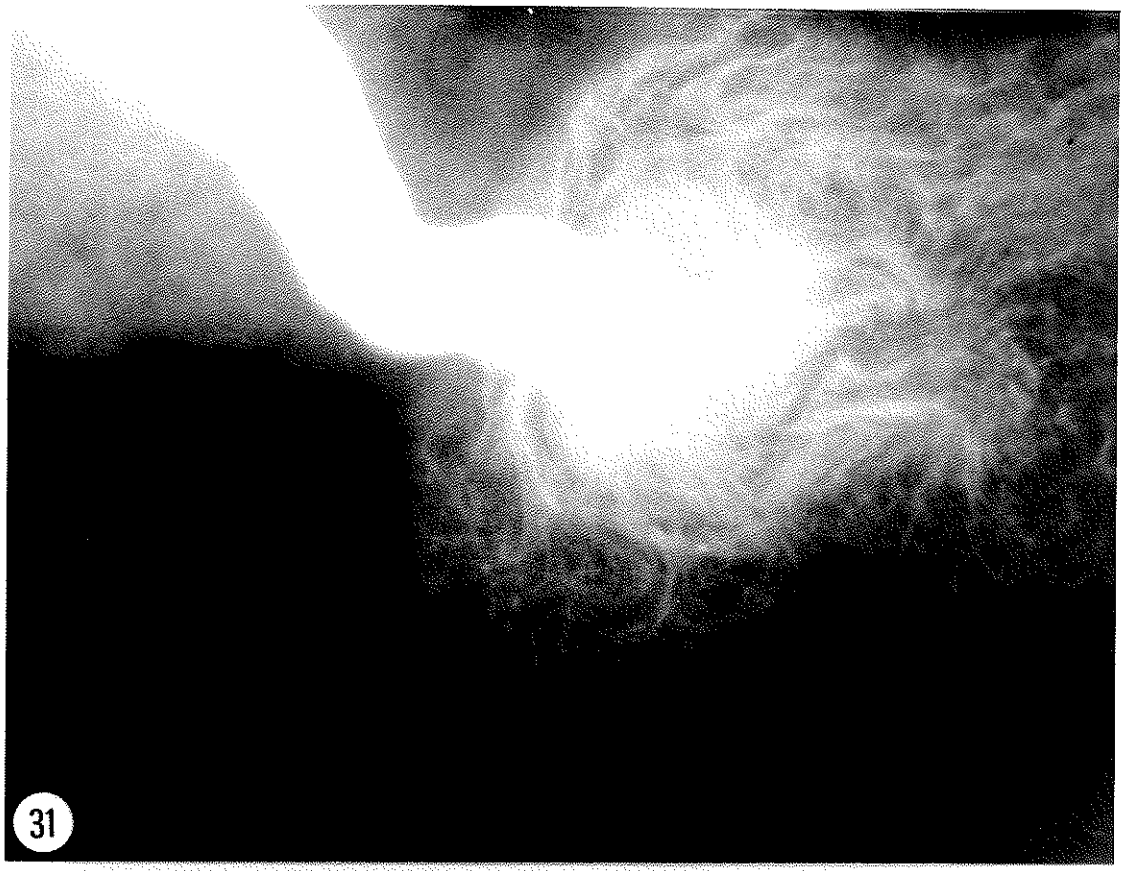
31

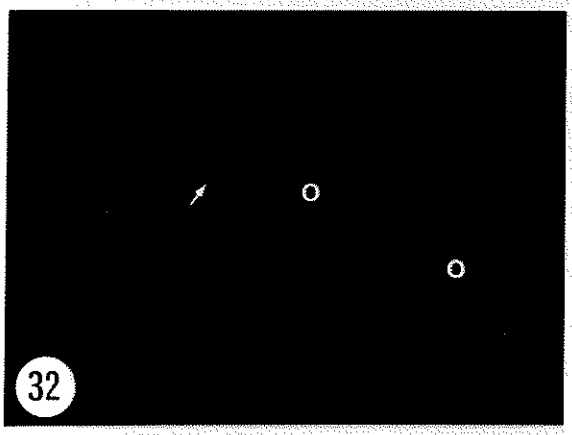
32

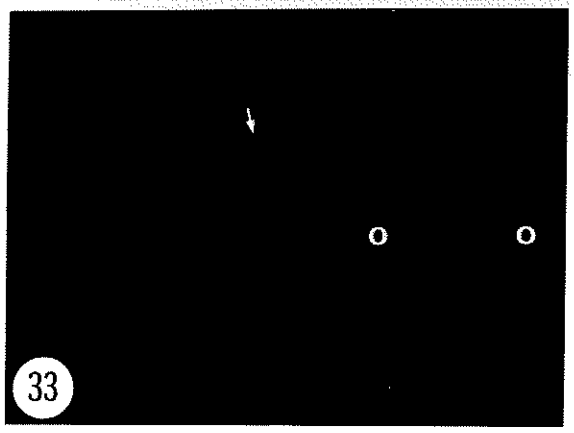
33

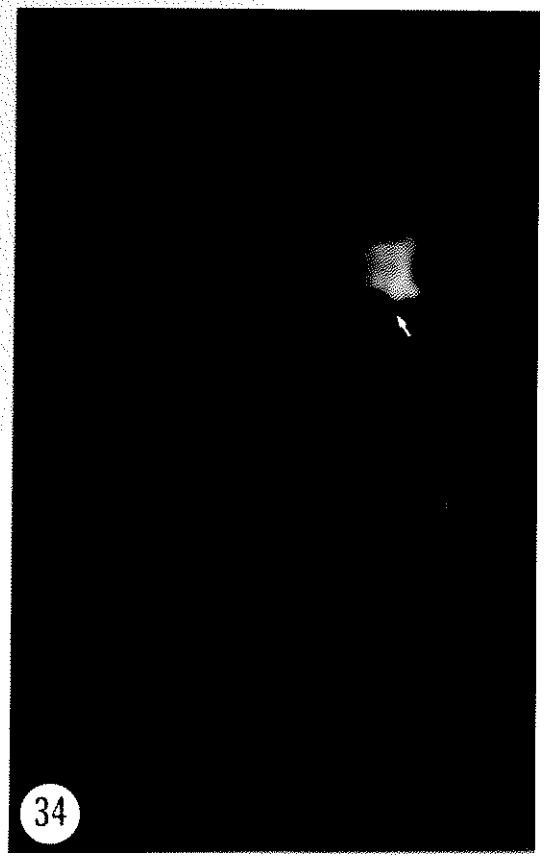
34

PLATE 7

Figure 35. Western blots of SDS-PAGE gels of *Rhodnius* ovary homogenates (O) and twice-cycled porcine tubulin (P) which were stained with the monoclonal antibodies: anti-α-tubulin (TAT-1) (Lane 1); anti-Tyr-tubulin TUB 1A2 (Lane 2 and 3); anti-Glu-tubulin (ID5) (Lane 4 and 5) and anti-acetylated-tubulin C3B9 (Lane 6 and 7). Lane 8 shows the pre-stained MW markers with protein sizes indicated to the right in kilodaltons (kDa) (Sigma P1677, MW 30-120 kDa). The porcine tubulin stained positively with all 3 antibodies. The ovarian homogenate stained positively (arrows) with the anti-tyrosinated and anti-acetylated α-tubulin antibodies but negatively (*) with the anti-detyrosinated α-tubulin antibody.

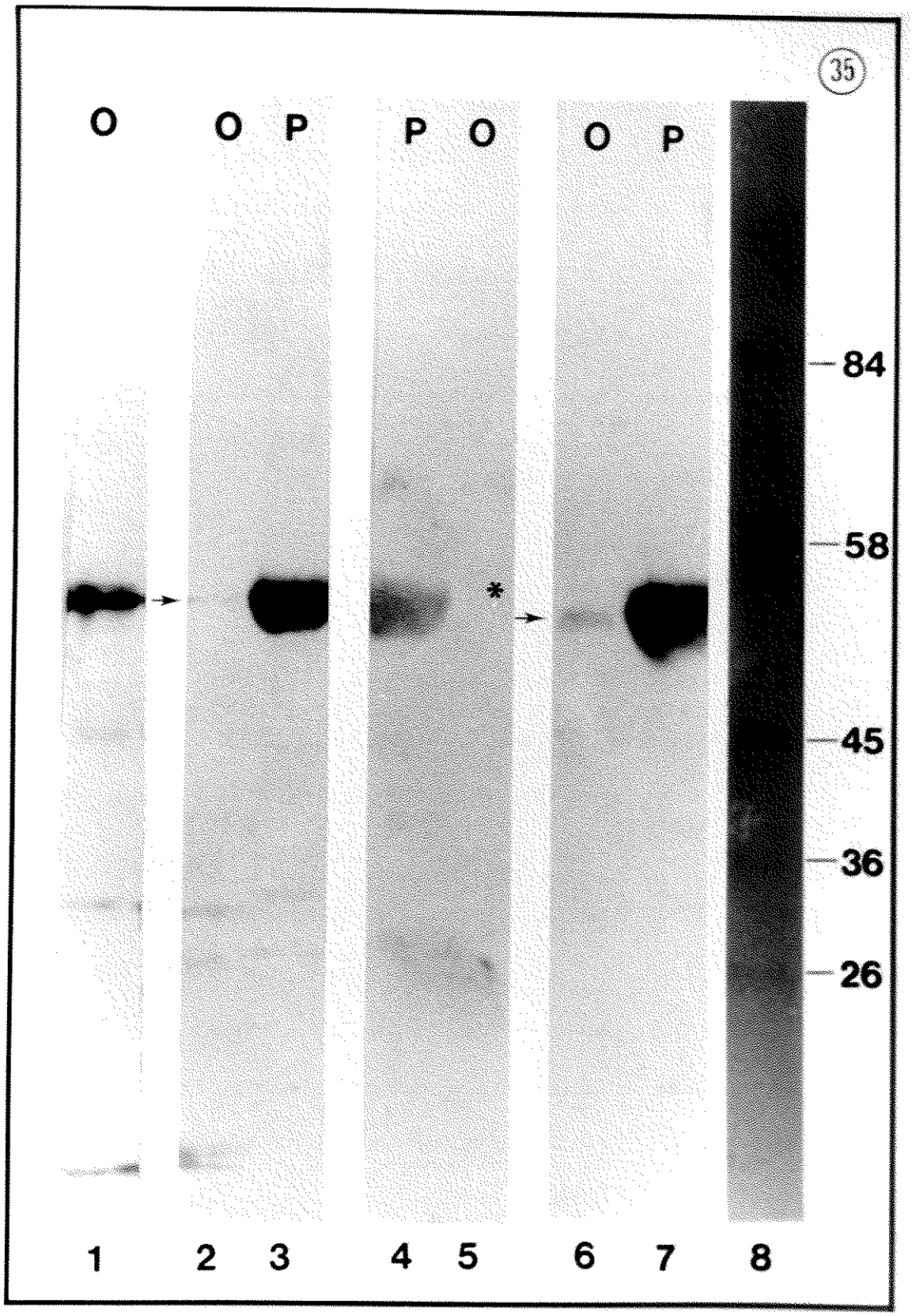
35
O
O P
P O
O P
84
58
45
36
26
*
1 2 3 4 5 6 7 8

DISCUSSION

These results indicate that the majority of trophic cord MTs are modified by an acetylase enzyme. Since acetylated α-tubulin has been shown to be an important marker of MT turnover and stability, the array of stable MTs is virtually indistinguishable from the total MT array in all cords examined. This suggests that the majority of MTs are selected for modification.

The low level of Glu-tubulin was not surprising in light of the intensity of the Tyr-tubulin staining seen within the cords. In most organisms most MTs stain with either Tyr or Glu antibodies, suggesting that together they make up the entire cellular array (Gundersen and Bulinski, 1991). The fact that no band was observed with the glu-tubulin antibody following Western blot analysis could be due to too low a concentration or absence of this isoform within the homogenate or that the modification was lost during tissue processing.

These results show that the trophic cord MTs are extensively acetylated but to a much lesser degree detyrosinated. Does the relative distributions of these tubulin modifications correlate with the known cold and drug stability of the trophic cord MTs? Can one draw conclusions about the structural characteristics of these MTs and the relative tubulin isoform distributions? What functional roles may these modifications contribute to the telotrophic ovariole? These questions will now be addressed.

Modifications, MAPs and MT Stability

Modified subsets of MTs may cause more effective or more specific MT interactions with specific MAPs (Gundersen and Bulinski, 1991). These interactions may then impart the drug and cold stability. Tyr-MTs have generally been observed to be cold and drug-labile (Baas and Black, 1990). The trophic cord MTs appear to have intact tyrosine residues at the carboxy termini of α-tubulin from immunocytochemical and immunoblotting results. Although they are tyrosinated, which is typical of more dynamic MTs, they appear to be substantially and selectively modified by an acetylase enzyme. This may play a role, either directly or indirectly in conferring cold and drug resistance. A correlation between the presence of posttranslational modifications of tubulin, MAP binding and cold and drug resistance exists in other systems.

A subset of MTs in the midbodies and flagella of the spermatogenic cells of the crane fly *Nephrotoma suturalis* are both acetylated and resistant to cold depolymerization (Wilson and Forer, 1989). Kim and colleagues (1989) showed that 80 percent of acetylated tubulin in brain extracts is found within the cold stable fraction. Margolis et al. (1986) speculated that MAPs confer cold resistance to this fraction by binding to the walls of acetylated MTs. As well, cod MTs which are highly acetylated and mainly detyrosinated are very resistant to colchicine depolymerisation (Billger et al., 1991). The lack of disassembly in the presence of colchicine is MAP-dependent as stability is increased in the presence of MAPs. Cod MAPS consist of MAP2 but not MAP1 and two other

MAPs not yet characterized (Billger et al., 1991). Some MAPs competitively inhibit colchicine binding to tubulin (Nunez et al., 1979). Stoichiometric binding of colchicine causes disassembly and inhibits assembly of MTs isolated from various sources as tubulin has one high affinity site for colchicine (Weisenberg and Taylor, 1968). In neuronal tissue, Binder and associates (1985) discovered that *tau* was localized only in axonal MTs. Its expression, along with other high molecular weight MAPs, coincides with the time of appearance of posttranslational modifications within axons (Matus and Riederer, 1986). Takemura et al., (1992) found that fibroblasts transfected with MAP2c or *tau* formed MT bundles which were similar to the long parallel arrays of MTs found in neuronal dendrites and axons. These MTs were stabilized against MT depolymerizing agents and were enriched in acetylated α-tubulin (Takemura et al., 1992). Transfection with MAP-1B did not cause bundling but the MTs showed slightly more stabilization and were also enriched in acetylated α-tubulin. None of the transfected cells had a pronounced enrichment of Glu-MTs (Takemura et al., 1992). This showed that these MAPs stabilize MTs and affect the state of posttranslational modifications of tubulin (Takemura et al., 1992).

There is probably more than one mechanism causing MT stability. In lower eukaryotes like the myxamoeba, *Physarum polycephalum,* the colchicine stability seems to be intrinsic with respect to tubulin, as isolated tubulin is assembly competent *in vivo* as well as *in vitro* in the presence of colchicine (Quinlan et al., 1981) and has a very low affinity for colchicine (Roobol et al., 1989). Since many modified MTs have higher resistance to anti-MT agents at their (+) ends, it has

been proposed that end stabilization occurs in these MTs, possibly by MT capping proteins, such as Gb4, found at the posterior end of *Trypanosoma brucei* MTs (Rindisbacher et al., 1993). These capping proteins would slow the turnover rate of these MTs and modifications may result following this stabilization.

Comparative Studies

My immunocytochemical findings in *Rhodnius* ovarioles differed quite significantly from those on *Notonecta* and *Oncopeltus* ovarioles reported by Harrison et al. (1991). This was somewhat unexpected considering some similarities in the MT properties. *Notonecta*, the backswimmer, is often found in water which may drop below 1°C, has also been shown to have trophic cord MTs which are highly resistant to cold and the anti-MT agents colchicine and nocodazole (Stebbings and van Bueren, 1981; Huebner, unpublished results). Since nocodozole binds to tubulin monomers the equilibrium of MT polymer and soluble tubulin monomers shifts towards the monomer (Dustin, 1984). This suggests the trophic cord MTs in both of these species are not turning over very rapidly. However *Notonecta* has been reported to be resistant to vinblastine sulphate as well as griseofulvin and maytansine (Stebbings and van Bueren, 1981) the latter two of which have not been investigated in *Rhodnius*.

If posttranslational modifications do play a direct role, or an indirect role via MAP binding, in increasing MT stability this may explain the presence of modified tubulin within the trophic cords of these two insects. One may also speculate

that the extensive detyrosination of the cords in *Notonecta* decreases the ability of vinblastine sulphate to disrupt the MT pattern, perhaps by blocking drug binding sites. It has been shown that colchicine and vinblastine sulphate have separate binding sites and therefore do not compete (Wilson and Friedkin, 1987). In other systems MTs disassemble very quickly, often within minutes, in the presence of anti-MT agents. However, the trophic cord MTs in *Rhodnius* are extraordinarily stable, lasting from hours to days in similar conditions, so it is curious that detyrosination does not occur here. Other α-tubulins have been reported which have different C-terminal residues, so one might ask whether all the C-terminal regions of *Rhodnius* α-tubulins can serve as substrates for detyrosination by a carboxypeptidase enzyme. In fact, *Drosophila,* has an isotype of α-tubulin (α_4) which has Asp-Glu-Phe at its C-terminus (Therkauf et al., 1986) and consequently cannot be detyrosinated.

Low levels of detyrosination have been observed in other systems as well. *Artemia*, the brine shrimp is able to develop for the first 15 hours of post-gastrula growth in the absence of Glu-tubulin in any of its cells (Langdon et al., 1991). In *Drosophila* embryos, all MT arrays contained tyrosinated α-tubulin but MTs rich in Glu-tubulin were not found in early stages of development, and only first detected after CNS condensation in neuron processes and in sperm tails. This was in contrast to the distribution of MT arrays containing acetylated α-tubulin which were detected as early as the cellular blastoderm stage. The lack of Glu-tubulin in early development was not a result of rapid turnover rate of MTs as found by taxol experiments (Warn et al., 1990). The question as to why Glu-tubulin does

not appear concurrently with acetylated α-tubulin could be due to low or absent levels of carboxypeptidase which cannot generate detectable Glu-tubulin (Warn et al., 1990). In fact, *Schizosaccharomyces pombe* contains tubulin with a C-terminal tyrosine residue, but it lacks Glu MTs suggesting the carboxypeptidase enzyme is not present (Alfa and Hyams, 1991). The very stable MT array of the marginal band in toad erythrocytes, there is no detectable Glu-tubulin (Gundersen and Bulinski, 1986). Consequently Glu-tubulin may not be necessary for stabilization of some subsets.

The lack of extensive Glu-MTs within the cord may be a result of variations in the intracellular distribution of ligase and/or carboxypeptidase activity. Since acetylated and Glu-tubulin are both enriched in MTs with slower turnover rates and decreased sensitivity to drug-induced depolymerization than the majority of cytoplasmic MTs, it seems likely that these forms of α-tubulin may substitute for each other depending on their availability in the cell. It is possible that they give different signals to the cell for different functions which have yet to be discovered (Gundersen and Bulinski, 1991). In *Rhodnius* ovarioles it appears that detyrosination is not directly involved in the stability of the MTs. If tubulin modification is required for MT stability, in *Rhodnius* acetylation of the cord MTs appears to be sufficient.

Unfortunately, there is little information on the stability of the MTs in the trophic cord MTs of *Oncopeltus*, which is a terrestrial insect like *Rhodnius*. These MTs do not show significant amounts of either Acet- or Glu-tubulin modifications. *Oncopeltus* has been shown to be sensitive to vinblastine

sulphate (Woodruff and Anderson, 1984) but it would be very interesting to see if the uniformly Tyr-MTs in these trophic cords had heightened sensitivities to cold or other anti-MT agents. In the case of these three insect species it appears that correlations cannot be drawn between the climate and the stability of trophic cord MTs as *Rhodnius*, a native of the tropics, has cold-stable MTs.

If the presence or absence of posttranslational modifications is linked to stable MTs produced by MAPs it is important to examine the MAP distribution within these insects. Using electron microscopy, most trophic cord MTs in all species examined show a clear zone surrounding each of the MTs (Stebbings and Bennett, 1975) suggesting the cord MTs do not have any visible projections such as MAPs. The spacing of the MTs also varies between species. Species showing rapid oogenesis, like *Rhodnius* and *Oncopeltus*, show wider cords (up to 35 μm in *Rhodnius* (Huebner, 1981)) with greater inter-MT spacing (Hyams and Stebbings, 1977). Species with slower oogenesis, like *Notenecta*, have narrower cords (up to 15 μm) (Macgregor and Stebbings, 1970) with tighter MT arrangements (Hyams and Stebbings, 1977). The organization of MTs into precisely spaced parallel arrays probably involves MT-MT associations and MAPs have been shown to be important for MT spacing (Black, 1987).

Anastasi and colleagues (1991) isolated a MAP-like protein from *Oncopeltus* which migrated electrophoretically between MAP 1 and MAP 2. This MAP was not present in *Notonecta*, indicating that the MAP composition varies between these two species. This may account for both spacing differences between MTs and differences in posttranslational modifications (Harrison et al., 1991). The

tubulin composition also seems to vary. In *Notonecta*, two α-tubulin isoforms have been identified (Sharma and Stebbings, 1985), one which stains for both Tyr- and Glu-tubulin antibodies on 2-D Immunoblots (α_1), and a slightly more acidic species (α_3) which stains with anti-acetylated antibodies (Harrison et al., 1991). *Oncopeltus* has one tubulin isoform which only stains with Tyr-specific antibodies on 2-D Immunoblots (Harrison et al., 1991).

Using indirect immunocytochemistry I screened ovariole sections for MAP 1, MAP 2 and *tau*. No staining was observed for either of the high molecular weight structural MAPS. It is possible that these MAPs are absent in the cords, or they are at a low level undetectable by epifluorescence. *Tau* however was observed within a redundant cord. This is very interesting as it has not been observed in other telotrophic ovarioles. The onset of redundancy in cords is much later in *Rhodnius*, occurring at mid-vitellogenesis (Huebner, 1981) as opposed to *Notonecta* and *Oncopeltus* cords, which detach from an oocyte entering vitellogenesis (Bennett and Stebbings, 1979; Woodruff and Anderson, 1984). Upon redundancy the MTs in all telotrophic ovarioles become closely packed bundles (Bennett and Stebbings, 1979). In *Notenecta* these tightly packed bundles persist for some time before depolymerization and resorption very slowly occurs, suggesting that the packing is not related to the stability of these MTs (Lane and Stebbings, 1994). In *Rhodnius*, depolymerization rapidly follows MT packing (Huebner, 1981) suggesting the MT reorganization affects MT stability. From my results, it appears that *tau* may play a role in MT packing and ultimately cord resorption. In *Oncopeltus*, a decrease in MT spacing during

redundancy corresponds to the time when cytoplasmic transport stops (Bennett and Stebbings, 1979). *Tau* has been shown to inhibit organelle movement (Hirokawa, 1994) which is obviously important in a non-functioning, redundant cord.

Functional aspects

It appears that these tubulin modifications do play some role in trophic cord MT stability. I will now discuss what functions stable subsets of MTs may have in the insect telotrophic ovariole.

Two important general functions of MTs are to provide structural stability to maintain cell shape and to provide a polarized cytoskeleton for directional transport of organelles. As expected, MTs carrying out these functions tend to be stable (Bulinski and Gundersen, 1991). Posttranslational modifications are a quick and reversible mechanism to create covalently distinct tubulin molecules which may alter the MT function during the early stages of differentiative events (Bulinski and Gundersen, 1991). Modifications have been proposed to demarcate selective subsets of MTs which accumulate posttranslational tubulin modifications with age (Greer and Rosenbaum, 1989). Because of the dynamic instability of MTs, most MTs are prone to depolymerization and many MT configurations will occur and be replaced by others. Only those MT subsets which are protected from depolymerization will persist as they have been differentiated from the majority of MTs (Schulze and Kirschner, 1986).

This is consistent with the formation and function of the trophic cords in the telotrophic ovariole. Just prior to the adult molt, MTs arise at the oocytes and extend toward the nurse cells (Valdimarsson and Huebner, 1989). To meet the demands of the telotrophic ovariole, a highly extensive and stable MT network must be established to function as a conduit for nurse cell-produced cytoplasmic components. These cords increase in length and girth as the MTs simultaneously extend in length and number (Valdimarsson and Huebner, 1989). The development of this MT array is the final step in the formation of a functional adult ovariole (Lutz and Huebner, 1981). Hence, these MTs must be stable to produce this cellular morphogenesis and create the exaggerated polarity seen between the nurse cells and the oocytes. Therefore stability is required to form these MT networks and secondly to maintain them.

Consistent with other findings, the trophic cord MTs are probably stabilized selectively based on their particular cellular location. Cellular cues, likely from the nurse cells and/or oocytes, demarcate these MTs such that they will be stabilized and the cord formation will continue and be maintained for as long as needed. This is probably due to the presence of unknown stabilization sites, the number and distribution of which will determine the structure and composition of the MT array (Bulinski and Gundersen, 1991). If there are relatively few stabilization sites, dynamic MT may coexist with stable MTs. Other factors like MT bundling may also affect the stability and final array of MTs within the trophic cords.

In other systems, attenuated MT arrays show similarities to *Rhodnius* trophic cord MTs. In *Chlamydomonas reinhardtii* the axoneme MTs are acetylated at the

time of MT elongation and deacetylated during flagellar resorption (Brunke et al., 1982). Falconer et al., (1989) reported the establishment of the stable acetylated, MT bundle in immature and mature axons. During neuronal differentiation, the MT bundle is extended to form a neurite. The acetylated MTs form a bundle of parallel MTs which is colchicine-stable, although no MAPs have been detected when probed with a wide range of anti-MAP antibodies (Falconer et al., 1989). They suggested that the establishment of a stable, acetylated MT bundle takes place very early in neurogenesis before morphological change has occurred. A transient increase in polymerized MTs occurs during neuronal commitment resulting in MT bundle formation. This could occur by either the formation of lateral interactions between MTs via MAPs, forming a stable and acetylated bundle, and/or MT elongation until they reach a structure, becoming "end-stabilized" and acetylated (Kirschner and Mitchison, 1986). Regardless of the order of acetylation and bundling, this new MT array seems to confer polarity on the differentiating cell and is present before the neurites extend (Falconer et al., 1989).

In other neuron studies, Tyr-MTs were found at the axonal tip which is consistent with an elongation mechanism which occurs presumably on stable MTs at their "fast-growing" or (+) ends (Arregui et al., 1991). Variations in modifications along polarized MT arrays also occurs in other systems. Sherwin and Gull (1989) have shown that in trypanosomes a gradient of tyrosination appears towards the assembling end of a single MT while the remainder is largely detyrosinated. They proposed that the modification may arise by MAP-

based associations between the MTs in this stable region. Such a gradient was not obvious in *Rhodnius* trophic cords but immunoelectron analysis is necessary to confirm this.

The formation of the stable trophic cord MT array appears to be linked to the timing of oogenesis. *Notonecta* has a very slow period of oogenesis, lasting weeks to months, in which up to 30 oocytes are undergoing oogenesis including vitellogenesis simultaneously (Harrison et al., 1991). Since *Notonecta* has such a lengthy period of oogenesis, it is not surprising that the long-lived MTs within the cord are both acetylated and detyrosinated (Harrison et al., 1991). On the other hand, *Oncopeltus* has a very rapid developmental cycle with 5 or 6 oocytes undergoing development and vitellogenesis simultaneously and in which oogenesis may be completed in a matter of days (Harrison et al., 1991). *Oncopeltus* may have such a rapid period of oogenesis that the MT polymers do not exist long enough to be substantially detyrosinated (Harrison et al., 1991). The presence of unmodified tubulin may allow for provision of labile MTs involved in rapid trophic cord extension and morphological remodelling.

Rhodnius also shows a relatively rapid period of oogenesis, which can be completed within a week, which may explain why the MTs are not modified to the extent seen in *Notonecta*. In *Rhodnius*, the trophic cord MTs may not exist long enough to be substantially detyrosinated. However, in *Rhodnius* only the terminal oocyte in each ovariole is vitellogenic, and the penultimate oocytes are suspended in development until the terminal follicle is ovulated (Huebner, 1981). Hence there is a high level of regulation both spatially and temporally within the

ovariole. This coordinated arrest of oocyte development may be why the trophic cord MTs show substantially more modification than *Oncopeltus.*

The appearance of Glu-MTs within the oocytes of *Rhodnius* indicates that these MTs may be exposed to an oocyte-specific carboxypeptidase not seen within the cords or elsewhere within the ovariole. Glu-staining was not observed in either *Notonecta* or *Oncopeltus* oocytes (Harrison et al., 1991). However, in polytrophic ovarioles, the nuclei are held tightly in position by a dense MT network within *Drosophila* oocytes (Gutzeit, 1986) which have also been shown to be extensively detyrosinated (Warn et al., 1990). There is evidence showing that there is a temporal and spatial interrelationship between the localization of Golgi and MTs containing Glu-tubulin (Skoufias et al., 1990). It appears these MTs play a role in establishing and maintaining the organization of the Golgi elements within an interconnected supraorganellar system (Thyberg and Moskalewski, 1993). In *Rhodnius* ovarioles, the oocytes contain the majority of the cytoplasmic machinery such as the Golgi apparatus. Selective detyrosination may occur in the oocytes to allow anchorage of this cytoplasmic component in a juxtanuclear position.

Transport

MTs in the trophic cords play an obvious structural role by participating in the cytoplasmic linkage between each oocyte and the nurse cell syncytium. But these stable MTs can also function as tracks, supporting the movement of nurse

cell produced RNA and/or organelles. This suggests a function for posttranslational modifications of tubulin that accumulate on stable MTs since they can signal biochemically different stable MTs from dynamics MTs. These selected MTs may be selected for unidirectional transport to the oocytes via MT motors. Supporting evidence has been found in other systems.

The distribution and development of acetyl-MTs *in vivo* and *in vitro* has been shown to be consistent with a role in organelle transport as seen in the adult rat cerebellar axons (Cambray-Deakin and Burgoyne, 1987), which are known to contain relatively stable MTs. Developmentally, acetylated MTs are expressed in cerebellar granule cell axons *in vivo* and *in vitro* during early stages of neurite extension, well before synaptic vesicles are transported along the neurite (Cambray-Deakin and Burgoyne, 1987). When astrocyte cells are given short-term exposures to colchicine and nocodazole, the tyr-MT network is removed but the distributions of acetyl-MTs, glial filaments and mitochondria remain unchanged suggesting that the colocalised acetyl-MTs and glial filaments are involved in the intracellular transport of organelles and/or in the control of their cytoplasmic distribution (Cambray-Deakin et al., 1988).

In *Notonecta*, ribosomes make up 75 percent of the trophic cord volume (Stebbings and Bennett, 1976) while sparse mitochondria are localized to the periphery of the cords (Macgregor and Stebbings, 1970). The closer packing of the MTs within this species may preclude the passage of mitochondria through the cords (Hyams and Stebbings, 1977). Although a few cytoplasmic components have been seen to move relatively quickly, the movement of most

ribosomes throughout the cords *Notonecta* is very slow (20 μm/hour). Thus synthetic flow has been proposed as the primary means of transport in species with long reproductive cycles (Macgregor and Stebbings, 1970).

Oncopeltus cords, like *Rhodnius* contain large numbers of mitochondria and ribosomes dispersed throughout the widely spaced MTs in the trophic cords (Hyams and Stebbings, 1977; Huebner, 1981). MT-based movement of mitochondria has been observed in *Oncopeltus* (Stebbings and Hunt, 1987) so synthetic flow as the primary means of transport is not likely in species which exhibit rapid oogenesis.

Interestingly, the distribution of Tyr-tubulin mimics that of mitochondria within the cords of all three species examined. The presence of Tyr-tubulin (or absence of Glu-tubulin) may affect mitochondrial distribution and/or transport. Or perhaps, these dynamic MTs require an immediate source of energy for their restructuring. More detailed studies are required to support this theory as correlations between tyrosinated MTs and mitochondrial distributions have not been observed in other systems.

CONCLUSIONS

In the telotrophic ovariole, ribosomal and messenger RNAs specifically accumulate in the oocyte early in development and trophic cords provide a mechanism to establish this cytoplasmic asymmetry. These cords consist of a parallel array of stable MTs. The known drug and cold stability of these MTs appears to be linked to the presence of posttranslational modifications of tubulin. Specifically, acetylation of α-tubulin is dramatic indicating that this modification directly, or indirectly plays a role in MT stability due to its restricted localization within this specialized cytoskeletal region. Detyrosination is not as prominent indicating that this modification is not linked to the cold and drug resistance observed in these MTs. If acetylation does not directly cause stability it is likely via MAPs. Since most cords did not show staining for MAP1 or MAP2 or *tau* there may be other MAPs present causing this high degree of stability.

If only a marker for stability, the brilliant staining seen with the anti-acetylated antibody clearly identifies this MT subset found within the trophic cords of the adult telotrophic ovariole of *Rhodnius*. These stable MT subsets may contribute to the maintainance of the asymmetric morphology by enhancing the rigidity of the axis along which nurse cell-oocyte transport occurs. These stable polymers may also act as nucleating structures for further MT elongation. As well, stable MTs may serve as tracks supporting the movement of organelles or vesicles.

Rhodnius ovarioles vary significantly from other telotrophic ovarioles examined. The extensive acetylation seen within the cords is likely linked to the

high regulation of oogenesis which is unique to species containing telotrophic ovarioles. Future work on the cause and regulation of this stable MT array will be important for understanding MT dynamics and function in producing cellular morphogenesis and allowing selective, regulated transport during oogenesis.

LITERATURE CITED

Alfa, C.E. and J.S. Hyams. 1991. Microtubules in the fission yeast *Schizosaccharomyces pombe* contain only the tyrosinated form of α-tubulin. Cell Motil. Cytoskel. **18**: 86-93.

Allen, C.and G.G. Borisy. 1974. Structural polarity and directional growth of microtubules from axonemes of *Chlamydomonas*. J. Mol. Biol. **90**: 381-401.

Allen, R.D., Weiss, D.G., Hayden, J.H., Brown, T.D., Fujiwake, H. and M. Simpson. 1985. Gliding movement of and bidirectional movement along single native microtubules from the squid axoplasm: Evidence for an active role of microtubules in cytoplasmic transport. J. Cell Biol. **100**: 1736-1752.

Amos, L.A., Linck, R.W. and A. Klug. 1976. Molecular structure of flagella microtubules. In *Cell Motility*, R. Goldman, T. Pollard and J. Rosenbaum, eds. Cold Spring Harbor Laboratory, pp. 847-868.

Anastasi, A., Hunt, C. and H. Stebbings. 1990. Isolation of microtubule motors from an insect ovarian system: characterization using a novel motility substratum. J. Cell Sci. **96**: 63-69.

Anastasi, A., Hunt, C. and H. Stebbings. 1991. Characterization of a nucleotide-sensitive high molecular weight microtubule-associated protein in the ovary of a hemipteran insect. Cell Motil. Cytoskel. **19**: 37-48.

Arce, C.A., Hallack, M.E., Rodriguez, J.A., Barra, H.S. and R. Caputto. 1978. Capability of tubulin and microtubules to incorporate and to release tyrosine and phenylalanine and the effect of the incorporation of these amino acids on tubulin assembly. J. Neurochem. **31**: 205-210.

Arregui, C., Busciglio, J., Caceres, A. and H.S. Barra. 1991. Tyrosinated and detyrosinated microtubules in axonal processes of cerebellar macroneurons grown in culture. J. Neurosci. Res. **28**: 171-181.

Baas, P.W. and M.M. Black. 1990. Individual microtubules in the axon consist of domains that differ in both composition and stability. J. Cell Biol. **11**: 495-509.

Barra, H.S., Rodriguez, J.A., Arce, C.A. and R. Caputto. 1973. A soluble preparation from rat brain that incorporates into its own proteins [^{14}C]arginine by a ribonuclease-sensitive system and [^{14}C]tyrosine by a ribonuclease-insensitive system. J. Neurochem. **20**: 97-108.

Bennett, C.E. and H. Stebbings. 1979. Redundant nutritive tubes in insect ovarioles: The fate of an extensive microtubule transport system. Cell Biol. Int. Rep. **3**: 577-583.

Billger, M., Stromberg, E. and M. Wallin. 1991. Microtubule-associated proteins-dependent colchicine stability of acetylated cold-labile brain microtubules from the Atlantic cod, *Gadus morhua*. J. Cell Biol. **113**: 331-338.

Binder, L.I., Dentler, W.L. and J.L. Rosenbaum. 1985. The distribution of *tau* in the mammalian central nervous system. J. Cell Biol. **101**: 1371-1378.

Black, M.M. 1987. Comparison of the effects of microtubule-associated protein 2 and *tau* on the packing density of *in vitro* assembled microtubules. Proc. Natl. Acad. Sci. USA **84**: 7783-7787.

Brady, S.T., Tytell, M. and R.J. Lasek. 1984. Axonal tubulin and axonal microtubules: biochemical evidence for cold stability. J. Cell Biol. **99**: 1716-1724.

Brady, S.T., Lasek, R.J. and R.D. Allen. 1985. Video microscopy of fast axonal transport in extruded axoplasm: A new model for study of molecular mechanisms. Cell Motil. **5**: 81-101.

Bre, M.M., Kreis, T.E. and E. Karsenti. 1987. Control of microtubule nucleation and stability in Madin-Darby canine kidney cells: the occurrence of noncentrosomal, stable detyrosinated microtubules. J Cell Biol. **105**: 1283-1296.

Brunke, K.J., Collins, P.S. and D.P. Weeks. 1982. Posttranslational modification of tubulin dependent on organelle assembly. Nature **297**: 516-518.

Brunt, A. 1970. Extensive system of microtubules in the ovariole of *Dysdercus fasciatus* Signoret (Heteroptera: Pyrrhocoridae). Nature (Lond.) **118**: 80-81.

Bulinski, J.C. and G.G. Gundersen. 1991. Stabilization and posttranslational modification of microtubules during cellular morphogenesis. Bioessays **13**: 285-293.

Cambray-Deakin, M.A. and R.D. Burgoyne. 1987. Posttranslational modifications of α-tubulin: acetylated and detyrosinated forms in axons of rat cerebellum. J. Cell Biol. **104**: 1569-1574.

Cambray-Deakin, M.A. and R.D. Burgoyne. 1988. Colocalization of acetylated microtubules, glial filaments, and mitochondria in astrocytes *in vitro*. Cell Motil. Cytoskel. **10**: 438-449.

Capco, D.G. and R.W. McGaughey. 1986. Cytoskeletal reorganization during early mammalian development: analysis using embedment-free sections. Dev. Biol. **115**: 446-458.

Capco, D.G., Krochmalnic, G. and S. Penman. 1984. A new method of preparing embedment-free sections for transmission electron microscopy: applications to the cytoskeletal framework and other three dimensional networks. J. Cell Biol. **98**: 1878-1885.

Cartier, M.-F. 1988. Role of nucleotide hydrolysis in the polymerization of actin and tubulin. Cell Biophys. **12**: 105-117.

Chu, D.T.W. and M.W. Klymkowsky. 1989. The appearance of acetylated α-tubulin during early development and cellular differentiation in *Xenopus*. Dev. Biol. **136**: 104-117.

Cleveland, D.W. and K.F. Sullivan. 1985. Molecular biology and genetics of tubulin. Annu. Rev. Biochem. **54**: 331-365.

Diggins, M.A. and W.F. Dove. 1987. Distribution of acetylated α-tubulin in *Physarum polycephalum*. J. Cell Biol. **104**: 303-309.

Dittmann, F., Weiss, D.G. and A. Munz. 1987. The bidirectional movement of mitochondria in the ovarian trophic cord of *Dysdercus intermedius* (Heteroptera) resembles axonal transport. Roux's Arch. Dev. Biol. **196**: 407-413.

Dustin, P. 1984. *Microtubules*. 2nd ed. Springer-Verlag New York Inc., New York. pp. 167, 462.

Eddé, B., Rossier, J., Le Caer, J.-P., Desbruyeres, E., Gros, F. and P. Denoulet. 1990. Posttranslational glutamylation of α-tubulin. Science **247**: 83-85.

Falconer, M.M., Vielkind, U. and D.L. Brown. 1989. Establishment of a stable, acetylated microtubule bundle during neuronal commitment. Cell Motil. Cytoskel. **12**: 169-180.

Gabeus, H.J., Graupner, G. and F. Cramer. 1983. Activity patterns of aminoacyl rRNA synthetases, rRNA methylases, arginyl-transferase and tubulin tyrosine ligase during development and ageing of *Caenorhabditis elegans*. Eur. J. Biochem. **131**: 231-234.

Gilbert, S.P., Allen, R.D. and R.D. Sloboda. 1985. Translocation of vesicles from squid axoplasm on flagellar microtubules. Nature **315**: 245-248.

Greer, K. and J.L. Rosenbaum. 1989. Post-translational modifications of tubulin. In: Warner FD, Satir, P and IR Gibbons (eds). In *Cell Movement. Vol. 2. Kinesin, dynein and microtubule dynamics.* Alan R. Liss, New York, NY. pp 47-66.

Gundersen G.G. and J.C. Bulinski. 1986. Microtubule arrays in differentiated cells contain elevated levels of a post-translationally modified form of tubulin. Eur. J. Cell Biol. **42**: 288-294.

Gundersen, J.C. and G.G. Bulinski. 1991. Stabilization and post-translational modification of microtubules during cellular morphogenesis. Bioessays **13(6)**: 285-293.

Gundersen, G.G., Kalnoski, M.H. and J.C. Bulinski. 1984. Distinct populations of microtubules: tyrosinated and nontyrosinated α-tubulin are distributed differently *in vivo*. Cell **38**: 779-789.

Gundersen, G.G., Khawaja, S. and J.C. Bulinski. 1989. Generation of a stable, posttranslationally modified microtubule array is an early event in myogenic differentiation. J. Cell Biol. **109**: 2275-2288.

Gutzeit, H.O. 1986. Transport of molecules and organelles in meroistic ovarioles of insects. Diff. **31**: 155-165.

Hallak, M.E., Rodriguez, J.A., Barra, H.S. and R. Caputto. 1977. Release of tyrosine from tyrosinated tubulin. Some common factors that affect this process and the assembly of tubulin. FEBS (Fed. Eur. Biochem. Soc.) Lett. **73**: 147-150.

Harrison, A., Stebbings, H. and J.S. Hyams. 1991. Different patterns of α-tubulin post-translational modification in ovarian nutritive tubes of two hemipteran insects. J. Cell Sci. **100**: 501-507.

Hirokawa, N. 1994. Microtubule organization and dynamics dependent on microtubule-associated proteins. Curr. Opin. Cell Biol. **6**: 74-81.

Hirokawa, N., Bloom, G.S. and R.B. Vallee. 1985. Cytoskeletal architecture

and immunocytochemical localization of microtubule-associated proteins in regions of axons associated with rapid axonal transport: The IDPN-intoxicated axons as a model system. J. Cell Biol. **101**: 227-239.

Hirokawa, N., Shiomura, Y. and S. Okabe. 1988. Tau proteins: The molecular structure and mode of binding on microtubules. J. Cell Biol. **107**: 1449-1459.

Houliston, E. and B. Maro. 1989. Posttranslational modification of distinct microtubule subpopulations during cell polarization and differentiation in the mouse preimplantation embryo. J. Cell Biol. **108**: 543-551.

Huebner, E. 1981. Nurse cell-oocyte interaction in the telotrophic ovaries of an insect, *Rhodnius prolixus*. Tiss. Cell **13**: 105-125.

Huebner, E. 1984. The ultrastructure and development of the telotrophic ovary. In: *Insect Ultrastructure Vol. 2.* (eds. R.C. King and H. Akai.) Plenum Publish, New York. pp. 3-48.

Huebner, E. and E. Anderson. 1970. The effects of vinblastine sulfate on the microtubular organization of the ovary of *Rhodnius prolixus*. J. Cell Biol. **46**: 191-198.

Huebner, E. and E. Anderson. 1972. A cytological study of the ovary of *Rhodnius prolixus*. III. Cytoarchitecture and development of the trophic chamber. J. Morphol. **138**: 1-40.

Huebner, E. and W. Diehl-Jones. 1993. Nurse cell-oocyte interaction in the telotrophic ovary. Int. J. Insect Morph. Embryol. **22**: 369-387.

Huebner E., Harrison R. and K. Yeow. 1995. A new feeding technique for experimental and routine culturing of the insect *Rhodnius prolixus*. Can. J. Zool. **72**: 2244-2247.

Hyams, J.S. and H. Stebbings. 1977. The distribution and function of microtubules in nutritive tubes. Tiss. Cell **9**: 537-545.

Hyams, J.S. and H. Stebbings. 1979. The formation and breakdown of nutritive tubes- Massive microtubular organelles associated with cytoplasmic transport. J. Ultrastruct. Res. **68**: 46-57.

Inoué, S. and H. Sato. 1967. Cell motility by labile association of molecules. The nature of mitotic spindle fibers and their role in chromosome movement. J. Gen. Physiol. Suppl. **50**: 259-292.

Kim, H., Binder, L.I. and J.L. Rosenbaum. 1989. Post-translational modifications of tubulin. In: Warner FD, Satir, P and IR Gibbons (eds). In *Cell Movement. Vol. 2. Kinesin, dynein and microtubule dynamics.* Alan R. Liss, New York, NY. pp 47-66.

Kirschner, M. and T. Mitchison. 1986. Beyond self-assembly: from microtubules to morphogenesis. Cell **45**: 329-342.

Laemmli, U.K. 1970. Cleavage of structural proteins during the assembly of the head of bacteriophage T_4. Nature **227**: 680-685.

Lane, J.D. and H. Stebbings. 1994. Independent regulation of microtubule spacing and microtubule stability following redundancy of nutritive tubes in telotrophic ovaries in hemiptera (insecta). Int. J. Insect Morphol. & Embryol. **23(4)**: 297-309.

Langdon, C.M., Freeman, J.A. and T.H. MacRae. 1991. Post-translationally modified tubulins in *Artemia*: prelarval development in the absence of detyrosinated tubulin. Dev. Bio. **148**: 147-155.

Le Dizet, M. and G. Piperno. 1986. Cytoplasmic microtubules containing acetylated α-tubulin in *Chlamydomonas reinhardtii*: spatial arrangement and properties. J. Cell Biol. **103**: 13-22.

L'Hernault, S.W. and J.L. Rosenbaum. 1983. *Chlamydomonas* α-tubulin is posttranslationally modified in the flagella during flagellar assembly. J. Cell Biol. **97**: 258-263.

L'Hernault, S.W. and J.L. Rosenbaum. 1985. *Chlamydomonas* α-tubulin is posttranslationally modified by acetylation on the e-amino group of a lysine. Biochemistry **24**: 473-478.

Lutz, D. and E. Huebner. 1981. Development of nurse cell-oocyte interactions in the insect telotrophic ovary of *Rhodnius*. Tiss. Cell **13**: 321-335.

MacGregor, H.C. and H. Stebbings. 1970. A massive system of microtubules associated with cytoplasmic movement in telotrophic ovarioles. J. Cell Sci. **6**: 431-449.

Margolis, R.L., Rauch, C.T. and D. Job. 1986. Purification and assay of a 145 kDa protein ($STOP_{145}$) with microtubule-stabilizing and motility behaviour. Proc. Natl. Acad. Sci. USA **83**: 4394-4398.

Maruta, H., Greer, K., and J.L. Rosenbaum. 1986. The acetylation of alpha-

tubulin and its relationship to the assembly and disassembly of microtubules. J. Cell Biol. **103**: 57-579.

Matus, A. and B. Riederer. 1986. Microtubule-associated proteins in the developing brain. Ann. N.Y. Acad. Sci. **466**: 167-179.

Miller, F.D., Naus, C.C.G., Durand, M., Bloom, F.E. and R.J. Miller. 1987. Isotypes of α-tubulin are differentially regulated during neuronal maturation. J. Cell Biol. **105**: 3065-3073.

Nauss, R.N. 1949. *Reticulomyxa* filosa gen. et sp. nov., a new primitive plasmodium. Bull. Torrey Bot. Club **76**: 161-173.

Nunez, J., Fellous, A., Francon, J. and A.M. Lennon. 1979. Competitive inhibition of colchicine binding to tubulin by microtubule-associated proteins. Proc. Natl. Acad. Sci. USA **76**: 86-90.

Olmsted, J.B. 1986. Microtubule-associated proteins. Annu. Rev. Cell Biol. **2**: 421-457.

Piperno, G., Le Dizet, M. and X. Chang. 1987. Microtubules containing acetylated α-tubulin in mammalian cells in culture. J. Cell biol. **104**: 289-302.

Porter, K.R. 1966. Cytoplasmic microtubules and their functions. In G.E.W. Wolstenholme (ed): *Ciba Foundation Symposium on Principles of Biomolecular Organization.* Churchill, London.

Preston, S., Deanin, G.G., Hanson, R.D. and M.W. Gordon. 1981. Tubulin:tyrosine ligase in oocytes and embryos of *Xenopus laevis*. Dev. Biol. **81**: 36-42.

Quinlan, R.A., Roobol, A., Pogson, C.I. and K. Gull. 1981. A correlation between *in vivo* and *in vitro* effects of the microtubule inhibitors colchicine, parbendazole and nocodazole on myxamoebae of *Physarum polycephalum.* J. Gen. Microbiol. **122**: 1-6.

Rindisbacher, L., Hemphill, A. and T. Seebeck. 1993. A repetitive protein from *Trypanosoma brucei* which caps the microtubules at the posterior end of the cytoskeleton. Mol. Biochem. Parasitol. **58**: 83-96.

Roobol, A., Pogson, C.I. and K. Gull. 1980. Identification and characterization of microtubule proteins from myxamboebae of *Physarum polycephalum.* Biochem. **189**: 305-312.

Sahenk, Z. and S.T. Brady. 1987. Axonal tubulin and microtubules: morphologic

evidence for stable regions on axonal microtubules. Cell Motil. Cytoskel. **8**: 155-164.

Sasse, R., Glyn, M.C.P., Birkett, C.R. and K. Gull. 1987. Acetylated α-tubulin in *Physarum*: Immunological characterization of the isotype and its usage in particular microtubular organelles. J. Cell biol. **104**: 41-49.

Satir, P. 1968. Studies on cilia. III. Further studies on the cilium tip and a "sliding filament" model of ciliary motility. J. Cell Biol. **39**: 77-94.

Schatten, H., Howard, C., Coffe, G., Simerly, C. and G. Schatten. 1988. Centrosomes, centrioles and post-translationally modified microtubules during fertilization. J. Zool. Sci. **5**: 585-601.

Schnapp, B.J., Vale, R.D., Sheetz, M.P. and T.S. Reese. 1985. Single microtubules from squid axoplasm support bidirectional movement of organelles. Cell **40**: 455-462.

Schneider, A., Sherwin, T., Sasse, R., Russel, D.G., Gull, K. and T. Seebeck. 1987. Subpellicular and flagellar microtubules of *Trypanosoma brucei brucei* contain the same α-tubulin isoforms. J. Cell Biol. **104**: 431-438.

Schulze, E. and M. Kirschner. 1986. Microtubule dynamics in interphase cells. J. Cell Biol. **102**: 1020-1031.

Schulze, E. and M. Kirschner. 1987. Dynamic and stable populations of microtubules in cells. J. Cell Biol. **104**: 277-288.

Schulze, E., Asai, D.J., Bulinski, J.C. and M. Kirschner. 1987. Posttranslational modification and microtubule stability. J. Cell Biol. **105**: 2167-2177.

Serrano, L., Diaz-Nido, J., Wandosell, F. and J. Avila. 1987. Tubulin phosphorylation by casein kinase II is similar to that found *in vivo*. J. Cell Biol. **105**: 1731-1739.

Sharma, K.K. and H. Stebbings. 1985. Electrophoretic characterization of an extensive microtubule-associated transport system in telotrophic ovarioles of *Notonecta glauca*. Cell Tiss. Res. **242**: 383-389.

Sherwin, T. and K. Gull. 1989. Visualization of detyrosination along single microtubules reveals novel mechanisms of assembly during cytoskeletal duplication in trypanosomes. Cell **57**: 211-221.

Sherwin, T., Schneider, A., Sasse, R., Seebeck, T. and K. Gull. 1987. Distinct localization and cell cycle dependence of COOH terminally tyrosinated α-

tubulin in the microtubules of *Trypanosoma brucei brucei*. J. Cell Biol. **104**: 439-446.

Skoufias, D.A., Burgess, T.L. and L. Wilson. 1990. Spatial and temporal colocalization of the Golgi apparatus and microtubules rich in detyrosinated tubulin. J. Cell Biol. **111**: 1929-1937.

Slautterback, D.B. 1963. Cytoplasmic microtubules. I. Hydra. J. Cell Biol. **18**: 367-388.

Stebbings, H. and C.E. Bennett. 1975. The sleeve element of microtubules. In *Microtubules and Microtubule inhibitors*. Borgers & M Brabander, North-Holland, Amsterdam. pp. 35.

Stebbings, H. and C. E. Bennett. 1976. The effect of colchicine on the sleeve element of microtubules. Exp. Cell Res. **100**: 419-423.

Stebbings, H. and J. van Beuren. 1981. Stability of microtubules from insect ovaries. Cell Biol. Int. Reports **5**: 705-710.

Stebbings, H. and C. Hunt. 1983. Microtubule polarity in the nutritive tubes of insect ovarioles. Cell Tiss. Res. **233**: 133-141.

Stebbings, H. and C. Hunt. 1987. The translocation of mitochondria along insect ovarian microtubules from isolated nutritive tubes; a simple reactivated model. J. Cell Sci. **88**: 641-648.

Sullivan, K.F. 1988. Structure and utilization of tubulin isotypes. Annu. Rev. Cell Biol. **4**: 687-716.

Summers, K.E. and I.R. Gibbons. 1971. Adenosine triphosphate-induced sliding of tubules in trypsin treated flagella of sea urchin sperm. Proc. Natl. Acad. Sci. USA **68**: 3092-3096.

Takemura, R., Okabe, S., Umeyama, T., Kanai, Y., Cowan, N.J. and N. Hirokawa. 1992. Increased microtubule stability and alpha tubulin acetylation in cells transfected with microtubule-associated proteins MAP1B, MAP2 or *tau*. J. Cell Sci. **103**: 953-964.

Theurkauf, W.E., Baum, H., Bo J. and P.C. Wensink. 1986. Tissue-specific and constitutive α-tubulin genes of *Drosophila melanogaster* code for structurally distinct proteins. Proc. Natl. Acad. Sci. USA **83**: 8477-8481.

Thompson, W.C., Asai, D.J. and D.H. Carney. 1984. Heterogeneity among microtubules of the cytoplasmic microtubule complex detected by a

monoclonal antibody to α-tubulin. J. Cell Biol. **98**: 1017-1025.

Thyberg, J. and S. Moskalewski. 1993. Relationship between the Golgi complex and microtubules enriched in detyrosinated or acetylated α-tubulin: studies on cells recovering from nocodazole and cells in the terminal phase of cytokinesis. Cell Tiss. Res. **273**: 457-466.

Tilney, L.G. and K.R. Porter. 1967. Studies on the microtubules in Heliozoa. II. The effect of low temperature on these structures in the formation and maintenance of axopodia. J. Cell Biol. **34**: 327-343.

Valdimarsson, G. and E. Huebner. 1989. The development of microtubular arrays in the germ tissue of an insect telotrophic ovary. Tiss. Cell **21**: 123-138.

Vale, R.D., Reese, T.S. and M.P. Sheetz. 1985a. Identification of a novel force-generating protein, kinesin, involved in microtubule-based motility. Cell **42**: 39-50.

Vale, R.D., Schnapp, B.J., Mitchison, T., Steuer, E., Reese, T.S. and M.P. Sheetz. 1985b. Different axoplasmic proteins generate movement in opposite directions along microtubules *in vitro*. Cell **43**: 623-632.

Warn, R.M., Harrison, A., Planques, V., Robert-Nicoud, N. and J. Wehland. 1990. Distribution of microtubules containing post-translationally modified α-tubulin during *Drosophila* embryogenesis. Cell Motil. Cytoskel. **17**: 34-45.

Webster, D.R., Gundersen, G.G., Bulinski, J.C. and G.G. Borisy. 1987. Differential turnover of tyrosinated and detyrosinated microtubules. Proc. Natl. Acad. Sci. USA **84**: 9040-9044.

Wehland, J. and K. Weber. 1987. Turnover of the carboxy-terminal tyrosine of α-tubulin and means of reaching elevated levels of detyrosination in living cells. J. Cell Sci. **88**: 185-203.

Weisenberg, R. and E.W. Taylor. 1968. Studies on ATPase activity of sea urchin eggs and the isolated mitotic apparatus. Exp. Cell Res. **53**: 372-384.

Wilson, K. and M. Friedkin. 1987(67?). The biochemical events of mitosis. II. The *in vivo* and *in vitro* binding of colchicine in grasshopper embryos and its possible relation to inhibition of mitosis. Biochem. (Wash.) **6**: 3126-3135.

Wilson, P.J. and A. Forer. 1989. Acetylated α-tubulin in spermatogenic cells of the crane fly *Nephrotoma suturalis*: kinetochore microtubules are selectively acetylated. Cell Motil. Cytoskel. **14**: 237-250.

Wolf, N., Regan, C.L. and M. Fuller. 1988. Temporal and spatial pattern of differences in microtubule behaviour during *Drosophila* embryogenesis revealed by distribution of a tubulin isoform. Development **102**: 311-324.

Woodruff, R.I. and K.L. Anderson. 1984. Nutritive cord connection and dye-coupling of the follicular epithelium to the growing oocytes in the telotrophic ovarioles in *Oncopeltus fasciatus*, the milkweed bug. Roux's Arch. Dev. Biol. **193**: 158-163.

CHAPTER 2: Microtubule Polarity and Transport

INTRODUCTION

Intracellular movement and cytoplasmic transport are essential properties of all cells. These movements are crucial, particularly during development. Without the reorganization of maternal factors and proper chromosomal migration during early development and cleavage, daughters cells will either lack essential cytoplasmic components or have unequal distributions of genetic information, respectively (Gilbert, 1990). Meroistic telotrophic ovarioles, which rely on import from nurse cells would lack components essential for further development without these transported contributions (Telfer, 1975).

Early light microscopy allowed scientists to directly observe movements occurring in cells although the mechanism behind these phenomena remained a mystery. Dujardin (1835) first observed movement of food vacuoles and "particles" along filopodial networks in protists. Chromosome migration, important in cell replication and heredity (Flemming, 1878), and cell shape changes important during embryogenesis, were also described a century ago (Davenport, 1895).

Research since then has demonstrated the importance of the cytoskeleton in cytoplasmic movements. Microtubules have been linked with cell shape, cell movement and intracellular transport. Important is their relative stability/instability (see Chapter 1), association with MAPs and their intrinsic polarity. Because MTs have a structural and growth asymmetry, it is not surprising that the polarity plays

an important role in the mechanism of MT-based transport.

Most MT research has been done on neural tissue. Neurons serve as ideal models for studying MT function because of their unique morphology and their extensive MT arrays. Vertebrate neurons are usually composed of a single, long axon and several dendrites which originate from the cell body. Functionally, the axon is specialized to transmit information over long distances as opposed to dendrites which receive and process information. They are also different structurally in terms of their shape and internal cytoplasmic components (Black and Baas, 1989). Axonal MTs have their plus ends oriented distal to the cell body (Heidemann et al., 1981) and can reach lengths up to 100 μM (Bray and Bunge, 1981), while dendrites contain MTs of mixed polarity with approximately fifty percent in each direction (Heidemann et al., 1981). Axons do not contain any of the cellular protein synthesis machinery as the cell body makes all the components necessary for its growth (Lasek and Brady, 1981). Consequently the highly polarized MT array gives structural support as well as directing the transport of organelles and proteins through the axoplasm (Black and Baas, 1989). There is great interest in how this MT array arises and functions in cytoplasmic transport.

While MT assembly can occur *de novo* by self-assembly of free tubulin subunits, it usually occurs by elongation from a nucleating structure or a MT template (Kirschner, 1978). MT nucleation is spatially regulated by discrete nucleating structures. The centrosomes are the main microtubule organizing centres (MTOCs) in the cell, usually located in a supranuclear position (Brinkley,

1985; Karsenti and Maro, 1986). The centrosome contains a fibrogranular matrix called the pericentriolar material which surrounds two short microtubule structures called the centrioles (Joshi, 1993). MTs appear to originate from the pericentriolar material. A novel tubulin, gamma(γ)-tubulin, which is very similar to α- and β-tubulin, is strictly localized to the pericentriolar material in MTOCs in many different organisms (Oakley and Oakley, 1989; Stearns et al., 1991). Because of its location, it is proposed to bind to the α- and β- heterodimers thus initiating MT formation and elongation (Oakley et al., 1990; Stearns et al., 1991). Gamma-tubulin is highly conserved and is essential for the formation of MTs in virtually all eucaryotic cell types examined thus far (Joshi et al., 1992). The (-) ends of the MTs are usually embedded within the nucleating structure while the (+) ends radiate away from it (Haimo et al., 1979; Heidemann et al., 1981). An important feature of MT nucleating structures is that they generate MT arrays of uniform polarity orientation (Oakley et al., 1990).

Polarity, along with MAPs, provides the molecular basis underlying MT-based cellular transport. Structural MAPs bind to assembled MTs already assembled increasing their stability (Sloboda and Rosenbaum, 1979; Murphy et al., 1977; see Chapter 1). Other MAPs are intricately involved in MT-based motility and are the mechanoenzymes or "motors" of cytoplasmic transport. The introduction of *in vitro* motility assays in the early 1980's, using the AVEC-DIC light microscopy technique, lead to the discovery and revealed functional aspects of these motors. Assays were initially developed using squid giant axon extracts of *Loligo pealeii* (Vale et al., 1985 a,b). MTs could be resolved and the movement

of optically detectable organelles and vesicles could be observed in real time in living tissue (Allen et al., 1981; 1982). As axonal MTs are oriented with their (+) ends toward the periphery, the polarity of movement was either (+) end-directed (anterograde) or (-) end-directed (retrograde) (Allen et al., 1982). These early motility assays led to the discovery that AMP-PNP (5'adenylylimidodiphosphate) caused organelles to bind and cease movement on MTs. This non-hydrolyzable analog of ATP was used for the purification of the first cytoplasmic translocator called kinesin (Vale et al., 1985c).

Kinesin was shown to "walk" over MTs causing the movement of kinesin-coated beads towards the (+) end of the MT (Vale et al., 1985d; Porter et al., 1987b). This ATPase was proposed to be the anterograde motor in fast axonal transport (Vale et al., 1985c). Since this soluble motor is unidirectional but bidirectional movement of organelles is observed along MTs both *in vivo* and *in vitro* (Brady et al., 1985; Vale et al., 1985a,b,d; Gilbert et al., 1985), the search for the retrograde motor intensified. This retrograde movement would have a similar direction of action as axonemal dynein. This ATPase, discovered years earlier in axonemes of eucaryotic cilia and flagella, is involved in their motility (Gibbons, 1965; Luck, 1984). Since vesicular transport was known to involve MTs and ATP hydrolysis, the existence of a cytoplasmic form of dynein was proposed (Bloom et al., 1984).

Direct evidence of cytoplasmic dynein came from the discovery of 5 MAPs which could be separated from MTs in neuronal tissue (Bloom et al., 1984). One of these, MAP 1C, is the least prominent and is structurally and functionally

distinct. It has ATPase activity that is stimulated in the presence of MTs (Paschal et al., 1987; Shpetner et al., 1988). The enzyme activity is greatly reduced in the presence of axonemal dynein inhibitors such as vanadate, NEM, and EHNA (Shpetner et al., 1988). MAP 1C is not affected by AMP-PNP which inhibits kinesin-based movement (Lasek and Brady, 1985). Unlike kinesin, which can produce motility along MTs by hydrolysis of the nucleotides ATP, GTP, UTP, CTP and ITP (Cohn et al., 1987), MAP 1C can only produce force in the presence of ATP (Shpetner et al., 1988). As well MAP 1C preferentially uses Mg^{2+}ATP as a substrate over Ca^{2+}ATP, whereas the opposite holds true for kinesin (Shpetner et al., 1988; Vale et al., 1985b). Another property of MAP 1C that distinguishes it from kinesin is that it cleaves into specific cleavage products when exposed to UV light in the presence of vanadate and ATP resulting in a selective inhibition of only retrograde transport *in vitro* (Gibbons et al., 1987; Lye et al., 1987; Paschal and Vallee, 1987; Porter et al., 1987a).

SDS-PAGE analysis shows that MAP 1C consists of an α and a β heavy chain with M_r of ~300 kDA (versus 115-135 kDa for the two α heavy chains found in kinesin) and sediments on sucrose gradients at 20S (versus 9.5S for kinesin), (Vale et al., 1985a; Bloom et al., 1984). Additional bands copurify with MAP 1C, giving strong evidence that it is a multisubunit protein complex (Paschal et al., 1987). Its total molecular weight is $1.2x10^3$ kDa, very close to that of axonemal dynein (Vallee et al., 1988). Scanning transmission electron microscopy (STEM), shows that MAP 1C is a two-headed particle on which the ATPase activity site is localized using photoaffinity analogues of ATP (Vallee et

al., 1988). The two heads are similar in appearance to those seen in *Tetrahymena* and sea urchin outer arm flagellar dynein (Johnson and Wall, 1983; Bell et al., 1979). Therefore it appears that MAP 1C has an ATP-sensitive binding site which probably forms a complex with MTs in the absence of ATP (Paschal et al., 1991). The heads are connected to a common base which is composed of at least four globular subdomains (Johnson, 1985; Goodenough and Heuser, 1984; Vallee et al., 1988). However MAP 1C does not appear to have the ATP-insensitive site found in axonemal dynein, which stably attaches this enzyme to MTs in axonemes (Vallee et al., 1989). These structural differences may very well be the cause of the functional differences between the dynein ATPases, as axonemal dynein interacts solely with MTs yet cytoplasmic dynein binds to both MTs and to its "cargo" such as membranous organelles (Vallee, et al., 1989). Cytoplasmic dynein may be an evolutionary predecessor of axonemal dynein (Pratt, 1989). The most important property of MAP 1C is that it induces MT movement along coated coverslips *in vitro* at a slightly faster rate (~1.25μm/sec versus 0.6μm/sec), and in an opposite direction, to that observed with kinesin (Paschal and Vallee, 1987; Vale et al., 1985c,d). This retrograde or "minus" end directed movement confirms that MAP 1C is the cytoplasmic dynein hypothesized for years.

In different systems the isolation and characterization of kinesin and cytoplasmic dynein has met with varied and sometimes contradictory results, perhaps reflecting differences in purification techniques or the existence of motor isoforms within and/or between organisms. Kinesin has been found in many cell

types including the sea urchin egg (Porter et al., 1987b), *Drosophila* (Saxton et al., 1988), bovine adrenal gland (Murofushi et al., 1988) and rat liver (Collins and Vallee, 1989). Several research teams discovered dynein-like ATPase activity in unfertilized sea urchin eggs (Weisenburg and Taylor, 1968; Pratt, 1980; Hisanaga and Sakai, 1980; Hollenback, et al., 1984; Asai and Wilson, 1985; Penningroth et al., 1985). They found two isoforms of dynein; one which appeared to be a precursor for axonemal dynein in the embryonic cilia which form at the late blastula stage of development (Porter et al., 1988), and another isoform which was proven likely to be cytoplasmic dynein, designated HMr-3 (Scholey, et al., 1984). Cytoplasmic dynein-like forms have also been found and characterized in chick embryo fibroblasts (Schroer et al., 1989), *Paramecium* (Schroer et al., 1989), squid (Schnapp and Reese, 1989), *Dictyostelium* (Koonce and McIntosh, 1990), *Caenorhabditis elegans* (Lye et al., 1987) and rat liver and testis (Collins and Vallee, 1989; Neely and Boekelheide, 1988).

There is general agreement that MT-associated motors probably evolved to provide the force to transport components too large to move by simple diffusion quickly over long distances to specific locations in the cell (Schroer and Sheetz, 1991). Motors also play a role in the formation of the mitotic spindles and force generation during mitosis (Fuller and Wilson, 1992). Although both kinesin and cytoplasmic dynein use ATP to translocate themselves and/or their "cargo" along MTs, it is obvious that they differ enzymatically, structurally and functionally (Schnapp and Reese, 1986; Amos, 1987). Whether or not these are universal motors is unclear without further comparative work. New evidence is also

showing that other MT motors may exist (Shpetner and Vallee, 1989). With new biochemical and molecular techniques it is now possible to identify, isolate and characterize these enzymes from a variety of organisms; create *in vitro* reconstitutions of the molecular components of translocating systems; and use high resolution analysis to visualize organelle movements in living cells (Inoué, 1981). *In vitro* motility assays allow for exposure of the transport systems to pharmacological agents such as ATP analogs and ATP inhibitors to assess potential motors responsible for particle transport based on their known sensitivity to these agents (Vale et al., 1985c; Gilbert et al., 1985). Identifying and understanding the mechanisms underlying intracellular transport is an age-old problem and consequently this exciting area of cell biology is currently a "hotspot" for research.

The polarity of the trophic cord MTs in telotrophic ovarioles has been examined in only one insect species (Stebbings and Hunt, 1983). Considering the significant variations in MT structure and function that exists between insect species, it is important to determine MT polarity in other species to establish if common mechanisms exist. I investigated MT polarity in *Rhodnius*. Using hook decoration, I found that MTs were oriented in *Rhodnius* trophic cords with the (-) ends of the MTs located in the oocytes and the (+) ends extending towards the tropharium, similar to the observations made by Stebbings and Hunts in *Oncopeltus* (1983). This has structural implications on the assembly of the MTs and well as functional implications as to the directionality of transport which would likely be via a retrograde motor. In 1990, Anastasi and her colleagues

showed that while kinesin was present in another telotrophic ovariole system, immunological studies did not reveal its presence in the trophic cords. Kinesin has also been demonstrated in *Rhodnius* ovarioles (Huebner and Diehl-Jones, 1993). Application of exogenous isolated axonemal dynein to ovarioles of *Notonecta glauca* bound the cord MTs in an ATP-sensitive manner, implying that a similar native protein could be involved in trophic cord cytoplasmic transport (Stebbings and Hunt, 1985). A dynein-like band was detected in gels of *Oncopeltus fasciatus* ovariole protein, but no movement of latex beads occurred on MTs *in vitro*, possibly due to the small amount present in the extract (Anastasi et al., 1990). As well, AVEC-DIC was utilized to study transport in two other insect species. *Dysdercus intermedius* cords supported bidirectional movement of mitochondria (Dittmann et al., 1987), while *Oncopeltus* isolated cord MTs only supported retrograde movements (Stebbings and Hunt, 1987).

I investigated the role of motors in transport in *Rhodnius* trophic cords. I used indirect immunocytochemistry to screen the trophic cords for dynein and kinesin but a positive immunofluorescence signal was not detected. Subsequently I used AVEC-DIC to examine motility in the presence of dynein and kinesin inhibitors. I observed saltatory motions of particles showing movement towards the oocyte, ie. in a retrograde direction. This movement occurred at an average rate of 0.77 μm/second, and was ATP dependent. Organelle movement was sensitive to the motor inhibitors NEM and vanadate but unaffected by AMP-PNP. These results clearly indicate nurse cell-oocyte transport is MT-based and driven by a cytoplasmic dynein-like motor.

MATERIALS AND METHODS

Polarity Determination

Twice-cycled porcine brain tubulin was obtained for hook decoration of ovariole trophic cord MTs. The method of tubulin purification and hook decoration is as follows:

Tubulin Isolation

Tubulin was isolated from porcine tubulin following the twice-cycling protocol of Borisy et al., (1975). Three pig heads were obtained (Burns meats abbatoir, Winnipeg) and the brains were quickly removed and placed on ice within 30 minutes of slaughter. Superficial blood clots and vessels were removed and the brain was homogenized for 30 seconds in a prechilled Waring blender in 1.5 volume (ml)/ gram of tissue of ice-cold 100 mM PIPES (pH 6.94) containing 1.0 mM EGTA, 0.1 mM $MgSO_4$, 0.1 mM GTP and 4 M glycerol. The tissue was then homogenized (2-3 passes) with a motor driven pestle operated at 3000 rpm which disrupted the cells. The homogenate was cooled to 5°C by swirling on ice and centrifuged at 9000 $g_{(max)}$ in a Beckman Model J2-21M Centrifuge for 25 minutes at 4°C. The supernatant was transferred to several tubes and spun at 96,000 $g_{(max)}$ for 75 minutes at 4°C in a Beckman Model L8-55 Ultracentrifuge to produce supernatant called brain extract.

For the first cycle, the extract was made 1.0 mM in GTP (added dry) and brought to 37°C for an additional 30-45 minutes until viscosity was observed

indicating polymerization of MTs. The MT polymer was pelleted by centrifugation at 40,000 $g_{(max)}$ for 40 minutes at 37°C. The volume of the warm supernatant (H_1S) was recorded and the supernatant discarded. The MT pellet (H_1P) was resuspended in ice-cold polymerization buffer (100 mM PIPES (pH 6.94) containing 0.1 mM $MgSO_4$, 1mM EGTA and 1.0 mM GTP) using $1/7^{th}$ the H_1S volume and kept at 0°C for a total of 30 minutes to depolymerize the MTs. Monomers were resuspended with the aid of a Teflon-glass homogenizer. The depolymerized protein was centrifuged to remove contaminating microsomes and protein aggregates at 40,000 $g_{(max)}$ for 30 minutes at 0°C. The resulting cold supernatant contained the tubulin monomers and MAPs. The cold pellet (C_1P) was discarded.

For the second cycle, GTP was added to 1.0 mM to the extract and brought to 37°C for 15-30 minutes until polymerization occurred. The MT polymer was pelleted by centrifugation at 40,000 $g_{(max)}$ for 30 minutes at 37°C. The volume of the warm supernatant (H_2S) was recorded and discarded. After two cycles of purification the porcine brain MT protein (H_2P) was frozen in liquid nitrogen and stored at -80° C, maintaining full retention of polymerization activity. The expected yield of protein was from 0.3 to 0.7 mg H_2P per 1 g brain cortex homogenized. When needed, the MT pellet (H_2P) was resuspended in Hook buffer [500 mM PIPES (pH 6.94) containing 1 mM MgCl, 1mM EDTA and 1.0 mM GTP] using 0.4 the H_2S (supernatant) volume and kept at 0°C for a total of 30 minutes to depolymerize the MTs. The depolymerized protein was ultracentrifuged to remove oligomers and spontaneous polymers at 200,000 $g_{(max)}$

for 3 hours at 5°C. The resulting cold supernatant contained the tubulin monomers and MAPs. The cold pellet (C_2P) was discarded. Protein determination of the upper third of the supernatant was done using a Bradford assay (Biorad). The supernatant was stored in liquid nitrogen until just before use.

SDS-PAGE Analysis and Western Blotting

SDS-PAGE was performed on twice-cycled porcine tubulin to determine purification success. Samples of porcine tubulin were run on a 10% acrylamide (10%T, 2.7%C) resolving gel as described in Chapter 1. Gels were transferred to nitrocellulose and screened for 4 anti-tubulin antibodies as described in Chapter 1.

Hook decoration of Trophic cord MTs

Hook decoration was performed following the method of Heidemann and McIntosh (1980). *Rhodnius* ovarioles were desheathed in Rhodnius Ringers (without Ca^{2+}) then washed in 100 mM PIPES (pH 6.94) containing 1 mM EGTA and 1 mM $MgSO_4$ (PEM buffer). Each ovariole was then placed in 2 µl of elastase Type IV (1 mg/ml in PEM buffer) to digest the basement membranes for 7 minutes and then placed and microdissected in PEM buffer to isolate trophic cords. The tissue was transferred to Hook buffer containing double-strength of the following: 0.5% Triton X-100 (or Brij-58), 0.5% NaDOC and 0.2% SDS. Immediately before use, the tubulin was thawed and adjusted to a final

concentration of 4 mg/ml in Hook buffer containing (2x): 1mM GTP, 2.5% (v/v) DMSO and 20 µg/ml RNase. Hook buffer containing tubulin (2x) was added in an equal volume to the Hook buffer containing detergents. Ovarioles were incubated in this final Hook buffer at 4°C for 20 minutes to allow soluble tubulin to infiltrate the tissue, at room temperature for 5 minutes, and at 37°C for 30 minutes to allow protofilament hook decoration to occur.

Electron Microscopy

The ovarioles were fixed in 2% GTA in PEM buffer for 45 minutes. The ovarioles were then washed with PEM buffer and embedded in 3% melted agarose in the same buffer and put on ice to harden. Blocks of the supported tissue were cut out and placed in a vial containing a small amount of PEM buffer. The ovarioles were post-fixed in 1% OsO_4 in 100 mM sodium cacodylate buffer (pH 7.1) for 45 minutes, and then washed several times in the same buffer. Tissue was stained *en bloc* with 2% aqueous uranyl acetate for 1 hour followed by quick dehydration in an ice-cold 70%, 80%, 95%, and 100% EtOH series. The tissue was allowed to warm up to room temperature followed by 3 changes of room temperature 100% EtOH for 30 minutes each. The tissue was transferred to a 1:1 mixture of 100% EtOH and acetone for 15 minutes followed by 2 changes of acetone for 30 minutes each. Ovarioles were infiltrated in 1:1 acetone and Epon plastic (6 ml DDSA (dodecenyl succinic anhydride), 2.5 ml Epon 812, 2 ml Araldite 502) and 0.3 ml DMP (2,4,6-tri(dimethylaminomethyl) phenol) overnight. Each ovariole was embedded in degassed plastic in flat

molds for 2 days at 60° C. Tissue was orientated longitudinally in the block such that cords were closer to the face of the block and the tropharium located distally. The cords were aligned such that they (and internal MTs) would be cut in cross-section. Semi-thin sections were cut on glass knives and stained with Toluidine Blue to establish the orientation and tissue location before thin sectioning. Silver sections were cut on a Sorval Porter Blum MT2-B Ultramicrotome using a diamond knife at 2° and transferred to 200-mesh copper grids. The sections were stained with lead citrate (Venable and Coggeshall, 1965) for 2 minutes and examined with a Hitachi H7000 STEM.

Indirect Immunocytochemistry

Indirect immunocytochemistry of DGD-embedded ovariole sections using anti-motor antibodies was performed using immunofluorescence methods described in Chapter 1. Polyclonal antibodies to *Drosophila* kinesin were kindly supplied by Bill Saxton (U of Indiana). Pre-immune sera (R99) diluted 1:500 in PBS-BSA and anti-fly heavy chain (R1.5), diluted 1:5000, were both used. Monoclonal antibodies against dynein intermediate chain (clone 70.1) and heavy chain (clone 440.4) in chicken embryo brain were obtained from Sigma and also diluted in PBS-BSA (1:100 and 1:2000, respectively). Secondary antibodies were as described in Chapter 1.

Motility Assays (AVEC-DIC Microscopy)

Adult ovarioles, 3 to 4 days post-feed, were removed and desheathed in

Rhodnius Ringers (-Ca^{2+}). Ovarioles were microdissected using tungsten needles to expose trophic cords attached to the tropharium. The tissue was transferred to Motility Buffer without ATP (35 mM PIPES (pH 7.4) and 5 mM $MgS0_4$) (modified from Dabora and Sheetz, 1988) and placed on slides. A chromic acid cleaned coverslip, with corner drops of VALAP (Vaseline, lanolin, paraffin, 1:1:1) as spacers, was placed over the tissue. The height of the spacers allowed the tissue to be held without becoming artificially flattened. The VALAP droplets were slowly melted down by touching the corners of the coverslip glass using a heated wire just until the VALAP melted, attaching the coverslip to the slide preventing subsequent shifting of the coverslip and tissue. Ovarioles were exposed to various solutions by placing a drop of experimental solution at one edge of the coverslip and drawing away fluid at the opposite side using filter paper. Solutions were readded frequently to prevent dehydration. Motility was observed in the presence or absence of 1 mM ATP, 1 mM AMP-PNP, 2 mM NEM (N-ethylmaleimide), 5 μM sodium ortho-vanadate ($NaVO_4$), and 50 μM $NaVO_4$, all obtained from Sigma. The inhibitors were diluted in Motility Buffer + ATP and added after motility was supported in buffer alone. Three trials for each inhibitor were run to assess sensitivity.

A Zeiss Photo I microscope especially equipped for high resolution DIC was used for observation and video recording. Microscope illumination was with a 200 watt Mercury arc lamp and a heat filter and green light was selected using a narrow band pass 546 nm mercury green line filter. The DIC optics consisted of a 100x Plan objective (NA 1.25) equipped with an individual DIC Nicol slider and

the matched DIC Nicol beam splitter in the condenser and the appropriate polarizers. Video images were obtained with a Hammamatsu CCD Model C2400 with manual gain control and visualized using a video imaging system (Image 1) in a 486 PC computer and Sony Trinitron Super fine monitor. Video tape recordings were made on 0.5-inch S-VHS videotape using a Sony SV0-9500 MD videocassette recorder in real time for up to 30 minutes. With Image-1, still frames at selected time intervals were sequentially captured and recorded to analyze direction and rates of vesicular movements. Distances were calibrated using a micrometer recorded at the same objective powers used in the motility assays. Normal motility was determined by tracking and capturing still frames of 12 different mitochondria at 1-second intervals. The still frames of normal motility and inhibitor trials were photographed and printed at the same magnification as micrometer images. Distances were measured and rates determined. Sensitivity to inhibitors was determined by observing significant increases or decreases in motility following treatment. From this information, the trophic cord MT-based motility could be characterized and compared to MT-based movement in other systems.

Photography

Photography for gels, epifluorescent images and Image-1 data employed the same methods discussed in Chapter 1. Electron micrographs were taken on Kodak Electron Microscope Film 4489 and developed using D19 developer according to manufacturer's instructions.

RESULTS

Hook Decoration

Heidemann and McIntosh (1980) showed that the curvature of protofilament hooks formed on endogenous MTs is a reliable method to determine the intrinsic polarity of the MTs. The tissue is detergent-extracted and then incubated in a MT assembly mixture containing exogenous tubulin. During the incubation, asymmetric protofilament sheets assemble on the walls of endogenous MTs, appearing as hooks in cross-section when examined by electron microscopy. Special care must be taken throughout the procedure to monitor the orientation of the tissue.

Trial and error was necessary to optimize the variety of experimental conditions for hook formation. Optimal tubulin yield from porcine brain was achieved with including 4M glycerol in the initial homogenization buffer. Tubulin purification is verified in Figure 35, Chapter 1. Obtaining ideal hook formation came from varying detergent concentrations and type, using either Brij-58 and Triton X-100 to optimize access of the porcine tubulin to the trophic cord MTs (Figs. 3-6). Varying tubulin concentration as well as the length, number and temperature of incubations for hook assembly was also necessary. I found that using either Triton X-100 or Brij-58 at a concentration of 0.5 % gave sufficient cell lysis (Figs. 3-6) while higher concentrations extracted many of the endogenous MTs in earlier trials. A greater percentage of MTs were decorated

using Triton X-100 then Brij-58 as a detergent (Table I, rows A to E). As Triton X-100 is a stronger detergent, it likely allowed more of the porcine tubulin to diffuse into the trophic cords, thereby increasing the likelihood of MTs being decorated. More hooks per MT were also seen when this detergent was used (Figs. 5 and 6). Brij-58-extracted ovarioles had lower percentages of MTs being decorated (Table I, rows 1 to 6), and most decorated MTs showed only 1 or 2 hooks (Figs. 3-4). Tubulin at 2 mg/ml was the optimal concentration, as lower concentrations showed very little hook assembly in previous trials. Incubation at low temperatures for 20 minutes was found to be necessary to allow sufficient tubulin diffusion into the cords and incubation at 37°C for 30 minutes was determined as the optimal time for hook formation. Less than 30 minutes resulted in very short, and indistinguishable hooks on the trophic cord MTs. An initial trial, using 3 mg/ml tubulin and 45 minutes of incubation at 37°C, showed uninterpretable "rosettes" of hooks on MTs, possibly due to a slightly higher concentration of tubulin or the long 37°C incubation period (Fig. 2).

Many areas of trophic cords and trophic core were examined for MT polarity according to criteria used by Heidemann and McIntosh (1981) and Redenbach and Vogl (1991). Decorated MTs were classified as either "clockwise", "counterclockwise" or "ambiguous" (Table I). Clockwise-curving hooks indicate the observer is looking from the (+) towards the (-) end of the MT, while counterclockwise hooks indicate the observer is looking towards the (+) end of a MT (Heidemann and McIntosh, 1980). Hooks which formed on hooks (rosettes), MTs containing hooks in both directions, and closed hooks were considered

ambiguous. Percentages of hook configurations were determined by dividing the total hooks of either category by the total number of unambiguous decorated MTs (Table I).

I found that the majority of MTs, 93.5 % (Table I), had counterclockwise hooks. Only 6.5% of MTs showed clockwise protofilament hooks (Table I). Tissue orientation was maintained throughout the procedure such that the observer was looking from the oocyte region towards the tropharium. These results indicate that trophic cord MTs are oriented with their (-) or slow-growing ends in the oocyte and their (+) or fast growing ends towards the trophic core. Since most MTs were decorated with this hook configuration, the MT array was assumed to be unipolar. These results are summarized schematically in Figure 7.

Motility Assays

Indirect immunocytochemistry failed to reveal the presence of either dynein or kinesin within the trophic cords (Figs. 8-9). Consequently, live tissue was observed to determine MT and MT motor involvement in nurse cell-oocyte cytoplasmic transport.

In vitro motility assays require precise experimental conditions to support movement *in vitro* and to reactivate motility as close to *in vivo* conditions as possible. A hypotonic motility buffer (35 mM PIPES (pH 7.4)) was found to be optimal to support MT-based movement as higher concentrations significantly decreased movement. ATP concentrations above 10 mM also reduced motility.

$MgSO_4$ was also necessary for movement to occur. However there was little movement in the presence of EGTA at low concentrations. This could be due to chelation of Mg^{2+}ATP which appeared to be necessary for movement. Consequently, the final ideal motility buffer contained 35mM PIPES (pH 7.4), 5 mM $MgSO_4$ and 1 mM ATP.

Organelles which moved were membranous as movement ceased when tissue was detergent extracted with 0.05% Triton X-100. Most were spherical, and some elongated, rod-like organelles which were likely mitochondria (Figs. 10-11). Organelles varied in diameter from approximately 2 μm to 0.2 μm (the resolution limit of the light microscope) (Figs. 10-11). Only a fraction of the vesicles was moving at any one time. All particle motions occurred on an array of linear elements which were straight or curved and intersected one another at various points along the cord (Figs. 10-11). These were assumed to be MTs as they are the only cytoskeletal component identified in the trophic cord interior (Huebner and Gutzeit, 1986).

Organelles within the cords moved in a MT-based fashion towards the oocyte region only. These vesicles moved smoothly for up to 20 μm with an average velocity of 0.77 ± 0.19 μm/second (Mean + standard deviation, n=12). Organelle movements were saltatory, exhibiting frequent stops, starts and minor oscillations. These observations were very similar to what has been reported in other systems (Vale et al., 1985a,b).

The velocities of movements were usually uniform but often the rates and the distances moved varied for the same vesicle as it moved down the cord. The

times of rest also varied. Organelles showed oocyte-directed movement throughout the cord showing no preferential areas of traffic. Organelles occasionally switched from one linear element to another and also appeared to be pulled back and forth between the MT bundles. After a period of time, some organelles detached and showed Brownian movement, and periodically reattached to the linear elements often exhibiting movement again. Movement appeared to be less frequent and decline over time with a greater proportion of organelles showing Brownian movement.

Motility was not observed in either direction in the presence of 50 μM vanadate ($NaVO_4$) or 2 mM NEM (Table II). Organelles appeared to stop moving with the exception of Brownian movement within minutes of applying these specific inhibitors. In the presence of 1 mM AMP-PNP and 5 μM vanadate, movement did not appear to be affected and organelles moved with the same frequency, rate and direction as seen with Motility Buffer containing ATP alone (Table II). The directionality of transport was retrograde (towards the (-) ends of MTs) similar to cytoplasmic dynein action (Table III). The rate of movement was faster than that seen for kinesin (0.6 μm/s), but slower than that observed for cytoplasmic dynein (1.25 μm/s). Movement was ATP dependent as seen with dynein and kinesin-based motility (Table III). Like cytoplasmic dynein, the trophic cord MT-based movement was sensitive to 2 mM NEM and 50 μM vanadate but resistant to 1 mM AMP-PNP (Table III). However, the resistance of trophic cord MT motility to 5 μM vanadate was a characteristic similar to kinesin-based motility (Table III).

PLATE 1

Undecorated and Decorated Trophic Cord MTs

Figure 1. Electron micrograph of a cross-section through a trophic cord showing typical undecorated MTs. x180 000.

Figure 2. Electron micrograph of a cross-section through a trophic cord after a lengthy 37°C incubation period with a higher tubulin concentration (3 mg/ml). Note the heavily decorated MTs showing "rosettes" of hooks many of which were regarded as uninterpretable. x100 000.

Figure 3. Electron micrograph of an extracted trophic cord using 0.5% Brij-58, 2 mg/ml tubulin and 30 minutes of 37°C incubation in Hook Buffer. Many of the MTs are decorated (arrows) and show counterclockwise hooks when viewed from the oocyte towards the trophic core region. x65 000.

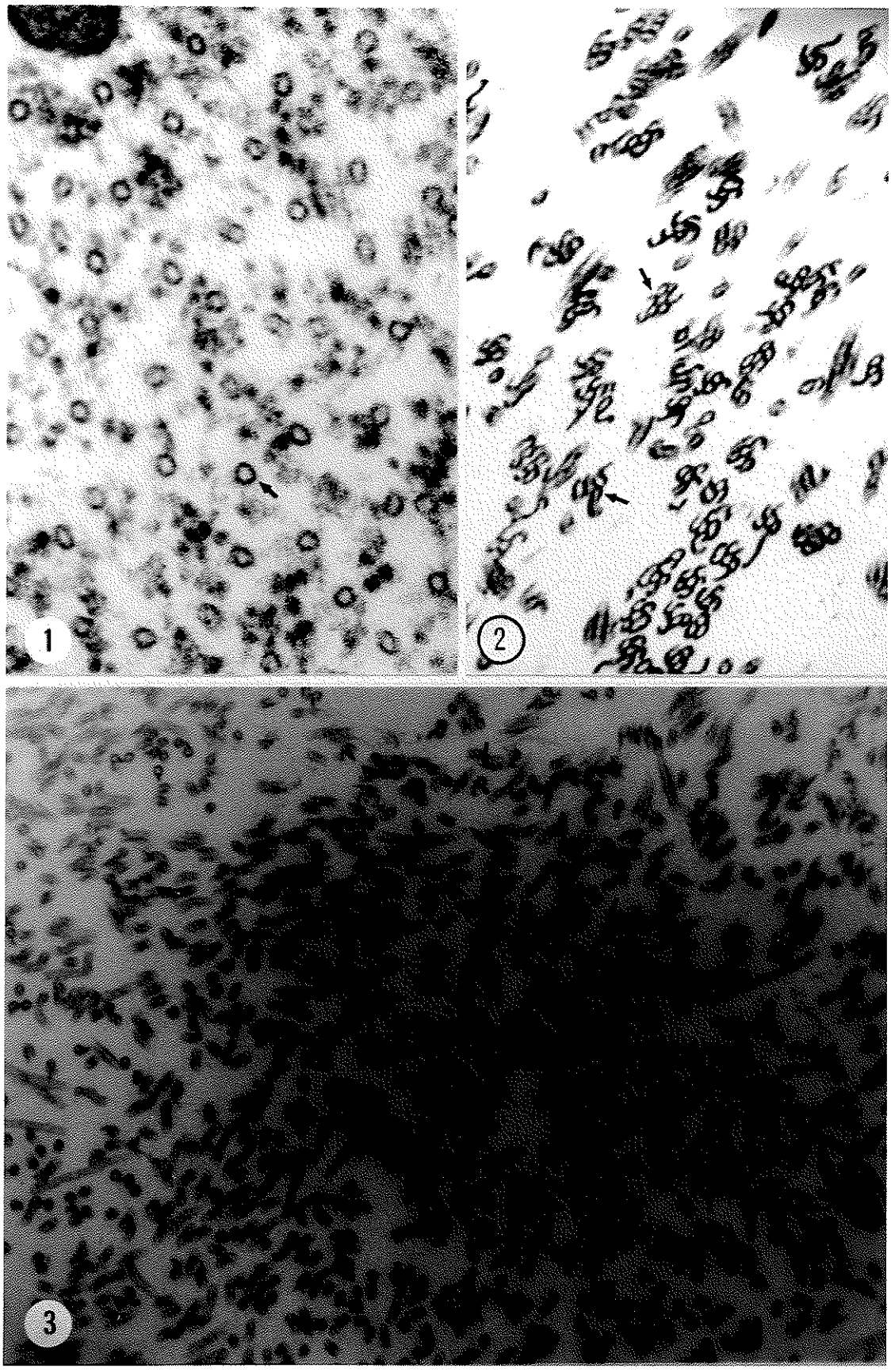
1
2
3

PLATE 2

Hook Decorated Trophic Cord and Trophic Core MTs

Figure 4. Electron micrograph of another region of an Brij-58 extracted trophic cord showing primarily counterclockwise hook decoration on the ovarian MTs (arrows). x55 000.

Figure 5. Cross-section TEM showing decorated MTs (arrows) of the trophic core following 0.5% Triton X-100 extraction, as viewed from the oocyte looking towards the tropharium. x25 000.

Figure 6. Trophic cord cross-section following extraction with 0.5% Triton X-100. The majority of hooks are counterclockwise (arrows) indicating that the microtubules have their (+) ends in the tropharium and their (-) ends in the oocyte. The inset shows a higher magnification of a typical decorated MT. x100 000, 575 000.

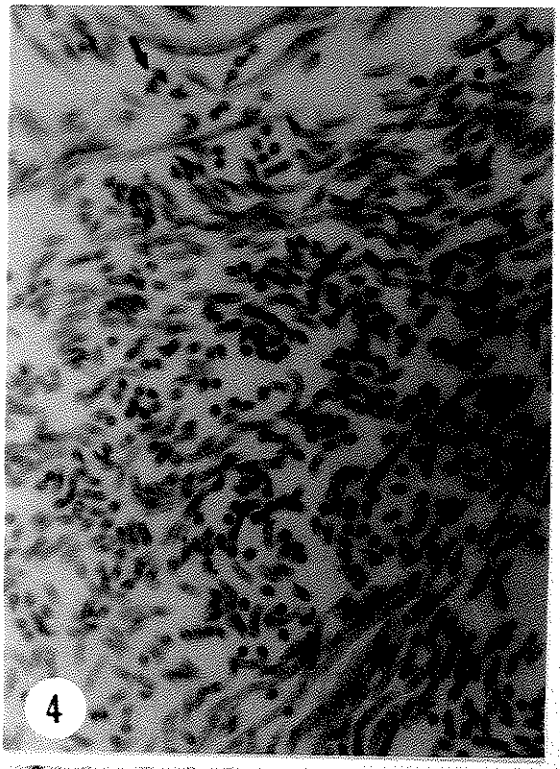

4

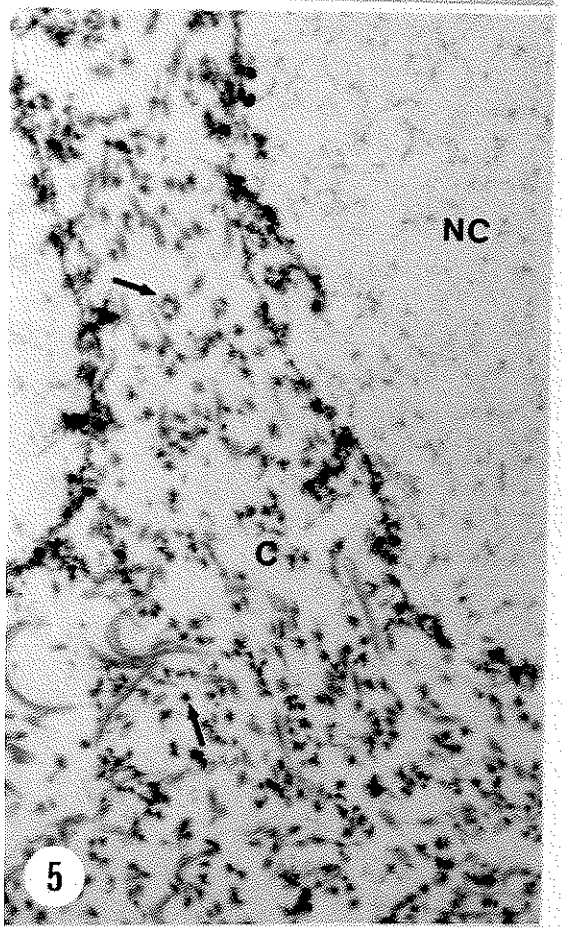

5

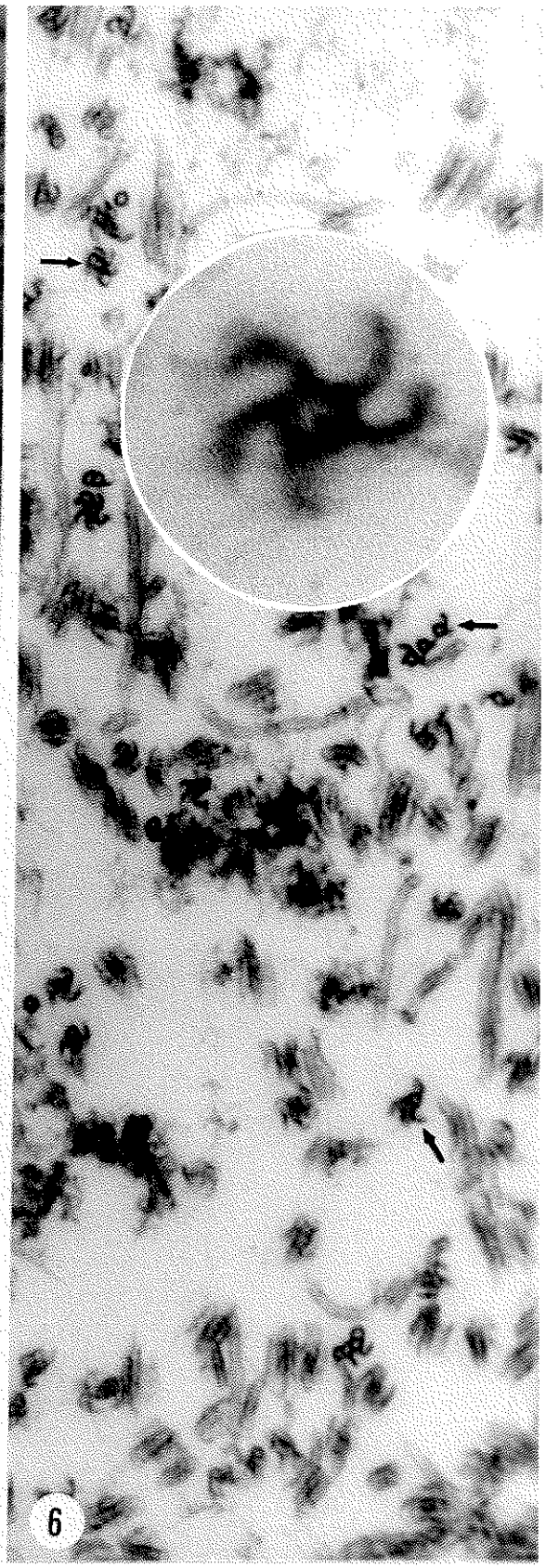

6

TABLE I: Hook Curvature for Oocyte-to-Nurse Cell Viewed Microtubules in Trophic Cords.

Section*	MTs with Counterclockwise Hooks	MTs with Clockwise Hooks	MTs with Ambiguous Hooks	Total Decorated MTs (%)§
A	37	1	15	100.0
B	23	7	15	97.8
C	48	10	14	91.1
D	42	3	12	100.0
E	50	5	14	86.3
1	42	2	2	41.8
2	56	1	0	40.7
3	48	0	0	44.0
4	35	1	0	63.2
5	41	1	1	53.7
6	39	1	1	41.4
Total	461	32	74	—
Percent*	93.5	6.5	—	—

* Table shows the number of MTs with 3 categories of hooks detailed in text in 11 cross-sections viewed from the oocyte towards the tropharium region using 0.5% Triton X-100 detergent (sections A-E) and 0.5% Brij-58 (sections 1-6).

§ The percentage of decorated MTs was calculated by counting the number of decorated MTs and dividing by the total MTs seen in the field.

* The total percentages of hooks were calculated for unambiguous decorated hooks.

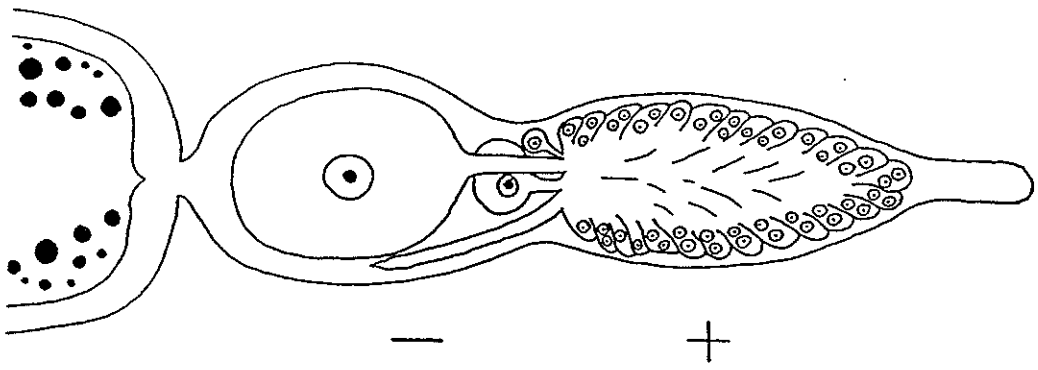

Figure 7. Summary diagram showing hook decoration results. Note the microtubule polarity of the *Rhodnius* telotrophic ovariole with the (+) ends in the tropharium and the (-) ends in the oocytes.

PLATE 3

Immunocytochemistry of Motors and AVEC-DIC Analysis

Figure 8. Immunofluorescence micrograph showing negative results in the ovariole when stained for anti-dynein antibody (Sigma, clone 70.1). x 600.

Figure 9. Negative results observed in the ovariole following immunofluorescent staining with a polyclonal anti-kinesin antibody (R 1.5). x700.

Figure 10. Light micrograph of a microdissected trophic cord (x 1000) showing insets (a to e) of stills taken from the video recorder at 1-second intervals. Arrows show movement of a presumptive mitochondria moving to the upper left towards the oocyte. (Bar= 3 μm).

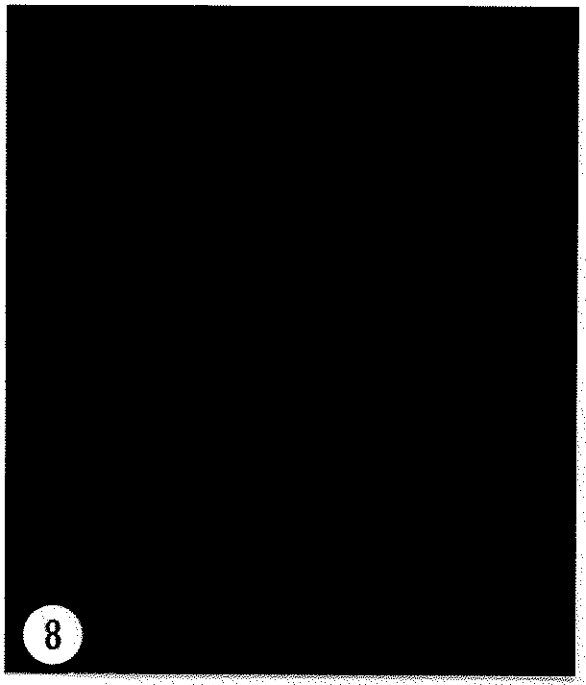
8

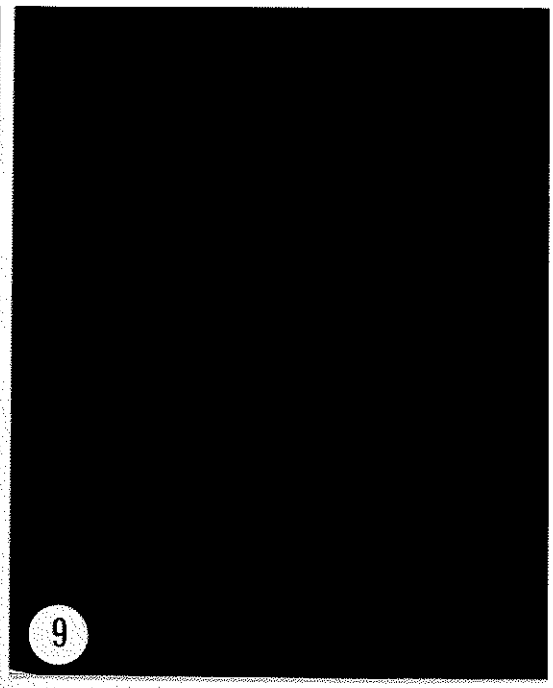
9

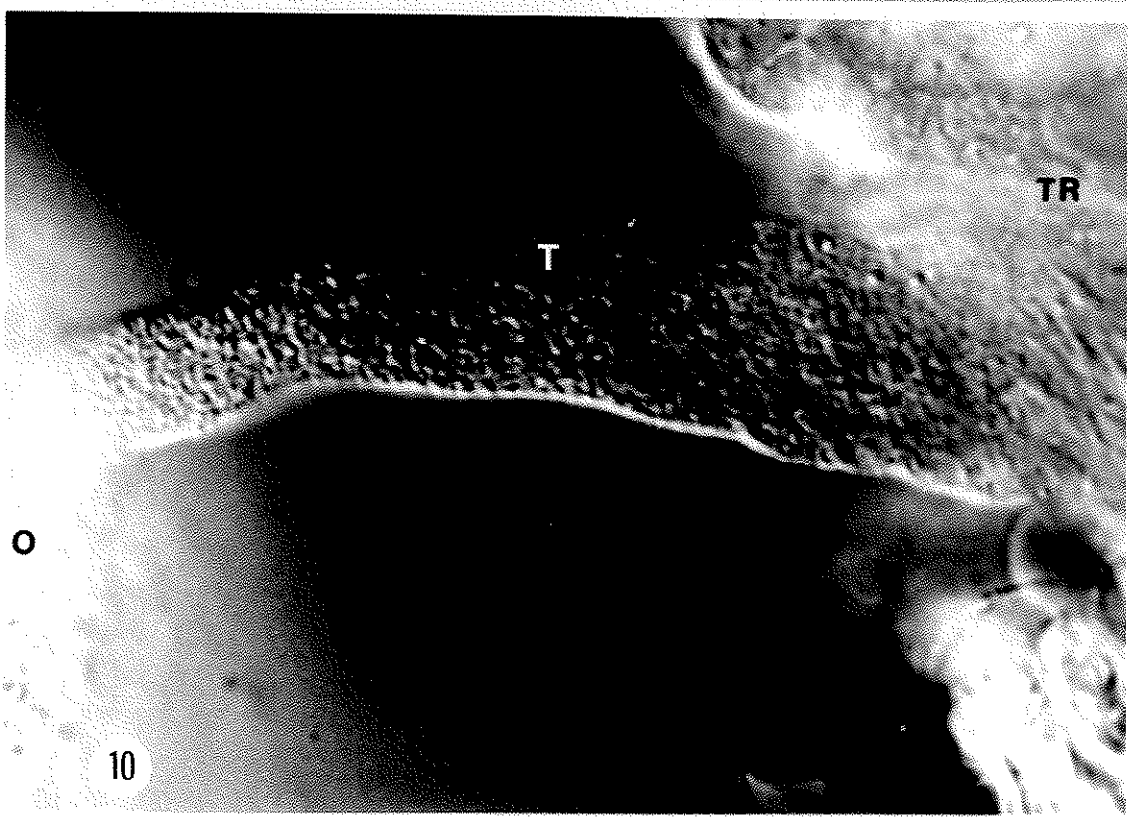
TR
T
O
10

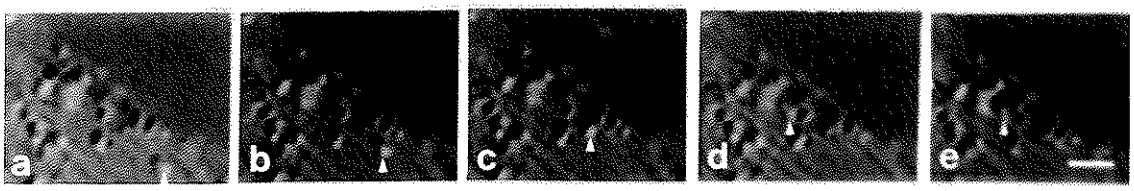
a
b
c
d
e

PLATE 4

Organelle Movement viewed using AVEC-DIC

Video Microscopy

Figure 11. Image-1 still frames taken at 1-second intervals (a to h) tracking the movement of a mitochondria (arrow) along distinctly visible tracks through an isolated trophic cord. The oocyte is in the upper left direction. (Bar= 5 μm)

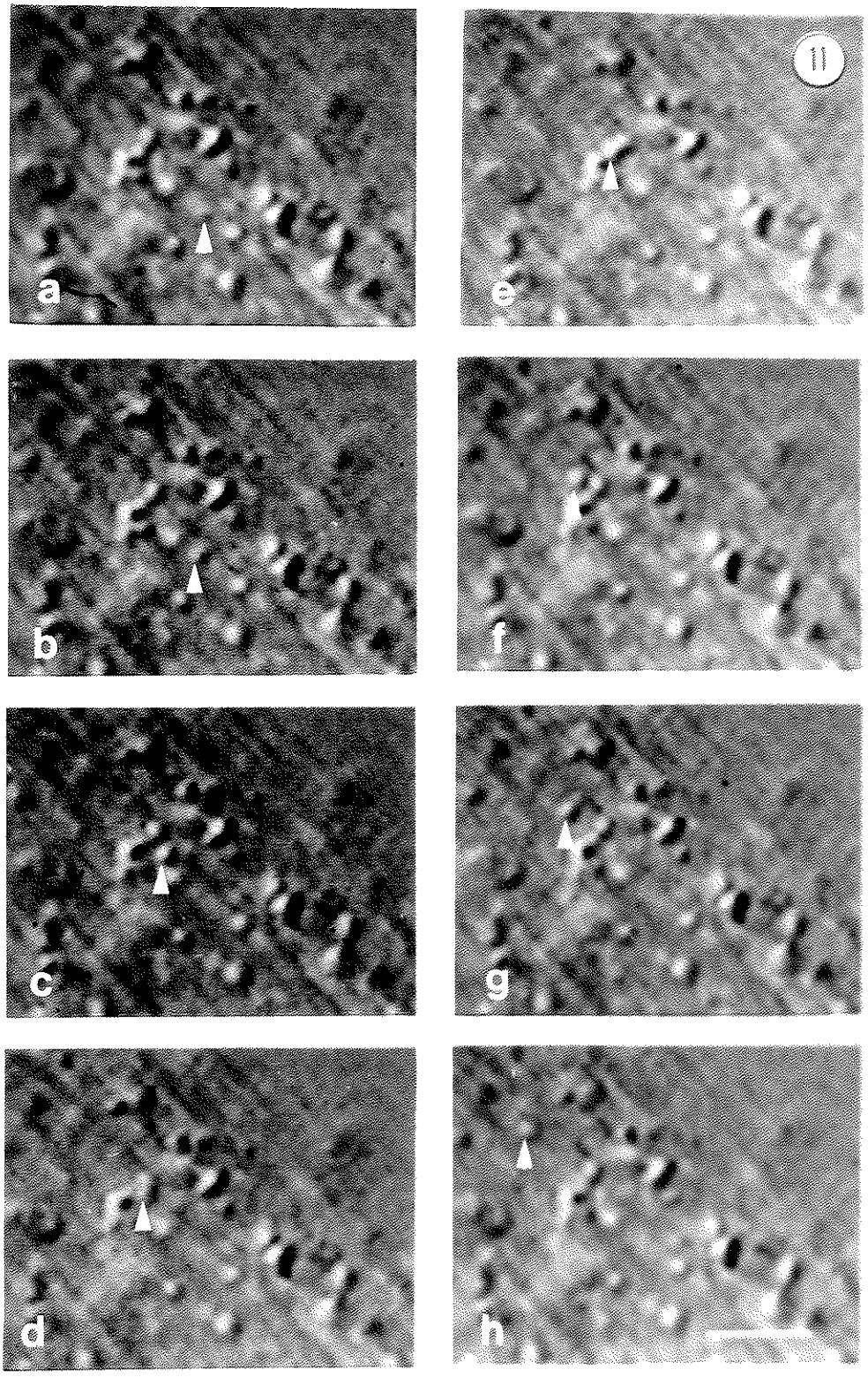
a
b
c
d
e
f
g
h
11

TABLE II: Effects of Motor Inhibitors Upon Motility* in Isolated Trophic Cords

Inhibitor§	Motility
None (Motility Buffer + ATP)	+
Motility Buffer without ATP	-
1 mM AMP-PNP	+
5 μM vanadate	+
50 μM vanadate	-
2 mM NEM	-

* The effect on motility was determined to be positive if a significant increase or decrease in motility was observed following treatment compared to normal motility (0.77 μM/s).

§ Inhibitors were diluted in Motility Buffer + ATP.

TABLE III: Comparison of Trophic Cord Motility Characteristics with Cytoplasmic Dynein* and Kinesin* -Driven Motility.

Characteristic	Trophic Cord	Cytoplasmic Dynein	Kinesin
Movement in Retrograde Direction	+	+	-
Rate of Movement	0.77 μM/s	1.25 μM/s	0.60 μM/s
Movement ATP-dependent	+	+	+
Sensitive to 1 mM AMP-PNP	-	-	+
Sensitive to 5 μM vanadate	-	+	-
Sensitive to 50 μM vanadate	+	+	+
Sensitive to 2 mM NEM	+	+	-

* Data from a variety of sources summarized in Brady, 1991.

DISCUSSION

MT Polarity

Based on hook decoration, the polarity of the trophic cord MTs was interpreted as having (-) ends in the oocytes and (+) ends in the tropharium. The method is not perfect as flagella axonemes, which have unipolar MTs, show at least 10% of MTs with opposite hook curvature (Heidemann, 1991) the vast majority (93.5%) of decorated MTs in *Rhodnius* were the same indicating unipolar MTs. As stated by Heidemann (1991), any deviations may be due to local conditions during the experiment which affect the interaction between hook protofilaments and the MTs, or perhaps because of biological variability of MTs.

This MT polarity is similar to the polarity described by Stebbings and Hunt (1983) in *Oncopeltus* trophic cords. Hook decoration has also revealed parallel MT arrays in many other systems having their (+) ends extending towards the periphery. These include chicken sensory neurites (Baas et al., 1987), cat post-ganglionic sympathetic fibers (Heidemann et al., 1981), frog olfactory neurons (Burton and Paige, 1981), teleost photoreceptors (Troutt and Burnside, 1988a) and melanophores (McNiven and Porter, 1986), and rat hippocampal neurons (Baas et al., 1988). As well, several cell types have unipolar MT arrays with their (-) ends directed peripherally. These include Sertoli cells (Redenbach and Vogl, 1991), MDCK (Madin Darby canine kidney) cells (Bacallao et al., 1989), teleost retinal pigmented epithelial cells (Troutt and Burnside, 1988b) and *Drosophila* wing epidermal cells (Mogensen et al., 1989). These studies support the

widespread acceptance and reliability of this technique.

Determining the polarity is important when considering the functional aspects of the insect telotrophic ovariole. These involve the role of MT polarity in the overall shape of the ovariole, the direction of organelle transport and the ultimate distribution of cellular organelles between the nurse cell and oocyte compartments.

Polarity and Trophic Cord MT Assembly

The polarity of trophic cord MTs in *Rhodnius* telotrophic ovarioles substantiates previous research on these MTs and raises some interesting questions about the origin, maintenance and eventual disassembly of these dramatic MT arrays. The development of trophic cords begins 6 days before the adult molt (Valdimarsson and Huebner, 1989). The cord MTs grow from the oocyte compartments towards the tropharium. As the cords increase in width and length, the MTs increase in length and number with a slight decrease in packing density in growing oocytes compared to the small, quiescent oocytes (Valdimarsson and Huebner, 1989). This packing density then remains the same until redundancy and bundling occurs (Huebner, 1981). The total tubulin within the ovariole increases coincidentally with MT growth from 6 days before molt until 1 day before molt after which it remains constant (Valdimarsson and Huebner, 1989). Whether the tubulin is produced in the nurse cells or oocytes is unknown. It is likely that the nurse cells synthesize the soluble tubulin which then diffuses

through the intracellular bridges to the oocyte where it is initially assembled. Because there is a continuous synthesis of tubulin while the MT arrays are being established, there is likely a high pool of tubulin subunits relative to MT polymers. This is critical because a lower subunit pool would cause net disassembly and the MT array could not be established. Conditions which favor MT assembly would contribute to potential MAP binding and/or acetylation of the MTs to generate a stable trophic cord MT array. During development, it is believed that the cords developing between each young oocyte and sibling nurse cell clusters intermingle in the larval tropharium region and undergo membrane fusions to produce the common, MT-packed trophic core during the larval to adult transformation (Valdimarsson and Huebner, 1989). According to my results, the trophic core which forms contains the (+) ends of the cord MTs which would imply a more dynamic MT domain. Like MTs in the polytrophic ovariole of *Drosophila* the dynamic instability of MTs in this region may allow populations to extend through ring canals; these perhaps becoming (+) end-stabilized preventing disassembly, via factors and MT-capping proteins in the nurse-cell cytoplasm (Therkauf et al., 1992). Ring canals associated with nurse cells have also been observed in 5th-instar larval *Rhodnius* ovarioles (Yeow and Huebner, 1994).

Although, the timing and oocyte origin of the cord MTs is known (Valdimarsson and Huebner, 1989), a nucleating centre has not been observed. This is true for all telotrophic species examined. Because the MTs are oriented with their (-) ends in the oocyte this is where an MTOC would be located if this is

how the MT array arises. Although there are MTs around the entire cortex of the oocytes (MacPherson and Huebner, 1993), the majority of the trophic cord MTs appear to extend from the apex of the oocyte. This might possibly be the region of a potential centrosome. However this is in an unusual location given that most centrosomes are located adjacent to the nucleus (Brinkley, 1985).

Recent research in *Drosophila* has generated interesting hypotheses about the establishment of these polarized MT arrays. In the polytrophic ovariole of *Drosophila*, a posterior MTOC within the oocytes nucleates an array of MTs, whose (+) ends extend through ring canals connecting all the cells in an egg chamber (Therkauf et al., 1993). This MTOC degenerates at the time when nurse-cell oocyte transport stops and the MTs then associate with the oocyte cortex. MT nucleation then appears to originate from the apical cortex and the MTs extend towards the posterior end (Therkauf et al., 1992). This reversal in polarity would then allow for anterior-posterior mRNA localization within the oocyte (Therkauf, 1994).

In *Rhodnius*, it is possible that, as in *Drosophila*, a maternal MTOC located at the posterior pole produces the oocyte cortical MT array observed by MacPherson and Huebner (1993), which then extends through the trophic cords. This MTOC then degenerates or loses its function, after which the MTs associate with the cortex of the egg. Since telotrophic ovarioles contain trophic cords with a much denser MT array compared to the oocyte cortex, further nucleation could occur at the apex of the oocytes. This could occur by a new MTOC turned on later in development. Although this explains how the MT may arise, it does not

explain the mechanics of redundancy which distinguishes trophic cord MT arrays from other systems examined.

During vitellogenesis of the T (terminal) oocyte, the cord decreases in diameter and closes at the apex of the oocyte while the MTs pack into bundles. Soon after the redundant cord is resorbed very quickly (Huebner, 1981). According to my polarity findings and observations on the stable redundant cord MTs, this would predict that the MTs disassemble at a faster rate in the trophic core where the (+) ends are located, while the slow-growing (-) ends of the MTs are drawn towards the tropharium. The MTs eventually all disassemble and tubulin subunits are presumably recycled into the growing ends of MTs in other cords. In most systems examined MT assembly and disassembly radiates away and towards the site of origin, respectively. However, in *Rhodnius* the MTs move in the opposite direction to their oocyte origin when the redundant cords retract, making this system highly unique. This also means that the MTs cannot be embedded in a stationary MTOC upon redundancy. For this reason, it is worthwhile to examine the establishment of the unipolar axonal MT array.

Axonal MTs are also not attached to a centrosome but are free in the cytoplasm (Bray and Bunge, 1981). There are two popular theories on the origin and maintenance of the axonal MTs with substantive evidence on both sides and aspects of both likely are involved. The first is that the cell body is responsible and the other is that local mechanisms exist within the axon itself for production of the MT array.

Axonal MTs have a 13-protofilament structure which is typical of MTs

assembled from a nucleating site such as a centrosome (Evans et al., 1985). The distribution of gamma-tubulin is restricted to the pericentriolar region within the soma only (Baas and Joshi, 1992). Therefore if gamma-tubulin is required for nucleation of axonal MTs, these MTs must first originate from the cell body and highly specialized mechanisms must exist to establish and maintain MT polarity orientation in the axon. Using experimental conditions which stopped MT assembly without depolymerizing existing MTs, Baas and Ahmad (1993) showed an increase in MT polymer in the axon simultaneously occurred with a decrease in polymer within the cell body. This indicated that preformed MTs were made within the cell body which then moved into the axon (Baas and Ahmad, 1993). It has been proposed that similar mechanisms are involved in shuttling polymerized MTs into the axon as found in organelle movement; that is, via motors (Baas and Ahmad, 1993). Unidirectional active transport mechanisms could move MTs into the axon with their plus ends leading, suggesting a dynein-like motor involvement (Joshi and Baas, 1993). The movement would be far slower considering the size of the MT polymer compared to an organelle. These MTs could move along neurofilaments, endoplasmic reticulum within the axon or other MTs themselves (Baas and Ahmad, 1993).

A similar mechanism for the origin of trophic cord MTs may exist in *Rhodnius*. An oocyte centrosome may produce MTs which then detach and move in a motor-dependent fashion along the cortex, endoplasmic reticulum or other MTs into the cords. This is consistent with other studies in *Rhodnius.* In the adult ovariole small cords are about 10 μm in width and grow as large as 35 μm

in diameter in the T-1 oocyte with a constant insertion of new MTs as they grow (Huebner, 1981). The larger cords which are as long as 1 mm in length contain up to 50 000 MTs with 100-250 MTs per μm^2. During vitellogenesis the cord to the T-1 oocyte increases in diameter at an inversely proportional rate to the decrease in width of the cord to the T oocyte. The T-1 oocyte then arrests its growth when the oocyte reaches approximately 400 μm in diameter until the T oocyte completes vitellogenesis (Huebner, 1981). It appears from my motility results that dynein is located in the cords and the presence of acetylated α-tubulin suggest MAP interactions. This could explain the MT arrangements during redundancy as they would not be attached to a nucleating site. Because redundancy appears to proceed from the oocyte end towards the trophic region it is likely under oocyte control (Woodruff and Anderson, 1984). Redundancy occurs at a time when the cortical MT network in *Rhodnius* oocytes undergoes dramatic alterations and reorganization at the onset of vitellogenesis (MacPherson and Huebner, 1993). At the same time. Ca^{2+} ion channels appear to open at the apex of the oocyte, resulting in a Ca^{2+} influx (Diehl-Jones and Huebner, 1993). This likely has implications on the trophic cord MTs if indeed their (-) ends are free in the cytoplasm as they will begin to disassemble allowing cord closure and separating these MTs from the oocyte cortex MTs which remain. Although it is possible that trophic cords originate in a similar manner to axonal MTs, further studies are needed to determine the source of MT nucleation, perhaps by screening the ovarioles with gamma-tubulin antibodies.

Although the MTs arise in the oocyte, most likely from a centrosome,

elongation within the cords must occur. Like axonal MTs, the cord MTs are often longer than the diameter of the cell body/ oocyte. Therefore substantial MT assembly must occur at the plus ends within these structures (Joshi and Baas, 1993). Over half of the MT mass of the axon is rich in tyrosinated α-tubulin while the other half shows both detyrosinated and acetylated α-tubulin (Baas and Black, 1990). These stable MTs may act as the nucleating structures within the axon (Brady et al., 1984; Black et al., 1984; Baas and Heidemann, 1986), and immunoelectron microscopic analysis shows many MTs with tyrosinated portions at the (+) ends of MTs in direct continuity with stable domains enriched in detyrosinated and acetylated MTs towards the (-) end (Baas and Black, 1990). This suggests that MTs assembly from preexisting stable MTs and uniform polarity is maintained. Labelling newly assembled MTs showed that the MTs elongate from the plus ends of preexisting MTs and no new polymers form *de novo* in the axon (Baas and Ahmad, 1993). Dynamic instability may allow many of these MTs to give up tubulin subunits for the elongation of other MTs, resulting in a shift during transit from large numbers of short MTs to a smaller number of longer MTs (Lasek, 1986).

Therefore the transport of MTs and their dynamic instability would work together to produce the characteristic MT array (Joshi and Baas, 1993). This is similar to the MT array in the subpellicar region of *Trypanosoma brucei* which has a unipolar configuration with the (+) ends located towards the posterior end of the cell (Robinson et al., 1995) and shows more dynamic, tyrosinated regions of the MT array in this region. It appears that as MTs are laid down between the

array they become selectively modified towards the more stable (-) end region of a MT perhaps by the formation of MAP cross-bridges (Sherwin and Gull, 1989). As well, Gard and associates (1990) observed that *Xenopus* previtellogenic oocytes in early diplotene did not have any functional MTOCs indicating inactivation of earlier maternal MTOCs while the acetylated MT arrays established earlier persisted (Gard et al., 1995). They proposed that these stable MT subsets then become the nucleating sites for future MT assembly (Gard et al., 1995).

In *Rhodnius* it is possible that not all the cord MTs are modified and some of the domains are exclusively tyrosinated and represent MTs which have been recently polymerized and inserted throughout the cord. These dynamic domains may also be found at the (+) ends of MTs in continuity with modified ends via acetylation. Acetylated MTs may act as the source of nucleation within the cords. Immunoelectron analysis using these antibodies would be necessary to verify these possibilities.

Polarity and Transport (AVEC-DIC Analysis)

Functionally, the polarity of the MTs in *Rhodnius* cords indicate that likely a minus-end directed MT motor such as cytoplasmic dynein is involved in nurse cell-oocyte transport. Although I did not observe dynein localized in the cords using indirect immunofluorescence this may be due to limited resolution or to low cross-reactivity reported for dynein antibodies. Howard Stebbings' lab also

attempted to determine the motor by analyzing axonemal dynein binding to the MTs (Stebbings and Hunt, 1985). However, this only shows that these MTs are competent to bind a dynein motor and does not give information about the transport mechanisms in the living system. Our lab and Stebbings' lab have attempted to purify MT motor proteins from whole ovarioles. A problems with this technique is that the amount of tissue from even hundreds of ovarioles is insufficient for adequate analysis of the enzymes. As well, motors are isolated from the entire ovariole, containing many cell types. This technique does not give information about the motor content and activities specifically within the trophic cords.

Consequently, I felt the most expedient approach was to observe organelle transport *in vitro* and assess the motor involvement using vesicle rates, direction of cytoplasmic transport and sensitivity of motility to various motor inhibitors. Several technical attempts made to observe fluorescently labelled exogenous and endogenous mitochondrial transport were unsuccessful as it was impossible to resolve single mitochondria once they passed into the cord with fluorescence microscopy, due to the thickness of the ovariole tissue. Application of confocal microscopy may solve this problem. Successful observations of motility *in vitro* was finally obtained by utilizing AVEC-DIC microscopy. This approach has been very successful for studying axonal transport as well as the regulation and direction of organelle movements along MTs in other systems such as chromatophores and *Reticulomyxa* (Rozdzial and Haimo, 1986; Koonce and Schliwa, 1986). Chromatophores can disperse or aggregate all of their pigment

granules at once and provide a good model to study particle translocation (Lynch et al., 1986). Protists such *Reticulomyxa* are also useful as they have thin processes to easily visualize transport along MTs (Travis et al., 1983).

When viewed with light microscopy using DIC optics, these organelles and vesicles appear as particles of different sizes and shapes attached to and/or moving along linear elements. Although one cannot identify these particles using DIC alone, their identity as mitochondria, lysosomes and other vesicles was determined using immunofluorescence in other systems (Hayden, 1988). Evidence for MT-based movement of Golgi vesicles and ER has also been observed (Cooper et al., 1990; Dunn et al., 1989). In *Rhodnius*, extensive studies using EM show that the cords are filled predominately with ribosomes and mitochondria and MTs as the sole cytoskeletal component present in the interior of the cords (Huebner, 1981). This suggests that the observed vesicles are likely mitochondria and the tracks which support their movement, the extensive MT array.

Organelles moved smoothly for up to 20 μm with an average velocity of 0.77 + 0.19 μm/s (Mean ± Standard Deviation, n=12) towards the oocyte. The movement towards the oocyte, based on the polarity determination of the MTs was therefore retrograde. In *Dysdercus* intact ovarioles, bidirectional movement of mitochondria occurred at rates of 3 μm/minute, much slower than seen in *Oncopeltus* which moved at rates of 7 μm/second in a retrograde direction only (Dittmann et al., 1987; Stebbings and Hunt, 1987). Like *Rhodnius*, *Oncopeltus* cords only exhibited unidirectional retrograde movement of vesicles on isolated

cord MTs but at a much faster rate of 7 μm/s. In *Dysdercus* the mitochondria exhibited a saltatory motion with slightly faster rates towards the oocyte as opposed to those moving towards the tropharium (Dittmann et al., 1987). Consequently, MT-based transport in *Rhodnius* was more similar to that in *Oncopeltus,* as both showed unidirectional transport of vesicles towards the oocyte.

The organelle movements I observed were usually saltatory, exhibiting frequent stops with slight oscillations and lengthy rest periods before moving again. Movement lasted for up to 20 seconds which is similar to that seen in axons (22-49 seconds) (Koles et al., 1982). Variations in velocity did occur as seen in axonal transport which varies from 0.1-2.0 μm/s (Koles et al., 1982). Oscillations between movements is also typical and occurs at rates of 0.02-0.05 Hz in axons (Koles et al., 1982). These observations were very similar to interrupted motion Type I which stops and starts in one direction only as observed in axonal transport (Weiss et al., 1986). Although the majority of the vesicles were stationary during observations times, this is also seen in *Dysdercus* cords and is typical of axonal transport (Dittmann et al., 1987; Koles et al., 1982). The frequent stops during transport are not unusual for saltatory movement. It has been suggested that an increase in cytoplasmic ADP following intense ATPase activity of the motors signals a stop in movement along the MTs (Bereiter-Hahn and Voth, 1983). Movement did not seem to occur preferentially along any particular subset of cord MTs. Interestingly, in lobster axons, only 25% of central axonal MTs are involved in vesicle transport (Miller et al., 1987).

The detachment of organelles over time that I observed, is also seen in other systems and may be due to a dilution effect or degradation of required cellular components and is not likely due to differences in the basic organelle transport mechanisms (Vale et al., 1985d).

Like *Oncopeltus*, there was little motility in the cords of intact ovarioles which were not microdissected, which could be due to limited resolution in this densely packed network (Stebbings and Hunt, 1987). The cord MTs seemed to disperse once they were partially exposed. The fraying of the cord MTs may be due to an ATP-dependent bundling mechanism which is released during motility experiments in the presence of ATP. This is also observed in *Reticulomyxa* and *Oncopeltus* (Koonce and Schliwa, 1986; Stebbings and Hunt, 1987).

Although is has been suspected that these cord MTs in *Rhodnius* functioned more than a sieve, this is the first evidence for direct MT involvement in nurse cell-oocyte transport. These results indicate a directed, and MT-based transport system in *Rhodnius*. Like axons, these unipolar MT arrays play a significant role in cytoplasmic transport.

Dynein Involvement

The rate of retrograde movement of 0.77 μm/s was faster then that of kinesin-based motility in squid axoplasm studies (0.6 μm/s) (Paschal et al., 1987). Although motility in trophic cords was slower than observed for cytoplasmic dynein (1.25 μm/s), the rates observed for cytoplasmic dynein are

from isolated, polymerized MTs in axoplasmic extracts, allowing maximum activity (Schnapp and Reese, 1989). Crowding within the isolated trophic cords may not allow for maximal motor rates. Squid axons show bidirectional movement which is predominately anterograde (Vale et al., 1985d). Organelle transport in axons appears to be in part, or entirely driven by kinesin and cytoplasmic dynein (Vale et al., 1985d; Paschal et al., 1987), which generate movement in opposite directions along the unipolar array (Heidemann et al., 1981).

Because retrograde movement was observed, and the MTs determined to be unipolar, a dynein-like motor must exist within the cord either in the cytoplasm or likely on the organelles to allow for this transport. Since particles appear to be pulled laterally from one linear element to another and back, there appears to be many retrograde motors on a single particle. It is possible that both dynein and kinesin motors exist in the cords but regulation systems favor retrograde motor activity. The presence of both motors may be the cause of the local oscillations of vesicles between movements. If this is the case, both motors must be present on the organelles because the oscillations occur too quickly for the exchange of one set of motors on the organelles for another. Since kinesin has not been demonstrated in the trophic core or cords this is less likely.

The rate and direction of transport was very dynein-like. To further determine the properties of the vesicle translocator I observed the motility in the presence of well-established motor inhibitors. Movement was monitered in the trophic cords in the presence of 1 mM AMP-PNP, 5 μM and 50 μM vanadate and 2 mM NEM. Movement was not affected by AMP-PNP and low concentrations of

vanadate but was inhibited by NEM and higher concentrations of vanadate.

In *Oncopeltus*, movement was sensitive to 1 mM AMP-PNP but not to 1 mM vanadate (Stebbings and Hunt, 1987), which indicatives kinesin-dependent movement. AMP-PNP stops anterograde movement in squid axon (Vale et al., 1985c). Although AMP-PNP weakens the interaction of myosin with microfilaments it stabilizes the binding of membrane-bound organelles to MTs (Brady, 1991). Kinesin shows relative resistance to sulphydryl oxidizing agents which abolish ATPase activity such as N-ethylmaleimide (NEM) at 3-5 mM concentrations unlike cytoplasmic dynein (Paschal and Vallee, 1987). My results show that kinesin is likely not the motor responsible for MT-based transport, due to its resistance to AMP-PNP and sensitivity to NEM.

Vanadate inhibits cytoplasmic dynein at low concentrations below 10 μM but kinesin at least 5-fold higher concentrations in squid axoplasmic extracts (Brady, 1991). Vanadate thus is an important tool when studying motors as in its anionic form it is a potent inhibitor of dynein ATPase activity and function. It acts as a phosphate analog and forms a stable dynein-ADP-vanadate complex with vanadate binding to the site normally occupied by the gamma-phosphate of ATP (Shimizu and Johnson, 1983). Motility in trophic cords was only affected by higher concentrations of vanadate in *Rhodnius*. Although low concentrations of vanadate did not affect transport this could be due to unique enzymatic characteristics of the presumptive motor or a failure of this inhibitor to affect motor functions due to penetration or dilution difficulties. Vanadate does not readily permeabilize membranes and has multiple cellular targets (Vallee and

Shpetner, 1990). With the exception of motility resistance to micromolar concentrations of vanadate, the results of the inhibitor studies further suggest that the trophic cord MTs are directly involved in cytoplasmic transport to the oocytes through the actions of an endogenous cytoplasmic dynein motor.

Cytoplasmic Components Transported

Since many unipolar MT arrays already described have been shown to support bidirectional transport of organelles, the polarity does not exclusively determine the directionality of transport. It does appear that once the motors and regulating signals are in place, the polarity of the MT becomes critical in selectively moving organelles. Apart from MT polarity and motor presence and action, it appears that inherent properties within organelles also exist which may affect directional cytoplasmic transport (Black and Baas, 1989). This is observed in melanophores when the MT-rich processes are cut, as a reversal in pigment aggregation along the MTs occurs simultaneously with the reversal in MT polarity (McNiven and Porter, 1986).

In neurons, it is proposed that organelles are selectively transported into either the axon or the dendrites based on the polarity orientation of the MTs (Black and Baas, 1989). Although individual MTs have been shown to support transport in either direction, it appears that certain organelles move preferentially towards the (+) or (-) ends (Allen et al., 1985). In axons, secretory vesicles move

towards the (+) ends of MTs while endosomes and multivesicular bodies move towards the (-) ends of MTs (Allen et al., 1985). Golgi elements are usually associated near the centrosome where the (-) ends of MTs are embedded, and will resume this position if MTs are abolished and then allowed to reform (Rogalski et al., 1984). Ribosomes also seem to move specifically towards the (-) ends of MTs (MacGregor and Stebbings, 1970). Golgi and ribosomes are excluded from axons which contain exclusively MTs with their (+) ends away from the cell body, but are very enriched in dendrites which have a mixed population of MTs (Black and Baas, 1989).

Although my results show that mitochondria and membrane-bound vesicles appear to move along the MTs in *Rhodnius*, it is not known if other components are transported by motor-based motility. Besides the numerous ribosomes and mitochondria in the system, ER has also been observed in the cords (Huebner and Diehl-Jones, 1993). In *Notonecta* although most ribosomes move at a slow rate not consistent with MT based motility, some polypeptides have been shown to move at different rates suggesting synthetic flow is not the only explanation for transport (Stebbings et al., 1985). An electrophoretic transport system also may play a role since both *Rhodnius* and *Dysdercus* ovarioles show a voltage gradient between the tropharium and the oocytes, and both support the movement of (-) charged ions and coated beads but not (+) charged proteins through the trophic cords to the more (+) charged oocytes (Huebner and Diehl-Jones, 1993; Munz and Dittmann, 1987).

The movement of messenger RNA also appears to be microtubule-dependent

in other systems. Destroying the MTOC in *Drosophila* abolishes mRNA localization in the oocyte (Therkauf et al., 1993) and the localization of *bicoid* and *oskar* mRNAs to the anterior region of the oocyte is colchicine sensitive (Pokywka and Stephenson, 1991; Ephrussi et al., 1991). This gives strong evidence that the nurse cell-oocyte MTs are involved in mRNA transport. Similarly, in *Xenopus*, localization of Vg1 mRNA to the posterior pole is sensitive to colchicine suggesting it is mediated by MTs (Yisraeli et al., 1990). In polytrophic ovarioles, the polarity of the MTs connecting the nurse cells and oocytes also indicates transport would likely be due to a retrograde motor. This is likely via the dynein-like motor isolated by Li and colleagues (1994). Kinesin may also be involved in anterior-posterior localization of messages in the mature oocyte when the polarity of MT reverses during oogenesis (Therkauf et al.,1993). Despite recent progress, the precise mechanisms by which mRNA transport is regulated are essentially unknown. Whether or not *Rhodnius* trophic cord MTs play a role in mRNA transport and distribution has yet to be determined.

It does appear that the distribution of mitochondria and other organelles in the *Rhodnius* telotrophic ovariole depends on the polarity orientation of the trophic cord MTs and perhaps the directional preference of transport of organelles involved. Likely, ribosomes and mitochondria in *Rhodnius* are selectively transported to the (-) ends of MTs based on their configurations. This may reflect selective interactions with directional motors such as dynein or kinesin.

CONCLUSIONS

The determination that trophic cord MTs have their (-) ends in the oocytes is in agreement with the observations of MT formation during ovariole morphogenesis. The polarity of these MTs also suggests retrograde nurse cell-oocyte transport is involved. Using AVEC-DIC microscopy and inhibitor studies, cytoplasmic dynein-like organelle translocation was confirmed. This was the first report in *Rhodnius* that vesicle transport was motor-mediated along the trophic cord MT array. The polarity of the MTs thus provides the structural basis for the selective transport of nurse-cell components via a retrograde motor. Consequently the generation of this stable, unipolar MT array and its motor interactions produce a physiologically significant spatial polarity in structure and metabolism essential for accumulation and compartmentalization of cytoplasmic components during oogenesis.

LITERATURE CITED

Allen, R.D., Allen, N.S. and J. Travis. 1981. Video-enhanced contrast, differential interference contrast (AVEC-DIC) microscopy: A new method capable of analyzing microtubule-related motility in the reticulopodial network of *Allogromia laticollaris.* Cell Motil. **1**: 292-302.

Allen, R.K., Metuzals, J., Tasaki, I., Brady, S.T. and S.P. Gilbert. 1982. Fast axonal transport in squid giant axon. Science **218**: 1127-1129.

Allen, R.D., Weiss, D.G., Hayden, J.H., Brown, T.D., Fujiwake, H. and M. Simpson. 1985. Gliding movement of and bidirectional movement along single native microtubules from the squid axoplasm: Evidence for an active role of microtubules in cytoplasmic transport. J. Cell Biol. **100**: 1736-1752.

Amos, L.A. 1987. Kinesin from pig brain studied by electron microscopy. J. Cell Sci. **87**: 105-111.

Anastasi, A., Hunt, C. and H. Stebbings. 1990. Isolation of microtubule motors from an insect ovarian system: characterization using a novel motility substratum. J. Cell Sci. **96**: 63-69.

Asai, D.J. and L.S. Wilson. 1985. A latent activity dynein-like cytoplasmic magnesium adenosine triphosphatase. J. Biol. Chem. **260**: 699-702.

Baas, P.W. and S.R. Heidemann. 1986. Microtubule reassembly from nucleating fragments during the regrowth of amputated neurites. J. Cell Biol. **103**: 917-927.

Baas, P.W. and M.M. Black. 1990. Individual microtubules in the axon consist of domains that differ in both composition and stability. J. Cell Biol. **11**: 495-509.

Baas, P.W. and H.C. Joshi. 1992. Gamma-tubulin distribution in the neuron: implications for the origins of neuritic microtubules. J. Cell Biol. **119**: 171-178.

Baas, P.W. and F.J. Ahmad. 1993. The transport properties of axonal microtubules establish their polarity orientation. J. Cell Biol. **120**: 1427-1437.

Baas, P.W., White, L.A. and S.R. Heidemann. 1987. Microtubule polarity reversal accompanies regrowth of amputated neurites. Proc. Natl. Acad. Sci. USA

84: 5272-5276.

Baas, P.W., Deitch, J.S. and Black, M.M. and G.A. Banker. 1988. Polarity orientation of microtubules in hippocampal neurons: uniformity in the axon and nonuniformity in the dendrite. Proc. Natl. Acad. Sci. USA **85**: 8335-8339.

Bacallao, R., Antony, C., Dotti, C., Karsenti, E., Stelzer, E.H.K. and K. Simons. 1989. The subcellular organization of Madin-Darby canine kidney cells during the formation of a polarized epithelium. J. Cell Biol. **109**: 2817-2832.

Bell, C.W., Fronk, E. and I.R. Gibbons. 1979. Polypeptide subunits of dynein 1 from sea urchin sperm flagella. J. Supramol. Struct. **11**: 311-317.

Bereiter-Hahn, J. and M. Voth. 1983. Metabolic control of shape and structure of mitochondria in situ. Biol. Cell. **47**: 309-322.

Black, M.M. and P.W. Baas. 1989. The basis of polarity in neurons. Trends Neurosci. **12**: 211-214.

Black, M.M., Cochran, J.M. and J.T. Kurdyla. 1984. Solubility properties of neuronal tubulin: evidence for labile and stable microtubules. Brain. Res. **295**: 255-265.

Bloom, G.S., Schoenfield, T.A. and R.B. Vallee. 1984. Widespread distribution of the major polypeptide component of MAP 1 (microtubule-associated protein 1) in the nervous system. J. Cell Biol. **98**: 320-330.

Borisy, G.G., Marcum, J.M., Olmsted, J.B., Murphy, D.B. and K.A. Johnson. 1975. Purification of tubulin and associated high molecular weight proteins from porcine brain and characterization of microtubule assembly *in vitro*. Ann. N.Y. Acad. Sci. **253**: 107-132.

Brady, S.T. 1991. Molecular motors in the nervous system. Neuron **7**: 521-533.

Brady, S.T., Tytell, M. and R.J. Lasek. 1984. Axonal tubulin and axonal microtubules: biochemical evidence for cold stability. J. Cell Biol. **99**: 1716-1724.

Brady, S.T., Lasek, R.J. and R.D. Allen. 1985. Video microscopy of fast axonal transport in extruded axoplasm: A new model for study of molecular mechanisms. Cell Motil. **5**: 81-101.

Bray, D. and M.B. Bunge. 1981. Serial analysis of microtubules of cultured rat

sensory neurons. J. Neurocytol. **10**: 589-605.

Brinkley, B.R. 1985. Microtubule organizing centres. Annu. Rev. Cell Biol. **1**: 145-172.

Burton, P.R. and J.L. Paige. 1981. Polarity of axoplasmic microtubules in the olfactory nerve of the frog. Proc. Natl. Acad. Sci. USA **78**: 3269-3273.

Cohn, S.A., Ingold, A.L. and J.M. Scholey. 1987. Correlation between the ATPase and microtubule translocating activities of sea urchin egg kinesin. Nature **328**: 160-163.

Collins, C.A. and R.B. Vallee. 1989. Preparation of microtubules from rat liver and testis: cytoplasmic dynein is a major microtubule associated protein. Cell Motil. Cytoskel. **14**: 491-500.

Cooper, M.S., Cornell-Bell, A.H. Chernjavsky, A., Dani, J.W. and S.J. Smith. 1990. Tubulovesicular processes emerge from trans-Golgi cisternae, extend along microtubules, and interlink adjacent trans-Golgi elements into a reticulum. Cell **61**: 135-145.

Dabora, S.L. and M.P. Sheetz. 1988. Cultured cell extracts support organelle movement on microtubules *in vitro*. Cell Motil. Cytoskel. **10**: 482-495.

Davenport, C.B. 1895. Studies in morphogenesis. IV. A preliminary catalogue of the processes concerned in ontogeny. Bull. Museum Comp. Zool. Harvard **27**: 171-199.

Diehl-Jones, W. and E. Huebner. 1993. Ionic basis of bioelectric currents during oogenesis in an insect. Dev. Biol. **158**: 301-316.

Dittmann, F., Weiss, D.G. and A. Munz. 1987. The bidirectional movement of mitochondria in the ovarian trophic cord of *Dysdercus intermedius* (Heteroptera) resembles axonal transport. Roux's Arch. Dev. Biol. **196**: 407-413.

Dujardin, F. 1835. Recherches sur les organismes inferieurs. Ann. Sci. Nat. **4**: 238-377.

Dunn, K.W., McGraw, T.E. and F.R. Maxfield. 1989. Iterative fractionation of recycling receptors from lysosomally destined ligands in an early sorting endosome. J. Cell Biol. **109**: 3303-3314.

Ephrussi, A., Dickinson, L.K. and R. Lehman. 1991. *oskar* organizes the germ plasm and directs localization of the posterior determinant *nanos*. Cell **66**:

37-50.

Evans, L., Mitchison, T.J. and M.W. Kirschner. 1985. Influence of the centrosome on the structure of nucleated microtubules. J. Cell Biol. **100**: 1185-1191.

Flemming, W. 1878. Beitrage zur kenntniss der zelle und ihrer lebensercheinungen, Theil II. Archiv. Mikrosk. Anat. **18**: 151-259.

Fuller, M.T. and P.G. Wilson. 1992. Force and contraction in the mitotic spindle. Cell **71**: 547-550.

Gard, D.L., Affleck, D. and B.M. Error. 1995. Microtubule organization, acetylation, and nucleation in *Xenopus laevis* oocytes: II. A developmental transition in microtubule organization during early diplotene. Dev. Biol. **168**: 189-201.

Gibbons, I.R. 1965. Chemical dissection of the cilia. Arch. Biol. (Leige) **76**: 317-352.

Gibbons, I.R., Lee-Eiford, A., Mocz, G., Phillipson, C.A., Tang, W.J.Y. and B.H. Gibbons. 1987. Photosensitized cleavage of dynein heavy chains. J. Biol. Chem. **262**: 2780-2786.

Gilbert, S.P., Allen, R.D. and R.D. Sloboda. 1985. Translocation of vesicles from squid axoplasm on flagellar microtubules. Nature **315**: 245-248.

Gilbert, S.F. 1990. *Developmental Biology*. 3rd ed. Sinauer Associates, Inc., Sunderland, Mass. pp. 249-279.

Goodenough, U.W. and J.E. Heuser. 1984. Structural comparison of purified dynein proteins with *in situ* dynein arms. J. Mol. Biol. **180**: 1083-1118.

Haimo, L.T., Telzer, B.R. and J.L. Rosenbaum. 1979. Dynein binds to and crossbridges cytoplasmic microtubules. Proc. Natl. Acad. Sci. USA **76**: 5759-5763.

Hayden, J.H. 1988. Microtubule-associated organelle and vesicle transport in fibroblasts. Cell Motil. Cytoskel. **10**: 255-262.

Heidemann, S.R. 1991. Microtubule polarity determination based on formation of protofilament hooks. Methods Enzymol. **196**: 469-477.

Heidemann, S.R. and J.R. McIntosh. 1980. Visualisation of the structural polarity of microtubules. Nature **286**: 517-519.

Heidemann, S.R., Landers, J.M. and M.A. Hamborg. 1981. Polarity orientation of axonal microtubules. J. Cell Biol. **91**: 661-665.

Hisanaga, S.I. and H. Sakai. 1980. Cytoplasmic dynein of the sea urchin egg. I. Partial purification and characterization. Dev. Growth Differ. **22**: 373-384.

Hollenbeck, P.J., Suprynowicz, F. and W.Z. Cande. 1984. Cytoplasmic dynein-like ATPase cross-links microtubules in an ATP-sensitive manner. J. Cell Biol. **99**: 1251-1258.

Huebner, E. 1981. Nurse cell-oocyte interaction in the telotrophic ovaries of an insect, *Rhodnius prolixus.* Tissue Cell **13**: 105-125.

Huebner, E. and H. Gutzeit. 1986. Nurse cell-oocyte interaction: A new F-actin mesh associated with the microtubule-rich core of an insect ovariole. Tissue Cell **18**: 753-764.

Huebner, E. and W. Diehl-Jones. 1993. Nurse cell-oocyte interaction in the telotrophic ovary. Int. J. Insect Morph. Embryol. **22**: 369-387.

Inoué, S. 1981. Video image processing greatly enhances contrast, quality and speed in polarization-based microscopy. J. Cell Biol. **89**: 346-356.

Johnson, K.A. 1985. Pathway of the microtubule-dynein ATPase and the structure of dynein: a comparison with actomyosin. Annu. Rev. Biophys. Chem. **14**: 161-188.

Johnson, K.A. and J.S. Wall. 1983. Structure and molecular weight of the dynein ATPase. J. Cell Biol. **96**: 669-678.

Joshi, H.C. 1993. Gamma-tubulin: the hub of cellular microtubule assemblies. Bioessays **15(10)**: 637-643.

Joshi, H.C. and P.W. Baas. 1993. A new perspective on microtubules and axon growth. J. Cell biol. **121**: 1191-1196.

Joshi, H.C., Palacios, M.J., McNamara, L. and D.W. Cleveland. 1992. Gamma-tubulin is a centrosomal protein required for cell cycle-dependent microtubule nucleation. Nature (Lond.) **356**: 80-83.

Karsenti, K. and B. Maro. 1986. Centrosomes and the spatial distribution of microtubules in animal cells. Trends Biochem. Sci. **11**: 460-463.

Kirschner, M.W. 1978. Microtubule assembly and nucleation. Int. Rev. Cytol. **54**: 1-71.

Koles, Z.J., McLeod, K.D. and R.S. Smith. 1982. A study of the motion of organelles which undergo retrograde and anterograde rapid axonal transport in *Xenopus*. J. Physiol. **328**: 469-484.

Koonce, M.P and M. Schliwa. 1986. Reactivation of organelle movements along the cytoskeletal framework of a giant freshwater amoeba. J. Cell Biol. **103**: 606-612.

Koonce, M.P. and J.R. McIntosh. 1990. Identification and immunolocalization of a cytoplasmic dynein in *Dictyostelium.* Cell Motil. Cytoskel. **15**: 51-62.

Lasek, R.J. 1986. Polymer sliding in axons. J. Cell Sci. Suppl. **5**: 161-179.

Lasek, R.J. and S.T. Brady. 1981. The axon: a prototype for studying expressional cytoplasm. Cold Spring Harbor Symp. Quant. Biol. **46**: 113-124.

Lasek, R.J. and S.T. Brady. 1985. Attachment of transported vesicles to microtubules in axoplasm is facilitated by AMP-PNP. Nature **316**: 645-647.

Li, M., McGrail, M., Serr, M. and T.S. Hays. 1994. *Drosophila* cytoplasmic dynein, a microtubule motor that is asymmetrically localized in the oocyte. J. Cell Biol. **126(6)**: 1475-1494.

Luck, D.J.L. 1984. Genetic and biochemical dissection of the eukaryotic flagellum. J. Cell Biol. **98**: 789-794.

Lye, R.J., Porter, M.E., Scholey, J.M. and J.R. McIntosh. 1987. Identification of a microtubule-based cytoplasmic motor in the nematode *Caenorhabditis elegans*. Cell **51**: 305-318.

Lynch, T.J., Taylor, J.D. and T.T. Tchen. 1986. Regulation of pigment organelle translocation. I. Phosphorylation of the organelle-associated protein p57. J. Biol. Chem. **261**: 4212-4216.

MacGregor, H.C. and H. Stebbings. 1970. A massive system of microtubules associated with cytoplasmic movement in telotrophic ovarioles. J. Cell Sci. **6**: 431-449.

MacPherson, S. and E. Huebner. 1993. Dynamics of the oocyte cortical cytoskeleton during oogenesis in *Rhodnius prolixus*. Tiss. Cell **25**:399-421.

McNiven, M.A. and K.R. Porter. 1986. Microtubule polarity confers direction to pigment transport in chromatophores. J. Cell Biol. **103**: 1547-1555.

Miller, R.H., Lasek, R.J. and M.J. Katz. 1987. Preferred microtubules for vesicle transport in lobster axons. Science **253**: 220-222.

Mogensen, M.M., Tucker, J.B. and H. Stebbings. 1989. Microtubule polarities indicate that nucleation and capture of microtubules occurs at cell surfaces in *Drosophila*. J. Cell Biol. **108**: 1445-1452.

Munz, A. and F. Dittmann. 1987. Voltage gradients and microtubules both involved in intercellular protein and mitochondria transport in the telotrophic ovariole of *Dysdercus intermedius.* Roux's Arch. Dev. Biol. **196**: 391-396.

Murofushi, H., Ikai, A., Okuhara, K., Kotani, S., Aizawa, H., Kumakura, K. and H. Sakai. 1988. Purification and characterization of kinesin from bovine adrenal medulla. J. Biol. Chem. **263**: 12744-12750.

Murphy, D.B., Johnson, K.A. and G.G. Borisy. 1977. Role of tubulin-associated protein in microtubule nucleation and elongation. J. Mol. Biol. **117**: 33-52.

Neely, M.D. and K. Boekelheide. 1989. Sertoli cell processes have axoplasmic features: an ordered microtubule distribution and an abundant high molecular weight microtubule-associated protein (cytoplasmic dynein). J. Cell Biol. **107**: 1767-1776.

Oakley, C.E. and B.R. Oakley. 1989. Identification of gamma-tubulin, a new member of the tubulin superfamily encoded by *mipA* gene of *Aspirgillus nidulans.* Nature (Lond.) **338**: 662-664.

Oakley, B.R., Oakley, C.E., Yoon, Y. and M.K. Jung. 1990. Gamma-tubulin is a component of the spindle pole body that is essential for microtubule function in *Aspergillus nidulans.* Cell **61**: 1289-1301.

Paschal, B.M. and R.B. Vallee. 1987. Retrograde transport by the microtubule-associated protein MAP 1C. Nature **330**: 181-183.

Paschal, B.M., Shpetner, H.S. and R.B. Vallee. 1987. MAP 1C is a microtubule-activated ATPase which translocates microtubules *in vitro* and has dynein-like properties. J. Cell Biol. **105**: 1273-1282.

Paschal, B.M., Shpetner, H.S. and R.B. Vallee. 1991. Purification of brain cytoplasmic dynein and characterization of its in vitro properties. Methods Enzymol. **196**: 181-191.

Penningroth, S.M., Rose, P., Cheung, A., Peterson, D.D., Rothaker, D.Q. and P. Bershak. 1985. An EHNA-sensitive ATPase in unfertilized sea urchin

eggs. Cell Motil. **5**: 61-75.

Pokrywka, N.J. and E.C. Stephenson. 1991. Microtubules mediate the localization of bicoid RNA during *Drosophila* oogenesis. Development **113**: 55-66.

Porter, M.E., Grissom, P.M., Pfarr, C.M., and J.R. McIntosh. 1987a. Vanadate-sensitized UV cleavage as a probe for dynein-like peptides. J. Cell Biol. **105**: 33a.

Porter, M.E., Scholey, J.M., Stemple, D.L., Vigers, G.P.A., Vale, R.D. and J.R. McIntosh. 1987b. Characterization of the microtubule movement produced by sea urchin egg kinesin. J. Biol. Chem. **262**: 2794-2802.

Porter, M.E., Grissom, P.M., Scholey, J.M., Salmon, E.D. and J.R. McIntosh. 1988. Dynein isoforms in sea urchin eggs. J. Biol. Chem. **263**: 6759-6771.

Pratt, M.M. 1980. The identification of a dynein-like ATPase in unfertilized sea urchin eggs. Dev. Biol. **74**: 364-378.

Pratt, M.M. 1989. Dyneins in sea urchin eggs and nerve tissue. In *Cell Movement. Vol. 2. Kinesin, Dynein and Microtubule Dynamics.* Alan R. Liss, Inc., New York, NY. pp.125-140.

Redenbach, D.M. and A.W. Vogl. 1991. Microtubule polarity in Sertoli cells: a model for microtubule-based spermatid transport. Eur. J. Cell Biol. **54**: 277-290.

Robinson, D.R., Sherwin, T., Ploubidou, A., Byard, E.H. and K. Gull. 1995. Microtubule polarity and dynamics in the control of organelle positioning, segregation, and cytokinesis in the trypanosome cell cycle. J. Cell Biol. **128**: 1163-1172.

Rogalski, A.A., Bermann, J.E. and S.J. Singer. 1984. Effect of microtubule assembly status on the intracellular processing and surface expression of an integral membrane protein of the plasma membrane. J. Cell Biol. **99**: 1101-1116.

Rozdzial, M.M. and L.T. Haimo. 1986. Bidirectional pigment granule movements of melanophores are regulated by protein phosphorylation and dephosphorylation. Cell **47**: 1061-1070.

Saxton, W.M., Porter, M.E., Cohn, S.A., Scholey, J.M., Raff, E.C. and J.R. McIntosh. 1988. *Drosophila* kinesin: characterization of microtubule motility and ATPase. Proc. Natl. Acad. Sci. USA **85**: 1109-1113.

Schnapp, B.J. and T.S. Reese. 1989. Dynein is the motor for retrograde axonal transport of organelles. Proc. Natl. Acad. Sci. USA **86**: 1548-1552.

Scholey, J.M., Neighbors, B., McIntosh, J.R. and E.D. Salmon. 1984. Isolation of microtubules and a dynein-like Mg^{2+}ATPase from unfertilized sea urchin eggs. J. Biol. Chem. **259**: 6516-6525.

Schroer, T.A. and M.P. Sheetz. 1991. Functions of microtubule-based motors. Annu. Rev. Physiol. **53**: 629-652.

Schroer, T.A., Steuer, D.R. and M.P. Sheetz. 1989. Cytoplasmic dynein is a minus-end directed motor for membranous organelles. Cell **56**: 937-946.

Sherwin, T. and K. Gull. 1989. Visualization of detyrosination along single microtubules reveals novel mechanisms of assembly during cytoskeletal duplication in trypanosomes. Cell **57**: 211-221.

Shimizu, T. and K.A. Johnson. 1983. Kinetic evidence for multiple dynein ATPase sites. J. Biol. Chem. **258**: 13841-13846.

Shpetner, H.S. and R.B. Vallee. 1989. Identification of dynamin, a novel mechanochemical enzyme that mediates interactions between microtubules. Cell **59**: 421-432.

Shpetner, H.S., Paschal, B.P. and R.B. Vallee. 1988. Characterization of the microtubule-activated ATPase of brain cytoplasmic dynein. J. Cell Biol. **107**: 1001-1009.

Sloboda, R.D. and J.L. Rosenbaum. 1979. Decoration and stabilization of intact, smooth-walled microtubules with microtubule-associated proteins. Biochemistry **18**: 48-55.

Stearns, T., Evans, L. and M. Kirschner. 1991. Gamma-tubulin is a highly conserved component of the centrosome. Cell **65**: 825-836.

Stebbings, H. and C. Hunt. 1983. Microtubule polarity in the nutritive tubes of insect ovarioles. Cell Tiss. Res. **233**: 133-141.

Stebbings, H. and C. Hunt. 1985. Binding of axonemal dynein to microtubules comprising the cytoplasmic transport system in insect ovarioles. Cell Biol. Int. Rep. **9**: 245-252.

Stebbings, H. and C. Hunt. 1987. The translocation of mitochondria along insect ovarian microtubules from isolated nutritive tubes; a simple reactivated model. J. Cell Sci. **88**: 641-648.

Telfer, W.H. 1975. Development and physiology of the oocyte-nurse cell syncytium. Adv. Insect Physiol. **11**: 223-319.

Therkauf, W.E. 1994. Microtubules and cytoplasm organization during *Drosophila* oogenesis. Dev. Biol. **165**: 352-360.

Therkauf, W.E., Smiley, S., Wong, M.L. and B.M. Alberts. 1992. Reorganization of the cytoskeleton during *Drosophila* oogenesis: implications for axis specification and intercellular transport. Development **115**: 923-936.

Therkauf, W.E., Alberts, B.M., Jan, Y.N. and T.A. Jongens. 1993. A central role for microtubules in the differentiation of *Drosophila* oocytes. Development **118**: 1169-1180.

Travis, J.L., Kenealy, J.F.X. and R.D. Allen. 1983. Studies on the motility of the forminifera. II. The dynamic microtubular cytoskeleton of the reticulopodial network of *Allogromia laticollaris*. J. Cell Biol. **97**: 1168-1176.

Troutt, L.L. and B. Burnside. 1988a. Microtubule polarity and distribution in teleost photoreceptors. J. Neurosci. **8**: 2371-2380.

Troutt, L.L. and B. Burnside. 1988b. The unusual microtubule polarity in teleost retinal pigment epithelial cells. J. Cell Biol. **107**: 1461-1464.

Valdimarsson, G. and E. Huebner. 1989. The development of microtubular arrays in the germ tissue of an insect telotrophic ovary. Tiss. Cell **21**: 123-138.

Vale, R.D., Schnapp, B.J., Reese, T.S. and M.P. Sheetz. 1985a. Movements of organelles along filaments dissociated from the axoplasm of the squid giant axon. Cell **40**: 449-454.

Vale, R.D., Schnapp, B.J., Reese, T.S. and M.P. Sheetz. 1985b. Organelle, bead, and microtubule translocations promoted by soluble factors from the squid giant axon. Cell **40**: 559-569.

Vale, R.D., Reese, T.S. and M.P. Sheetz. 1985c. Identification of a novel force-generating protein, kinesin, involved in microtubule-based motility. Cell **42**: 39-50.

Vale, R.D., Schnapp, B.J., Mitchison, T., Steuer, E., Reese, T.S. and M.P. Sheetz. 1985d. Different axoplasmic proteins generate movement in opposite directions along microtubules *in vitro*. Cell **43**: 623-632.

Vallee, R.B. and H.S. Shpetner 1990. Motor proteins of cytoplasmic microtubules.

Annu. Rev. Biochem. **59**: 909-932.

Vallee, R.B., Wall, J.S., Paschal, P.B. and H.S. Shpetner. 1988. Microtubule-associated protein 1C from brain is a two-headed cytosolic dynein. Nature **332**: 561-563.

Vallee, R.B., Shpetner, H.S. and B.M. Paschal. 1989. The role of dynein in retrograde axonal transport. Trends Neurosci. **12**: 66-70.

Venable, J.M. and R. Coggeshall. 1965. A simplified lead citrate stain for use in electron microscopy. J. Cell Biol. **25**: 407.

Weisenberg, R.C. and E.W. Taylor. 1968. Studies on ATPase activity of sea urchin eggs and the isolated mitotic apparatus. Exp. Cell Res. **53**: 372-384.

Weiss, D.G., Keller, F., Gulden, J. and W. Maile. 1986. Towards a new classification of intracellular movements based on quantitative analyses. Cell Motil. Cytoskel. **6**: 128-135.

Woodruff, R.I. and K.L. Anderson. 1984. Nutritive cord connection and dye-coupling of the follicular epithelium to the growing oocytes in the telotrophic ovarioles in *Oncopeltus fasciatus*, the milkweed bug. Roux's Arch. Dev. Biol. **193**: 158-163.

Yeow, K. and E. Huebner. 1994. Ring canal origin for the extensive F-actin mesh in the insect telotrophic ovary. Mol. Biol. Cell Suppl. **5**: 912a.

Yisraeli, J.K., Sokol, S. and D.A. Melton. 1990. A two-step model for the localization of maternal mRNA in *Xenopus* oocytes: Involvement of microtubules and microfilaments in the translocation and anchoring of Vg1 mRNA. Development **108**: 289-298.